To the Graduate Council:

I am submitting herewith a thesis written by Zeshaan Sher Mohammed entitled "EFFECT OF MOISTURE ABSORPTION ON SINTER QUALITY OF CENTRAL SOLENOID (CS) COIL PACK." I have examined the final electronic copy of this thesis for form and content and recommend that it be accepted in partial fulfillment of the requirements for the degree of Master of Science, with a Major in Mechanical Engineering.

Madhu S. Madhukar
Major Professor

We have read this thesis and
Recommend its acceptance:

J.A.M. Boulet

John D. Landes

Accepted for the Council:

Carolyn R. Hodges

Vice Provost and Dean of the Graduate School

(Original signatures are on file with the official student records)

EFFECT OF MOISTURE ABSORPTION ON THE SINTER QUALITY OF CENTRAL SOLENOID (CS) COIL PACK

A Thesis
Presented for the
Master of Science
Degree
The University of Tennessee, Knoxville

Zeshaan Sher Mohammed
December, 2010

Copyright ©2010 by Zeshaan Sher Mohammed
All rights reserved.

ACKNOWLEDGMENTS

I would first like to mention my professor, Dr. Madhukar, for supporting me during my graduate career. His guidance and advice over the past year has made getting my Master's possible. I have had Dr. Madhukar for several classes throughout my college career and after each one I have walked away with a better understanding of the mechanical world around me. The late nights spent at the lab taking pictures and starting soak ovens have not always been joyful but I appreciate his patience and support, and for that I thank him.

I would also like to thank all guys at the lab who have helped me with my research. Joe, Jim, and Bill who have spent countless hours machining dies, presses, and collars only for me to come back and need them modified. They did this each time without complaint and were grateful to help whenever possible. I would like to thank Steve for his help in the sintering of the samples. It was Steve who developed the heat treatment process the samples would need to go through in order to be sintered and stayed a few long nights at the lab ensuring the oven was working properly. I would like to thank Dr. Irick for allowing me to work at the Magnetic Development Lab (MDL) and assisting with ordering the materials needed for the experiments. The knowledge gained while working at MDL and attending the meetings was priceless. It is an honor to say I have worked on a piece of the future with the ITER project. I would also like to thank Gongyao at the University of Tennessee for his help in using the testing equipment needed to complete my research.

Special thanks go to Dr. Landes and Dr. Boulet for sitting on my thesis board and guiding me through my college career. Dr. Landes has taught me invaluable lessons on Solid Mechanics and Advanced Mechanics of Materials. His knowledge and humor will not soon be forgotten. Thank you to Dr. Boulet for being my academic advisor for the past several years and assisting me when I had questions and concerns about the undergraduate/graduate process.

Last but certainly not least I would like to thank my friends and family for helping me through this process. I would like to thank my loving girlfriend Evgeniya for spending hours with me in the lab while I tested samples and giving me encouragement when I got discouraged. I thank my dad for his help in teaching me how to polish samples. I thank my mom for the "hang in there" when things were rough.

Without the love and support throughout my college career I can honestly say I would not be where I am today. Thank you everyone!

ABSTRACT

Fusion energy has been said to be the solution to all the world's energy problems. The International Thermonuclear Experimental Reactor (ITER) is the flagship project to demonstrate the feasibility of fusion energy. The Central Solenoid (CS), an important component of the reactor, is needed to induce plasma current, to initiate, ramp-up, ramp-down, and to sustain plasma in a very controlled manner. In order to achieve this, the CS coil packs must be manufactured under controlled conditions. The CS conductor is an advanced cable-in-conduit Nb_3Sn superconductor. The CS cable will be made in long continuous sections but with thousands of meter of cable needed, splices will have to be made in the field during construction of the ITER reactor. With the ends of the CS cable being exposed to the environment for an unspecified amount of time, concern has been expressed about the effect of the cable exposure on the quality of the splice. As a result an experimental program, the subject of this thesis, was devised to replicate and expedite the environmental damage the cable may see while in the field.

The CS cable samples were exposed to 100% humidity at 60, 80, and 100^{o}C for periods ranging from one week to four weeks. Once the samples were soaked for a period of time they were then sintered as would be done in the field. After sintering the mechanical tests were done to determine the load required to push the sintered strands out of the copper sleeve. Initial results obtained with samples having the sleeve thickness of 1.25 mm (0.05 in) were inconclusive due to the presence of a fold in the copper sleeve formed during the compaction of the sleeve around the cable. To prevent the fold formation, another set of samples was prepared with thicker copper sleeve of 5 mm (0.20 in).

Results from these samples yielded data that was more conclusive and showed a possible correlation between aging temperature and sintering strength. The experimental data suggests that the thin oxide layer formed during the elevated temperature soak at 100% humidity may even be beneficial to the sinter quality.

TABLE OF CONTENTS

Page

INTRODUCTION 1
1.1 Balance 1
1.2 Energy 1
1.3 Nuclear Energy 2
1.4 ITER and Magnetic Suspension 4
1.4.1 Central Solenoid (CS) 4
MATERIAL 6
2.1 CS Superconductive Cable 6
2.2 Construction of CS Cable (Cable in Conduit) 7
BACKGROUND 15
3.1 Copper Oxidation/Corrosion 15
3.2 Copper Corrosion due to Atmosphere, Acid, and Oxygen 15
3.3 Sintering 18
3.4 Chromium and Sintering 20
3.5 Methodology 21
SAMPLE PREPERATION 22
4.1 Thin Wall Sample Preparation: 22
4.2 Thick Wall Sample Preparation 29
4.3 Sample Soaking 31
4.4 Sample Sintering 39
MECHANICAL TESTING 49
5.1 Thin Wall Testing Procedure 49
5.2 Thick Wall Testing Procedure 54
RESULTS AND DISCUSSION 55
6.1 Thin Wall Samples Results and Discussion 55
6.2 Thin Wall Sample Data Elimination 57
6.3 Analysis of Thin Wall Results 61

6.4 Analysis of Thick Wall Results 65
CONCLUSIONS AND RECOMMENDATIONS..... 71
7.1 Conclusions..... 71
7.2 Recommendations for Future Work 71
REFERENCES..... 73
APPENDIX..... 75

LIST OF TABLES

Table **Page**

3.2.1:Atmospheric Corrosion of Selected Copper Alloy…….…. 16
3.3.1: Effect of Copper Oxide Thickness on Tensile strength…….. 20
4.1.1: Sample Summary…… 29
4.3.1: Sample Soaking 1 Week……. 32
4.3.2: Sample Soaking 2 Weeks……... 33
4.3.3: Sample Soaking 1 Month…… 33
4.3.4: Thick Walled Sample Soaking Periods…….. 34
4.4.1: Thin Wall Sample Ramp Rate and Heat Cycles……. 39
6.4.1: ½” Sample X Average Peak Loads and Standard Deviation…….. 67

LIST OF FIGURES

Figure **Page**

1.2.1 U.S. Energy Consumption by Fuel Type Per Year…….. 2
1.3.1 General Diagram of Tokamak Magnetic Field…….3
1.4.1: Artist Rendering of Proposed ITER Fusion Reactor……...4
1.4.2: CS Coil in Relation to the Toroidal Field Magnets…….5
2.2.1: Billet Copper Drilled and Filled with Niobium-Tin Rods…….. 7
2.2.2: Filled Copper Billet Drawn Down and Shaped into Hexagonal Filament……. 8
2.2.3: Copper Billet Filled with 19 Hexagonal Filaments…… 9
2.2.4: Superconducting Wire Wrapped Around Central Copper Wire to Form Cable…..10
2.2.5: Final Superconducting Cable Containing 270 Wires……..11
2.2.6: Final Superconducting Cable Compacted in Copper Sleeve……...12
2.2.7a: Superconducting Wire at 25x…….13
2.2.7b: Superconducting Wire at 100x……..13
2.2.7c: Superconducting Wire at 500x……...14
3.2.1 A, B: Copper Corrosion Rates shown as Thickness loss vs. Time……...17
3.2.2: Corrosion Rate of Copper (mm/yr) vs Amount of Oxygen in Reacting Acid…….18
4.1.1: Ultrasonic Tank with Eight PVC Pipes……...23
4.1.2: Nitrogen Purge Placed Through Center of the Strand…….23
4.1.3: Strand Lowered into HCL with Nitrogen Purge……..24
4.1.4: Drying and Visual Inspection of Chrome Removed from Strand……...24
4.1.5: Val Power Hydraulic Crimper…….25
4.1.6: Press…….6
4.1.7: Die……26
4.1.8: Clamshell with Welding Wire…….27
4.1.9: Predictable vs. Unpredictable Folds……28
4.1.10: Marking of the Samples…….28
4.1.11: Samples after Cutting……29
4.2.1: Bar X Thick Wall Sample After Compaction and EDM…….30
4.3.1: Soaking Setup……..32
4.3.2: 1 Week Thin Wall Humidity Recordings Measured by Omega Sensors……35
4.3.3: 1 Week Thin Wall Temperature Recordings Measured by Omega Sensors……...35
4.3.4: Sample 16c After Soaking 50x……36
4.3.5: Sample 16c After Soaking 100x……..37
4.3.6: Sample 16c After Soaking 200x……..37
4.3.7: Sample 16c After Soaking 500x……..38
4.3.8: Visual Discoloration of Soaked Samples…….38

4.4.1: Thin Wall Sample Retort…….39
4.4.2: Thin Wall Retort End Cap and Compression Fitting……..40
4.4.3: Stainless Clips……..41
4.4.4: Clips Placed Between Samples……42
4.4.5: Complete Stack of Thin Wall Disk Samples……...43
4.4.6: Spring……...44
4.4.7: Stainless Tube Oven…….. 44
4.4.8: Retort on Rack…….45
4.4.9: Argon Gas Flow to Retort……...46
4.4.10: Argon Inflow……..46
4.4.11 Thick Walled Sample Retort……...47
4.4.12: Box Oven Used for Sintering Thick Wall Samples……...48
5.1.1: Press and Die……...49
5.1.2: Notches Cut into Press…….50
5.1.3: Die Inside Edge and Taper……...50
5.1.4: MTS Testing Setup……..51
5.1.5: Close-up of Disk sample Testing Setup……...52
5.1.6: Rigid Clamping Collar for Thin Wall Samples……...53
5.1.7: Rigid Clamping Collar Installed During Testing of Thin Wall Sample……..53
5.2.1: Press, Die, and Collar for Thick Wall Samples……...54
6.1.1: Thin Wall Disk Samples Pressed w/o Collar Demonstrating Stick Slip…….55
6.1.2: ¾” Disk sample Comparison of Collar vs. No Collar…….56
6.1.3: ¾” Disk sample Comparison of Collar vs. No Collar…….57
6.2.1: Disk sample 10a No Chrome Removal……58
6.2.2: Disk sample 2e…….59
6.2.3: Disk sample 11b……...59
6.2.4: Disk sample 3e…….60
6.2.5: Crushed Disk sample Data……...61
6.3.1: Soaked and Sintered ¾” Disk samples.……..62
6.3.2: Soaked and Unsintered ¾” Disk samples..……..……63
6.3.3: Soaked and Sintered ½” Disk samples……63
6.3.4: Soaked and Unsintered ½” Disk samples……64
6.3.5: Effect of the fold orientation with respect to the loading axis…….65
6.4.1: ½” Sample X Four Weeks 100˚C……66
6.4.2: Sample 1x (low load) Clean Sleeve vs. Sample 32x (high load) Wires in Sleeve..67
6.4.3: ½” Sample X Average Peak Loads vs. Time and Temperature……..68
6.4.4: ½” Sample 1x Pictures of Each Stage of Testing……69
6.4.5: Sample X Temperature and Humidity Recordings……..70

7.2.1: Suggested specimen design for establishing a quantitative relationship between moisture condition and sinter quality…….72
7.2.2: Lap shear test……...72

LIST OF ABBREVIATIONS AND SYMBOLS

TOKAMAK: Russian acronym for Torodial Magnetic Chamber
EAST: Experimental Advanced Superconducting Tokamak
KSTAR: Korea Superconducting Tokamak Advanced Research
NSTX: National Spherical Torus Tokamak
MAST: Mega Ampere Spherical Tokamak
ITER: International Thermonuclear Experimental Reactor
CS: Central Solenoid
Cu_2O: Cuprous Oxide
H_3PO_4: Phosphuric Acid
HCL: Hydrochloric Acid
CuO: Cupric Oxide
K: Kelvin (Temperature)
C: Celsius (Temperature)
I.D.: Inner Diameter
O.D.: Outer Diameter
V: Volume
L: Length
π: Ratio of the diameter of a circle to the circumference, represented as 3.14
EDM: Electro Discharge Machining

Chapter I

INTRODUCTION

1.1 Balance

William H. Danforth was the founder of Purina, the world's largest supplier of dry dog and cat food as well as cat box filler. Mr. Danforth was a sickly child growing up in Southeast Missouri and was "dared" by his teacher to become the healthiest boy in the class. That dare did Mr. Danforth well and he said that life can be viewed as an equally sided box. The four sides of this box are thought to be different aspects of a person's life. On the left side of the box Mr. Danforth would write "Physical" at the top "Mental" on the right side "Social" and on the bottom "Religion." The idea is people have four parts to their lives and that all four parts should be lived equally and developed equally [1].

The same principles can be expanded to that of a corporation or economy with the left side of the box being "Energy" on the top "Computation" on the right side "Communication" and on the bottom "Community." The community and communication aspects of the four-sided box are flourishing with the advent of the internet and cheaper/faster communications methods such as email, texting, video conferencing, etc. Speeds of computers have increased exponentially over the past few years thereby increasing the computational power that can now be achieved. However with more technologies being developed and a constantly progressing economy, the energy side of the box has been left without equal advancement.

1.2 Energy

Currently there are several different methods of producing energy; to name a few there are wind, solar, fossil fuels, biomass, hydroelectric, and nuclear. Each has advantages and disadvantages, but with the world's energy requirements growing quickly, only a few have the capability to meet such a need. Figure 1.2.1 is a diagram of the United Sates' energy consumption over the past few years with projections into the future.

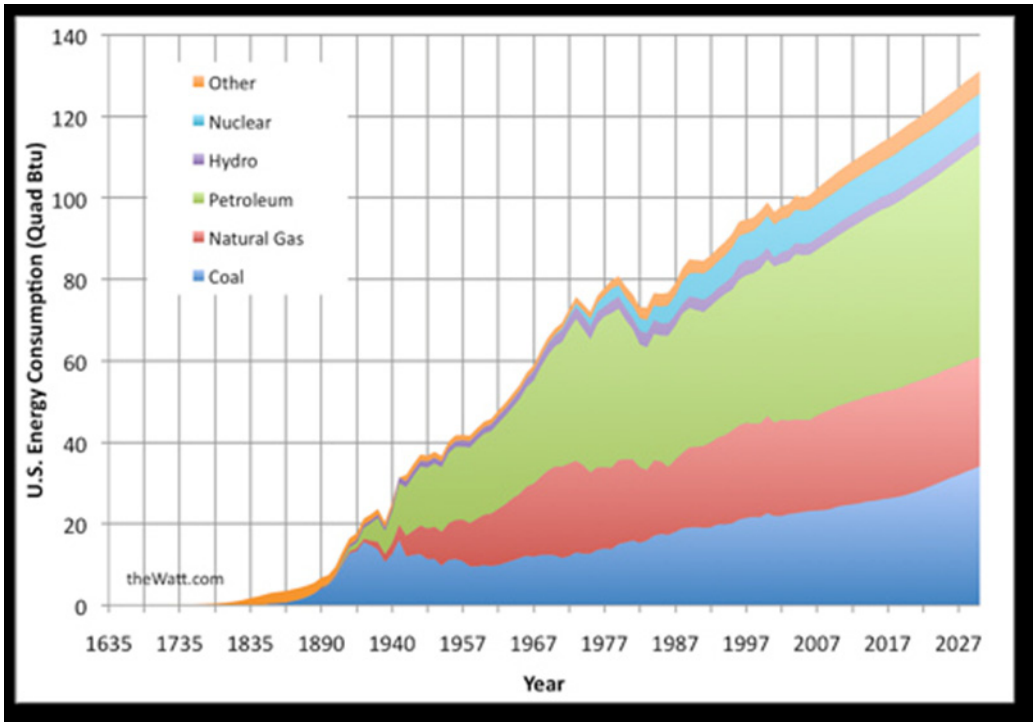


Figure 1.2.1 U.S. Energy Consumption by Fuel Type Per Year [2]

While arguments could be made about how accurate the projections for 2027 are, little doubt was expressed that the energy requirements will increase. According to the above graph, an increase in energy requirements means an increase in fossil fuel dependency. The problem with fossil fuels, other than the harm to the environment, is that they are a non-renewable energy source; while the exact time is debatable most believe the supply will run out. There are cleaner and safer forms of energy that are currently being developed. When complete these energies could replace part of the dependency on fossil fuels.

1.3 Nuclear Energy

Nuclear fission energy has large potential as an energy source. Relatively small amounts of uranium are needed to produce large amounts of energy. However, with fission energy there is radioactive waste and a concern that the waste could be used for weapons of mass destruction. Fusion energy on the other hand does not have such waste.

Nuclear fusion runs primarily on a mixture of deuterium and tritium which are inexhaustibly abundant. Deuterium is relatively abundant in the world's oceans, while tritium can be produced from deuterium each time it absorbs a neutron. The advantage is that once a fusion reaction has been started, it is largely self sustaining and produces little

to no harmful byproducts. However, fusion energy does have many challenges that need to be overcome in order for it to be a viable energy producer.

Currently, the largest challenge is the confinement of the reactor's plasma field, which can operate at temperatures in excess of 150 million ˚C. There are currently no materials, either natural or engineered, that can withstand such high temperatures. Several methods of confinement are known to exist, including gravity, lasers, and magnetic fields. Gravity has been used by the stars and the galaxy to produce energy for millions of years. Laser confinement utilizes laser beams to compress the plasma. One drawback to laser confinement is the extreme precision required in the process. Another is the plasma lasts for less than 1/10 of a nanosecond [3]. Magnetic field confinement is the most commercially feasible and was first developed with the TOKAMAK reactor designed by Russian scientists Andrei Sakharov and Igor Tamm.

Since the design of the TOKAMAK, several reactors have been built and several are currently in operation, including MAST in the United Kingdom NSTX in Princeton, New Jersey EAST in Hefei, China and KSTAR in Daejon, South Korea. A common feature in these fusion reactors is that they utilize magnetic fields for containment of the plasma. To do this several sets of magnets are used in multiple orientations, as seen in Figure 1.3.1.

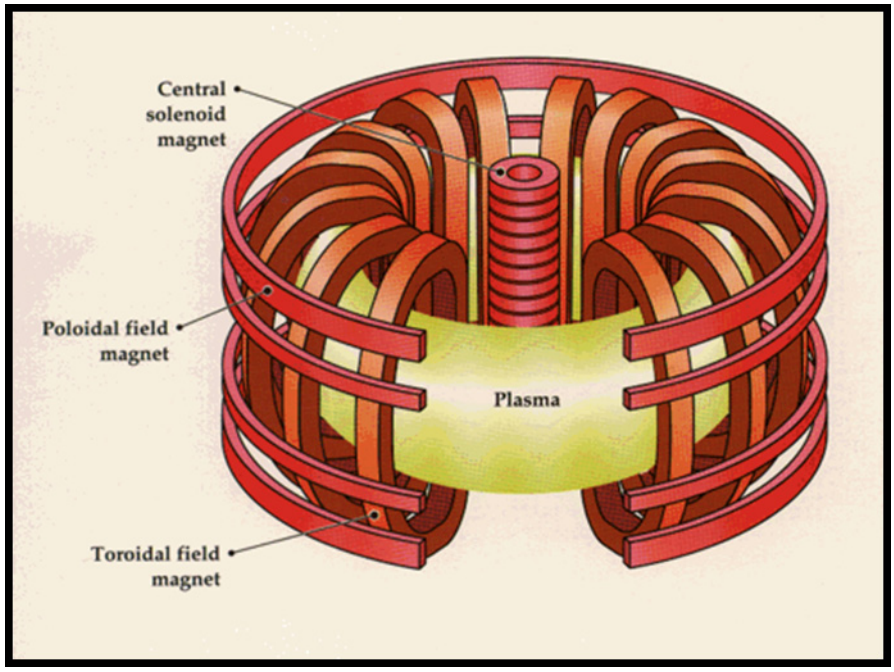


Figure 1.3.1 General Diagram of Tokamak Magnetic Field [3]

As seen in the diagram there are three main sets of magnets used to suspend the plasma during reaction: toroidal, poloidal, and central solenoid. Each set of magnets suspends and controls the flow of plasma and ensures that the plasma continues to flow in

a circular manner throughout the reactor. This same concept will be applied to the ITER project (formerly International Thermonuclear Experimental Reactor).

1.4 ITER and Magnetic Suspension

When a voltage is applied through a conducting wire, two forces are present, an electric force and a magnetic force. It is the magnetic force created by the voltage running through the wire that fusion reactors depend on to suspend the plasma during reactions. Making magnets from superconducting cable has several advantages. In theory, because the cable is superconducting, the electrical resistance reduces to zero at the characteristic temperature. As a result the heat generated and the power required are both very low. A superconducting magnet is also much lighter than traditional magnet because it does not require the heavy iron poles of traditional magnets [9].

The ITER reactor will consist of 48 magnetic elements that will generate a magnetic field 200,000 times that of the earth. Similar to the diagram in Figure 1.3.1, the ITER reactor will consist of 18 toroidal field magnets, 6 poloidal field magnets, a central solenoid and a set of correction coils [4]. Figure 1.4.1 shows an artist's rendering of what the inside of the ITER reactor will look like when completed.

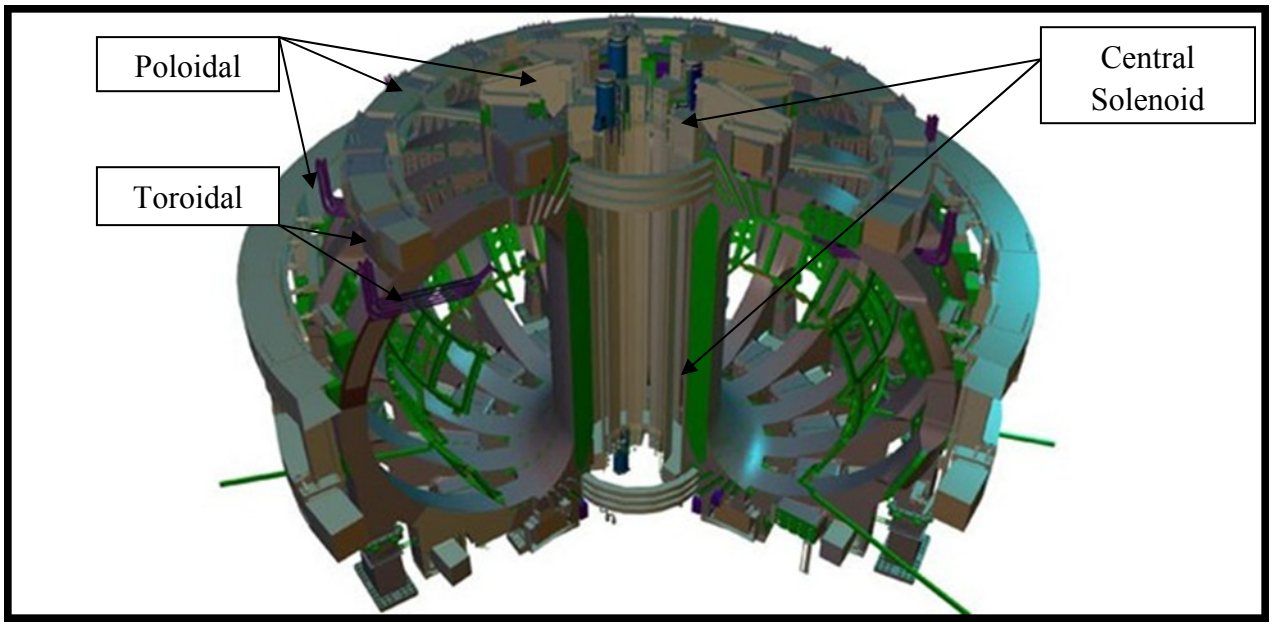


Figure 1.4.1: Artist Rendering of Proposed ITER Fusion Reactor [4]

1.4.1 Central Solenoid (CS)

The central solenoid will be manufactured by coiling CS superconducting cables into rings that will be placed at the center of the reactor. The Central Solenoid has been called the "backbone" of the reactor and acts as a giant transformer. Manufactured from

a copper and niobium-tin (Nb_3Sn) alloy, the CS coil is largely responsible for the inductive flux that drives the plasma and ensures vertical stability.

The CS coil is made of six independent coils that are held together utilizing a vertical pre-compression structure. To minimize joints, each coil will be manufactured in a pancake like fashion with lengths of conductor measuring up to 910 meters [4]. A picture of the CS coil in relation to the toroidal field coil can be seen in Figure 1.4.2 below.

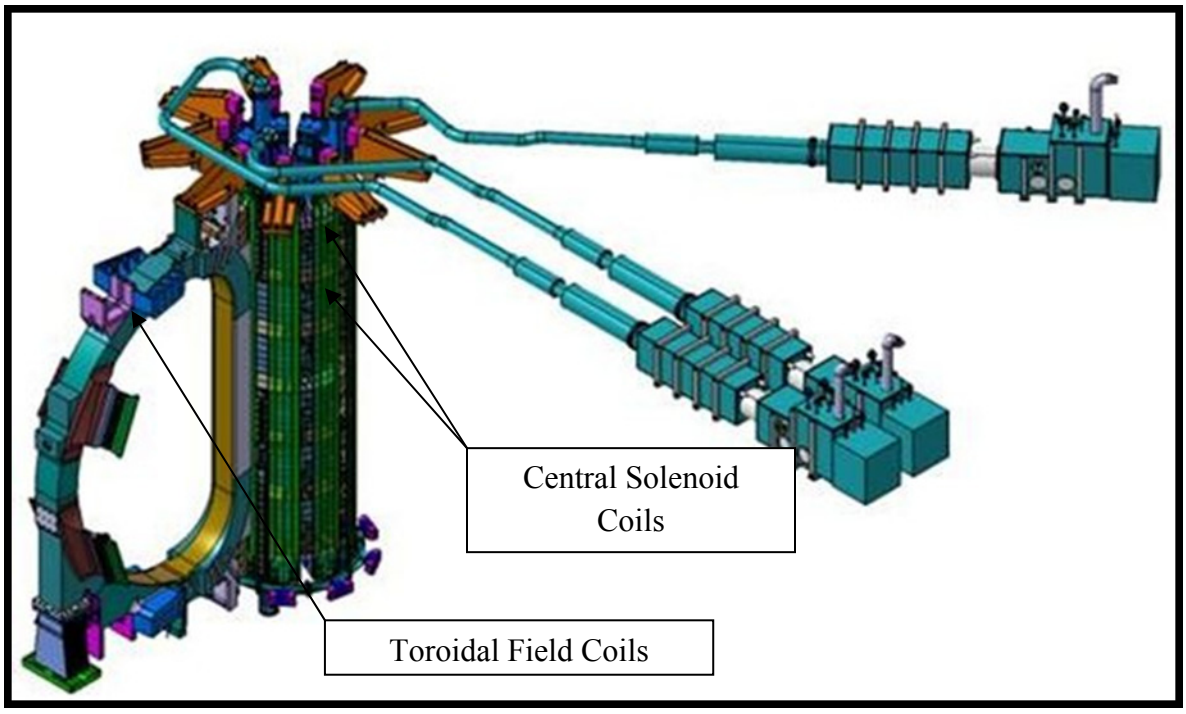


Figure 1.4.2: CS Coil in Relation to the Toroidal Field Magnets [4]

One issue with the CS coil is that even though care is taken to minimize joints, they are inevitable and will be needed. In order to ensure that proper current flow exists throughout the CS coil, joints will be spliced together, inserted into a copper sleeve and then sintered. The concern is that, between the time the wires are sintered and first cut, the CS superconducting wires will be exposed to the environment for an uncertain amount of time. During this exposure to the environment oxidation of the copper and other components will occur and could possibly have adverse effects on the sinter quality.

Chapter II

MATERIAL

2.1 CS Superconductive Cable

Super conductivity is defined as the ability of metals to transmit electricity with no losses. In addition, a superconductive metal also has special magnetic properties. Known as the Meissner effect, superconductive metals have the ability to bend magnetic field lines away from its self, while normal metals attract the magnetic field lines and allow them to pass through. A German professor named Alexander Meissner and his graduate student R. Oschenfeld discovered that when a superconducting material was placed in a magnetic field and then lowered beyond the transition temperature, the magnetic field was repelled away from the center of the material. The phenomenon was later explained by London brothers Fritz and Heinz. They explained that a voltage was applied to a superconductor which produced a surface current resulting in an internal magnetic field that exactly matched the applied magnetic field leaving the interior of the conductor with no field at all [9].

One problem with superconducting magnets is that as adjacent wires carry current, an attractive force is present between the wires. As the current fluctuates this can cause the wires to move or vibrate against each other causing heat to be produced. This would in turn cause a quenching of the superconducting state causing a large pulse of normal current that would in turn generate more heat due to resistance. The high heat generated could boil liquid helium causing an explosion leading to the destruction of the magnet. Another problem with superconducting wire is known as "flux slippage" where current flowing in the wire interacts with flux trapped in the wire in the form of flux lines or vortices. This phenomenon causes localized regions of heat known as "hot spots" within the wire and can have the same catastrophic effect as the wire's moving against one another. To dissipate the heat quickly, several strands of superconducting wire must be wrapped in an excellent heat conductor such as copper [9].

Most superconducting cable is made of an alloy consisting of niobium-tin (Nb_3Sn) or niobium-titanium (NbTi). While niobium-titanium cable is cheaper to manufacturer, the niobium-tin cable can be used in higher magnetic fields. The cables used in the CS coil consists of hundreds of smaller filament wires with some no larger than a human hair wound together in bundles to form larger cables. Each cable would then consist of thousands of smaller wires. The purpose of having such a large number of wires is to provide adequate surface area for the cooling process and the elimination of hot spots.

In order for the cable to be super conducting it needs to be as cold as possible. To achieve this liquid helium (the coldest liquid on earth) is piped through the middle of the cable at 4 K. However, to ensure conductivity even at these temperatures, careful manufacturing procedures must be followed.

The cable used in this experiment is constructed of the niobium-tin alloy and is enclosed in a copper sleeve. The niobium-tin alloy is a very brittle material and once sintered becomes even more brittle. Because of this, the alloy is encased in a copper matrix which not only lends mechanical stability but also provides a security measure. In the event an accidental rise in temperature causes the superconductor to stop carrying the current, the copper can carry the additional load [7].

2.2 Construction of CS Cable (Cable in Conduit)

Different manufacturing facilities have different methods of manufacturing superconducting cable. The process described below is a process used by one particular manufacturer; while the details of the process may vary, the overall principles remain the same. Manufacturing of the CS cable is a relatively simple process in which a billet cylinder of the base material (in this case copper) 25 cm (9.84 in) in diameter by 1 m (39.7 in) long is drilled with several holes as presented in Figure 2.2.1. The holes are then filled with rods of the super conducting niobium also seen in Figure 2.2.1.

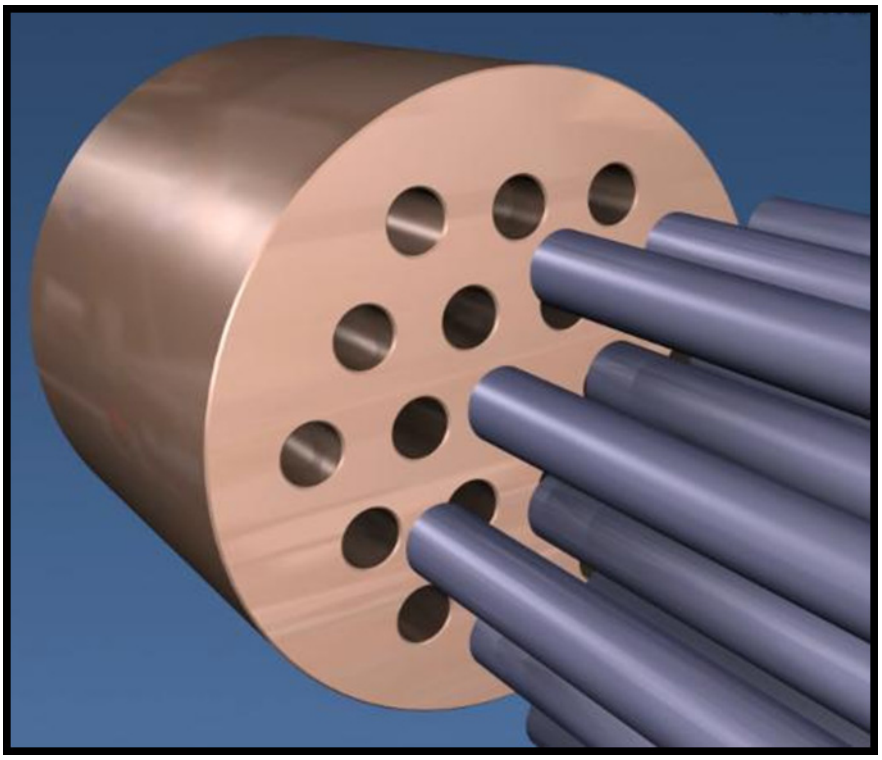


Figure 2.2.1: Billet Copper Drilled and Filled with Niobium-Tin Rods [7]

The next step requires the filled copper billet to be drawn down to a size of 2.5 cm (0.984 in) in diameter. The strand is then formed into a hexagonal filament as shown in Figure 2.2.2.

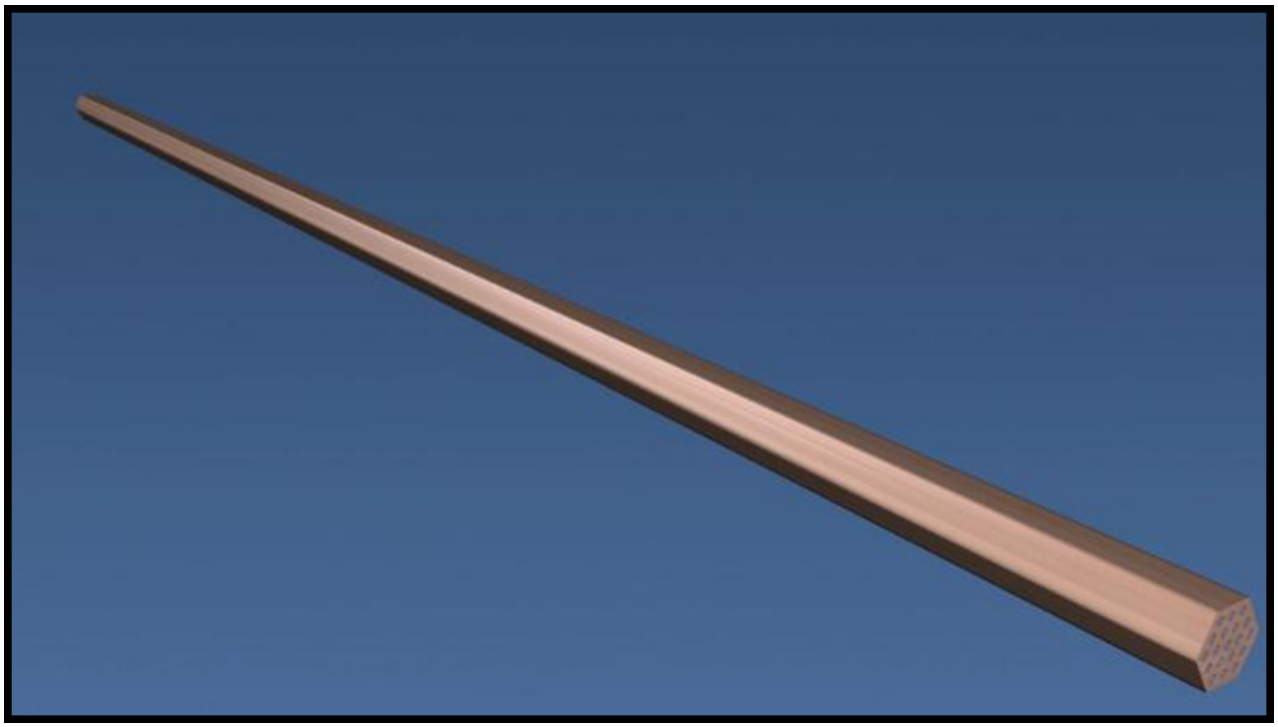


Figure 2.2.2: Filled Copper Billet Drawn Down and Shaped into Hexagonal Filament [7]

Next, another copper billet 25 cm (9.84 in) diameter by 1 m (39.37 in) long is drilled with a large center hole. The large hole is then filled with 19 of the above hexagonal filaments as shown in Figure 2.2.3.

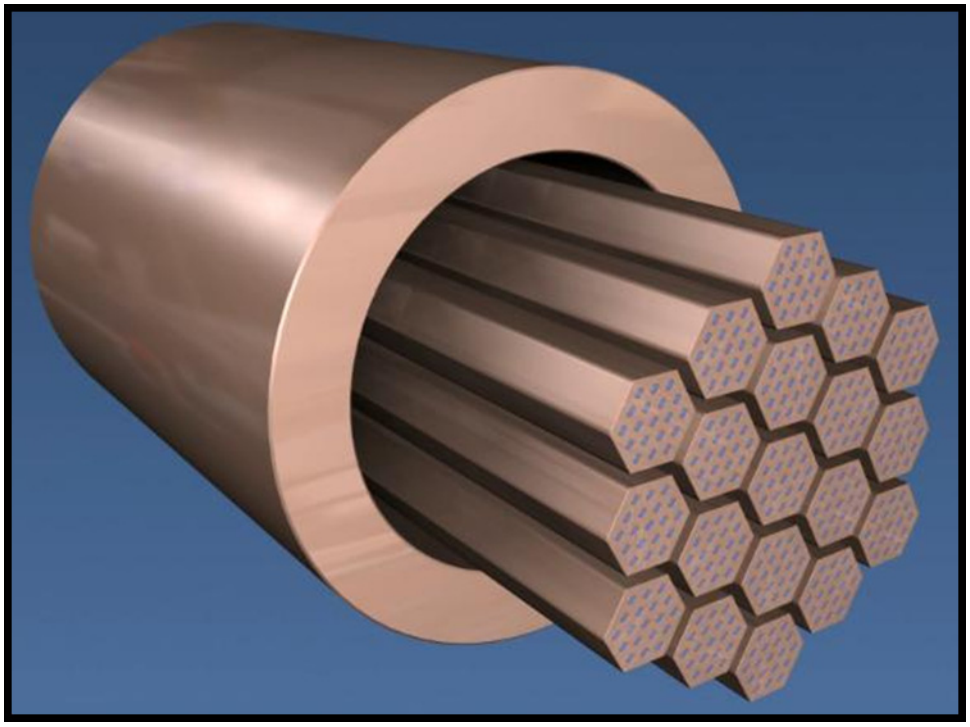


Figure 2.2.3: Copper Billet Filled with 19 Hexagonal Filaments [7]

The assembly is then drawn down to a diameter of 1 mm (0.04 in) to form the first complete super conducting wire. Six of these superconducting wires are wrapped around a central copper wire as pictured in Figure 2.2.4.

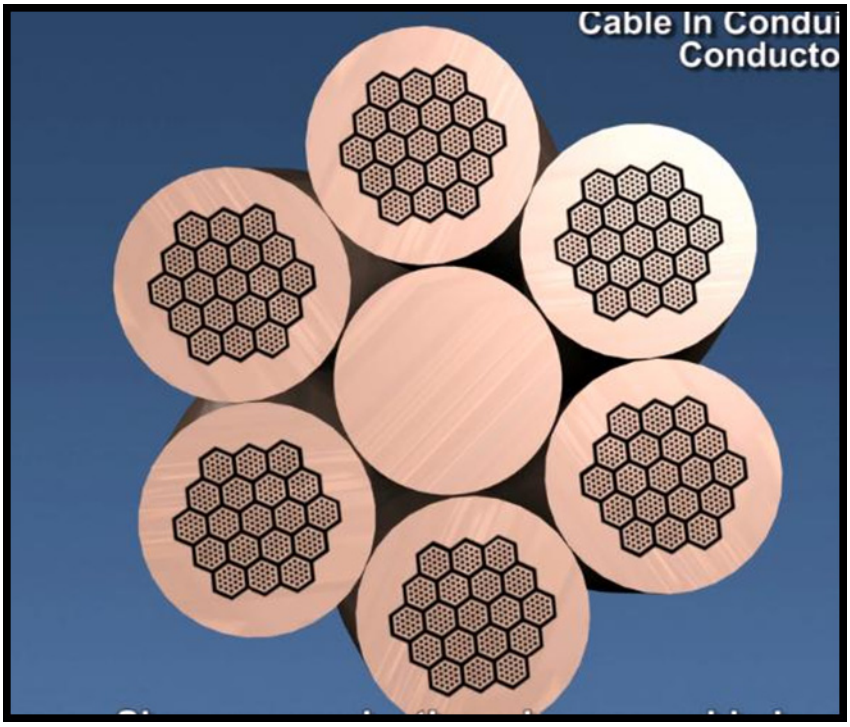


Figure 2.2.4: Superconducting Wire Wrapped Around Central Copper Wire to Form Cable [7]

Once one superconducting cable is formed, three of these are wound together to form a bundle. Three bundles are then twisted together to form larger bundles after which three of the larger bundles are twisted together to form an even larger bundle. Last, five of the "even larger" bundles are twisted together to form the superconducting cable containing a total of 270 wires as shown in Figure 2.2.5.

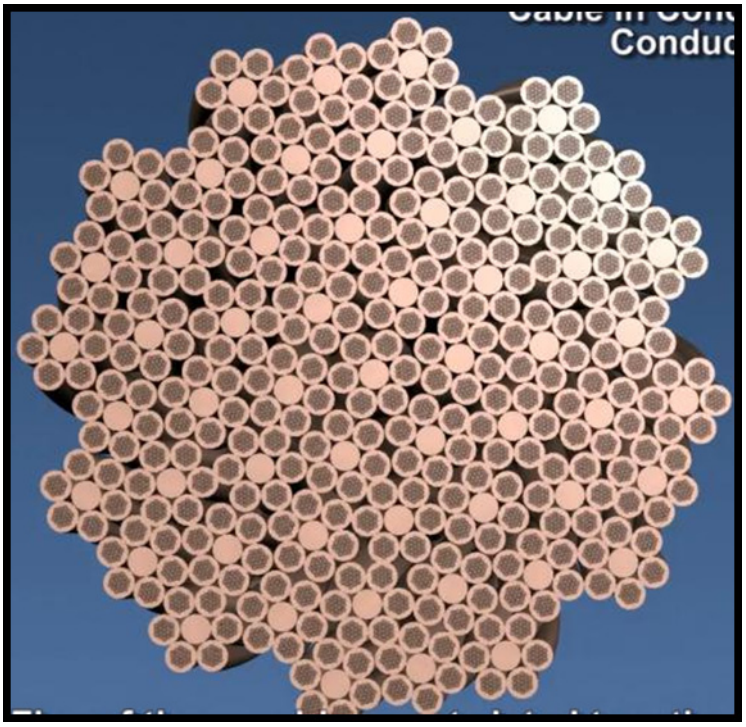


Figure 2.2.5: Final Superconducting Cable Containing 270 Wires [7]

The next step of the process involves inserting the 270 wire cable bundle into a copper sleeve and compacting it into a round shape. Figure 2.2.6 shows a picture of a sample of the final cable once it has been compacted in the copper sleeve. A note should be made that the cable used in the current experiment was wound with a stainless sleeve inserted into the middle as shown in the figure below. This is different than the above described manufacturing process because, the stainless sleeve was inserted to allow a better flow of the liquid helium required for superconductivity.

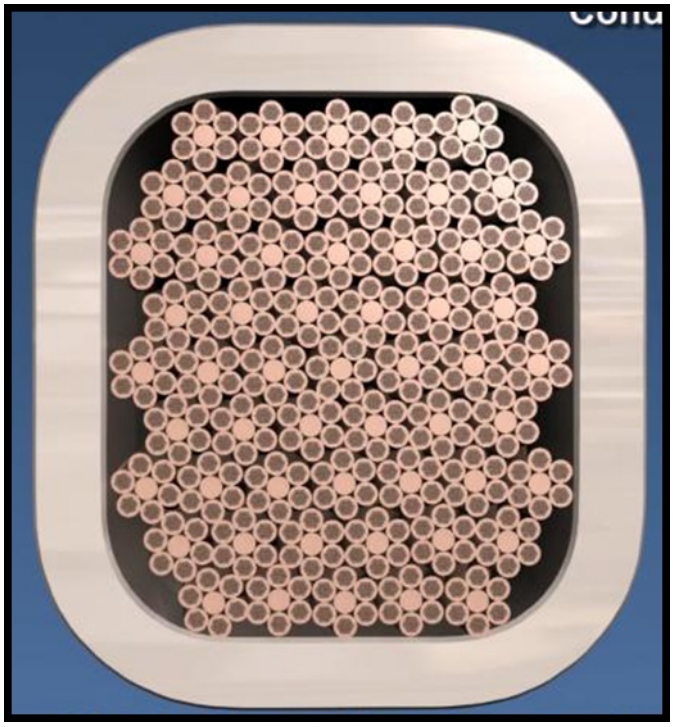


Figure 2.2.6: Final Superconducting Cable Compacted in Copper Sleeve

Figures 2.2.7 a-c show microscopic photos of the superconducting wire structure at magnifications varying from 25x to 500x. In each photo the hexagonal packing of the wires into cables is apparent as well as the different metals used to construct the wire.

Figure 2.2.7a shows the cable at 25x magnification. At this magnification the outline of solid copper strands can be seen mixed in between the superconducting wire pictured with the "dots." This would be the step highlighted in Figure 2.2.4 from above.

At 100x magnification the hexagonal packing of the niobium-tin can be seen in the copper matrix as shown in Figure 2.2.7b. At this magnification the original 19 hexagonal filaments can be counted. Taking a closer look at one of the hexagonal patterns pictured above yields an even more in depth view of the manufacturing process. Figure 2.2.7c is a picture of the cable taken at 500x.

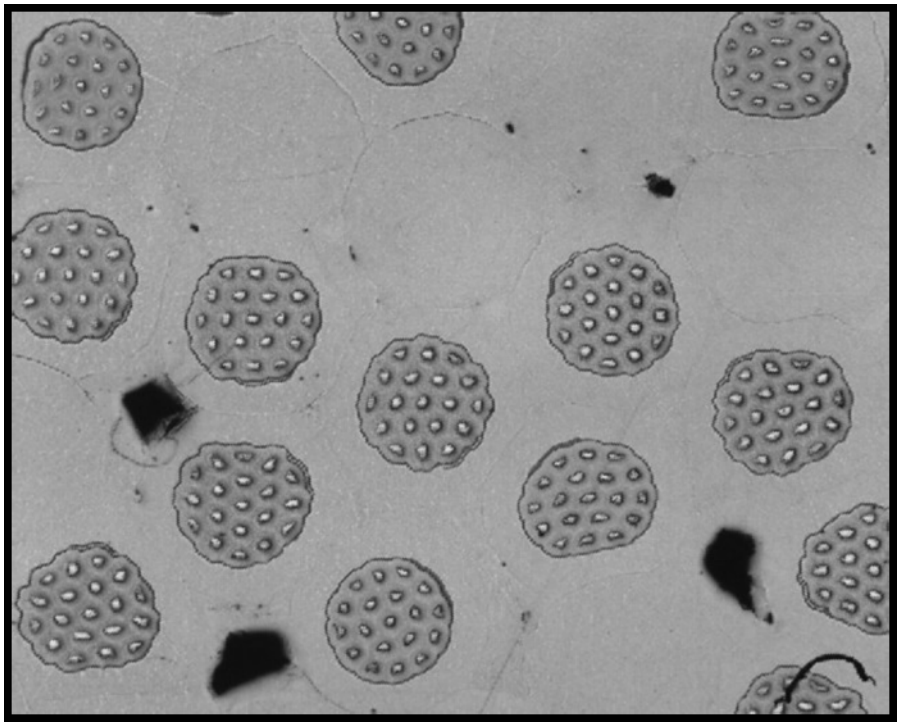


Figure 2.2.7a: Superconducting Wire at 25x

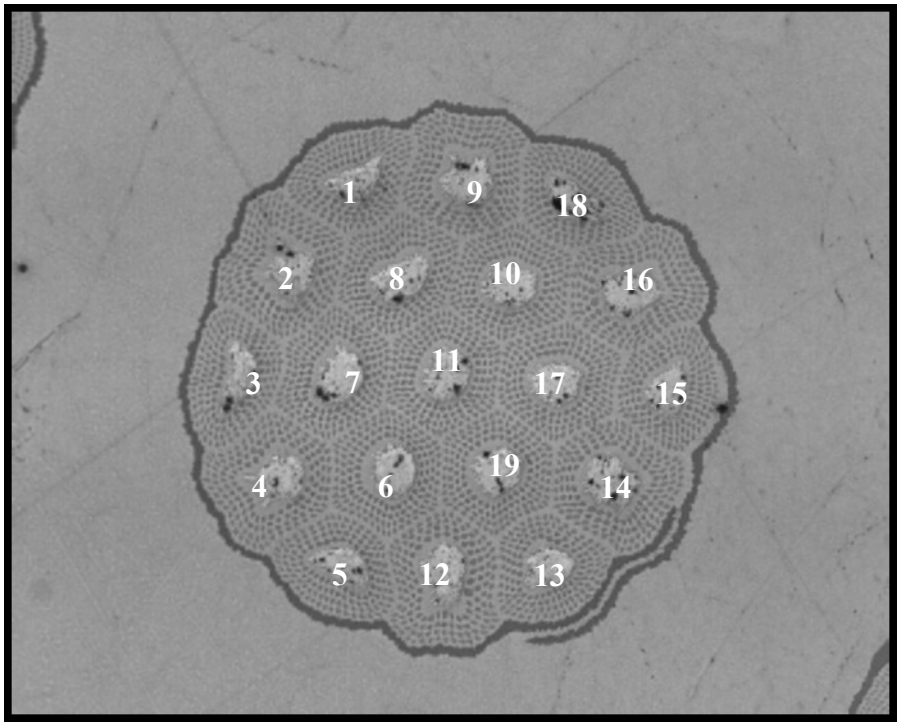


Figure 2.2.7b: Superconducting Wire at 100x

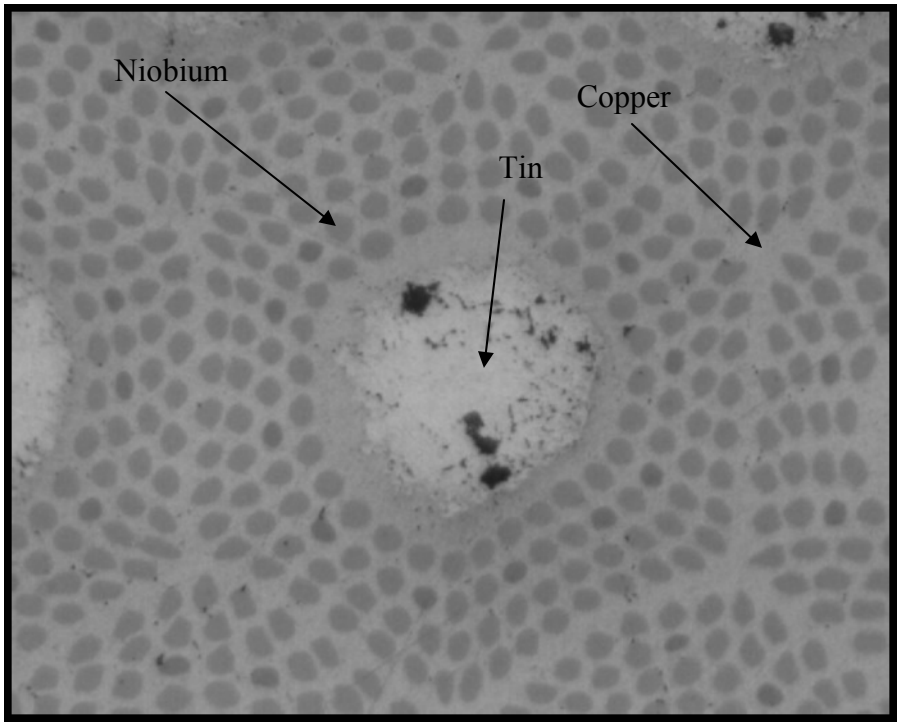


Figure 2.2.7c: Superconducting Wire at 500x

At 500x the different metals that make up the superconducting wire are clearly visible. The large circular area located at the middle of the hexagon is the niobium while the smaller dots that surround it are tin. The matrix the assembly is contained in is the copper that originally started out as billet at the very first step of the manufacturing process.

When the cable is viewed under a microscope, black voids appear throughout the assembly. While these voids appear to be infrequent in reality, almost one third of the cable is voids. This serves to provide adequate surface area for the helium to transport the heat generated by the magnet allowing for the super cool conditions the cable needs to conduct. This is the primary difference between cable in conduit magnets and wire wound magnets. Cable in conduit magnets are cooled directly through the middle of the cable from the inside out allowing for greater efficiency vs. the wire wound magnets which are indirectly cooled either by the outer or inner surfaces [7].

Chapter III

BACKGROUND

3.1 Copper Oxidation/Corrosion

Copper and its alloys are widely used in a variety of industrial fields because of high resistance to corrosion and excellent conductive properties. Several other advantages of copper include ease of fabrication, methods of joining, and range of attainable mechanical properties. In unpolluted air, water, and de-aerated non-oxidizing acids, copper deteriorates in negligible amounts. Several examples of copper artifacts have been found buried deep beneath the earth's surface or in rural areas with little to no degradation.

At ambient temperatures and in aqueous environments copper and its alloys form a protective film that consists mainly of cuprous oxide or Cu_2O. This protective film is a p-type semiconductor and follows the chemical process as seen below.

$$4Cu + 2H_2O \rightarrow 2Cu_2O + 4H^+ + 4e^- \text{ (anode)}$$

and

$$O_2 + 2H_2O + 4e^- \rightarrow 4(OH)^- \text{ (cathode)}$$

which gives a net reaction of

$$4Cu + O_2 \rightarrow 2Cu_2O$$

In order for the corrosion process to proceed beyond the initial forming of the oxide layer, electrons must first travel through the outer cuprous oxide film. If further protection from oxidization is required, doping of the outer layer with alloys such as tin, aluminum, zinc, iron, and nickel can be used to reduce the conductivity of the Cu_2O film and significantly reduce the corrosion rates [5]. At higher temperatures a different form of oxide can be found known as cupric oxide which is black in color.

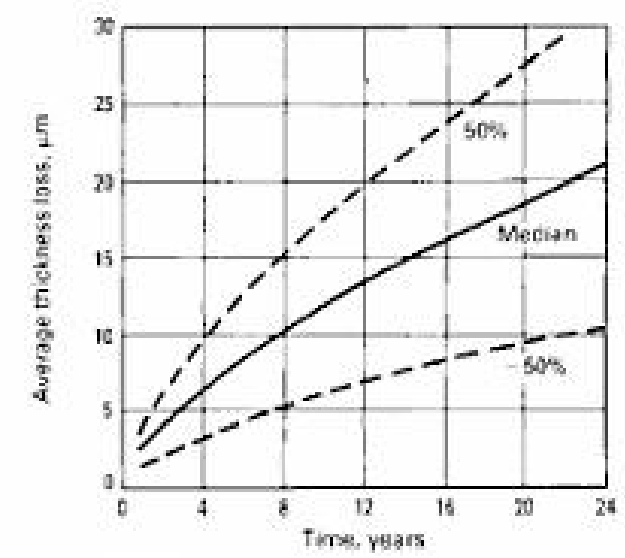
3.2 Copper Corrosion due to Atmosphere, Acid, and Oxygen

Several comprehensive studies that have been conducted over a 20 year period have concluded that copper is a suitable material for atmospheric exposure. Table 3.2.1 (as adapted from, "Copper and Copper Alloys") below shows the corrosion loss of common copper alloys as sample thickness (μm) per year when exposed to atmospheric conditions.

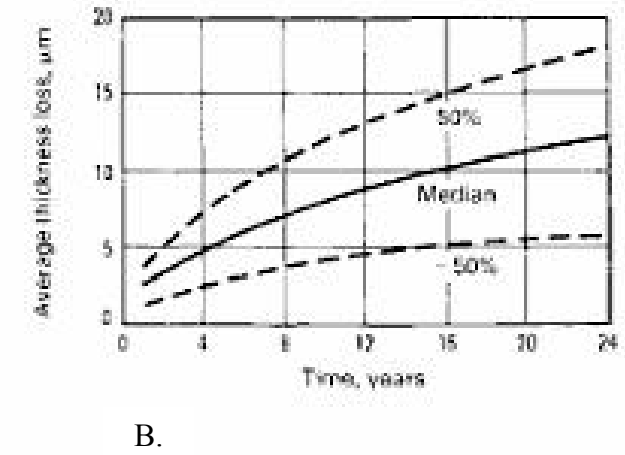
Table 3.2.1:Atmospheric Corrosion of Selected Copper Alloy [5]

Atmospheric Corrosion of Selected Copper Alloys vs. Location						
	Altoona, PA	New York, NY	Key West, FL	La Jolla, CA	State College, PA	Phoenix, AZ
Alloy	µm/yr	µm/yr	µm/yr	µm/yr	µm/yr	µm/yr
C11000	1.40	1.38	0.56	1.27	0.43	0.13
C12000	1.30	1.22	0.51	1.42	0.36	0.08
C23000	1.88	1.88	0.56	0.33	0.46	0.10
C26000	3.05	2.41	0.20	0.15	0.46	0.10
C52100	2.24	2.54	0.71	2.31	0.33	0.13
C61000	1.63	1.60	0.10	0.15	0.25	0.51
C65500	1.65	1.73	-	1.38	0.51	0.15
C44200	2.13	2.51	-	0.33	0.53	0.10
70-Cu-29Ni-Sn	2.64	2.13	0.28	0.36	0.48	0.10

As mentioned earlier, an exposed copper surface forms a protective patina consisting of Cu_2O that increases the resistivity to corrosion. Copper exposed to a marine environment can often form an additional layer of copper chloride or copper carbonate with a deeper layer of cuprous oxide. The formation of these layers is visible in the different colors they produce. Cuprous oxide has a distinct, red color while copper carbonate and copper chloride have a distinct, green color. While the rate of corrosion of copper varies from marine to industrial to a rural environment, the rate does decrease as the protective patina/oxide forms. Figures 3.2.1A,B show the average thickness loss as a function of time for varying copper alloys.



A.



B.

Figure 3.2.1 A, B: Copper Corrosion Rates shown as Thickness loss vs. Time [5]

Figure A is shown for copper, silicon bronze, and phosphor bronze. Figure B is shown for brass, aluminum bronze, nickel silver, and copper nickel. The median rate loss of thickness is shown as a solid line in the middle of each graph. The two dashed lines located above and below the median line was a variance in thickness loss by as much as 50% due to environmental differences between the samples. While copper does resist atmospheric corrosion, several factors can cause accelerated corrosion. Those factors are high humidity, high temperature (either ambient or solar), proximity to the ocean, and presence of pollutants which may cause the formation of an acid.

Copper is widely used in applications involving acid. There is a fairly large difference between the acids that affect copper and those that do not. Acids which are non-oxidizing such as phosphoric acid (H_3PO_4) and hydrochloric acid (HCL) do not react

with copper so long as the amounts of air and ferric ions are low. Given the amount of aeration in the acid, the corrosion rate of copper nickel alloys (in HCL acid at 25˚C (75˚F)) can range from 0.004 to 7.6 mm/yr. High oxidizing acids such as nitric acid (HNO_3) should not be used around copper as the rate of corrosion can reach 240 mm/yr. However, with any acid the rate of corrosion of copper can be varied by changing the concentration of the acid, temperature, and aeration levels, as shown in Figure 3.2.2 below [5].

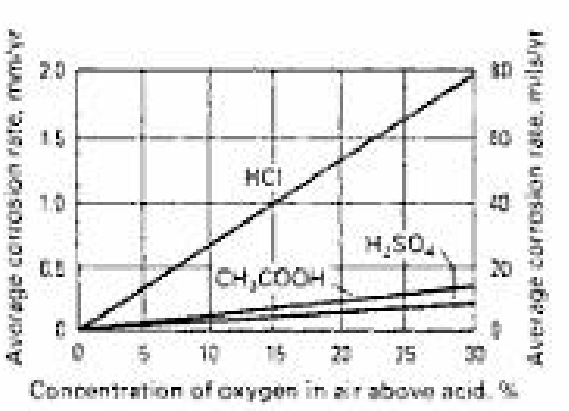


Figure 3.2.2: Corrosion Rate of Copper (mm/yr) vs. Amount of Oxygen in Reacting Acid [5]

Unlike the presence of oxygen in acid which increases the rate of corrosion dissolved oxygen in the atmosphere and water prevents corrosion as it promotes the formation of a brown and green hued copper oxide. The higher the temperature the faster the production of oxide occurs and the result is mainly a black copper oxide. Unlike oxides of iron, copper oxides form a protective barrier covering the metal and preventing the formation of further oxidation. When introduced to hydrogen gas flow the black oxide can be reduced back to pure copper leaving a shiny patina [10].

3.3 Sintering

According to many different sources sintering is the process of heating a powdered metal or ceramic to just below its melting point causing grain growth among the particles. The process is often used in applications where different alloys or grades of materials are being used, for example brake pads on a car or filters used in purification of oil, fuel, or air. One advantage to sintering is that the process leaves a porous surface which can be good for lubrication or diffusion. In general, the process of sintering is one normally reserved for that of iron or steel parts. However, in certain high conductivity applications copper is sintered [6].

In the case of this experiment solid copper wire alloyed with niobium and tin will be compacted into a solid copper conduit and then sintered. In general sintering takes

place in three different phases. The first phase consists of neck growth between the particles but powdered particles retain their shape, in the second phase most of the densification takes place and the individual particles begin to lose their shape and diffuse into one another as the pores become rounded and grain growth occurs, in the third phase isolated pores shrink and the densification proceeds at a lower rate. During sintering, movement of particles is generally attributed to one of four types of mechanisms: 1. diffusional flow, 2. evaporative/condensation, 3. viscous flow, 4. plastic flow.

During sintering several different factors play into the quality and density of the final product. The pressure and temperature the powder was compacted at initially has an effect on the densification of the final product. In general most powder compacting takes place as cold compaction, in which the powder is placed in closed dies and punches on top and bottom are used to apply the desired force. Typically, compacted densities are 80-90% of the density of the material [5].

Activated sintering is a process in which the activation energy required for diffusion is lowered thereby accelerating the sintering process. Advantages of activated sintering are lowered sintering temperatures and shorter sintering times. Activated sintering can also yield added properties such as higher strength and better conductivity. Several different methods of activated sintering include adding physical or chemical treatments to the powder or adding a reactive gas to the sintering process. Interestingly enough, activated sintering has been found to take place in copper samples containing a thin layer of copper oxide on the particle surface. The reason is that copper oxide is partly soluble in the copper matrix. This causes the oxygen from the oxide to diffuse into the copper leaving behind highly active copper surfaces that can sinter more efficiently. However, the effect of the oxide layer can vary greatly as thicker layers of oxide contain too many oxide to oxide reactions and can inhibit the activation effects. Ideally for a reaction to benefit from a layer of oxide the thickness needs to be in the range of 40 to 60 nm [5]. The improved properties can be found in Table 3.3.1.

Table 3.3.1: Effect of Copper Oxide Thickness on Tensile Strength [5]

Thickness of oxide films on powder, nm	Tensile strength of sintered compact(a) MPa	ksi
Coarse copper powder		
0	29	4.2
40	51	7.4
80	38	5.5
120	21.5	3.1
160	15.7	2.2
200	7.8	1.1
Fine copper powder		
0	120	17.4
20	130	18.8
60	143	20.7
100	137	19.8
140	129	18.7
180	122	17.7
220	114	16.5

(a) Pressed at 414 MPa (30 tsi), sintered at 600 °C (1110 °F) for ½ h in H_2. Source: Ref 13

The CS cable used in this report is made of copper, tin, and niobium. In order for the copper and tin to alloy liquid phase sintering occurs. Liquid phase sintering is the process in which temperatures are lower than the melting point of the copper (1083°C, high melting point constituent) but higher than the melting point of the tin (231.9°C, low melting point constituent). As noted earlier, as densification occurs and the expansion of the pores takes place, the now liquid tin is free to move throughout the copper matrix. When cooled the tin is locked inside the copper and niobium thus forming the copper, tin, and niobium alloy.

3.4 Chromium and Sintering

Once the basic cable has been manufactured through the drawing process described in Chapter II, the cable is plated with chromium and wrapped in a foil insulator before being sent to the customer where the copper (or other metal) sleeve is inserted over the cable and compacted. Before the sleeve can be inserted over the cable the insulation foil must be removed. The cable will be constructed in long sections; however, because continuous cable is needed in order to construct the CS magnet these long sections will have to be spliced together.

The chromium is in place to prevent the wires from sintering together and causing a disturbance in the magnetic field. This is only applicable in the lengths of the cable where no joints will be found. Chromium has a much higher melting point than the sintering temperatures reached by the treatment. On average, chromium melts at 1907 ˚C while the temperatures seen during treatment are in the range of 650 ˚C. This allows the

diffusion of the tin throughout the copper-niobium wire without the copper melting into the neighboring wires. At the joints, however, the desired effect is to have the copper strands melt together as much as possible to form a uniform cable that has as low of an impedance as possible. To do this the chromium must be removed from the joint utilizing an ultrasonic acid bath. [7][8].

3.5 Methodology

The CS Cable is an integral part of the ITER fusion reactor. As with any superconducting wire the key to success lies in its ability to conduct current with no resistance. In order to introduce as few flaws as possible the CS cable will be produced in lengths reaching 910 meters, however splices will need to be made. The concern with the splices is that cable will sit exposed to the elements for an undetermined amount of time before the splice will be performed.

For a quality splice to be made a series of steps will need to be performed. The first involves the removal of a chromium coating found on the wire. The second step involves interlacing the strands in a staggered pattern followed by the insertion of the cable into a copper sleeve. Once inside the sleeve the cable splice will be compacted and then sintered. The purpose of this project is to re-create that process and attempt to quantify any changes to the quality of the sintering from the CS cables being exposed to the elements.

The time frame that the CS cables could be exposed to the elements could be years or a few months. In order to best replicate the possible damage done to cable from the environment a series of ovens were setup to expedite the effects of the environment. Each oven was set at a different temperature and contained a jar that would keep the cable samples at constant humidity.

The samples were prepared in a manner similar to how the splices would be performed in the field during the construction of the reactor and tested in order to determine the quality of the sintering.

Testing the samples consisted of a shear test in which the mechanical strength of the sintering between the copper wires and the copper sleeve was the focus. The idea being that samples with different soaking temperatures would require a different amount of force to separate from the copper sleeve. Using this ideology samples were constructed and the experimentation began.

Chapter IV

SAMPLE PREPERATION

4.1 Thin Wall Sample Preparation:

Five lengths of CS Super Conducting cable were cut from a larger roll of cable and given labels “A” through “E”. Each bar then had the chrome coating covering the wires removed by an ultrasonic acid bath.

To remove the chrome from the copper wire an eight step procedure was developed. A special tank was built in which eight PVC pipes were partially submerged in a larger tank containing water. The larger tank was then hooked to an ultrasonic cleaner that would send ultrasonic waves through the water and into the PVC pipes. Figure 4.1.1 is a photo of this tank. The PVC pipes were then filled with different liquids required for the chrome removal process. To start the process, nitrogen gas was purged through the center tube of the conductor. This was done to keep the copper from reacting with the Hydrochloric acid (HCL). Next, the strand was removed from the acid and rinsed in the next pipe containing tap water. The strand was then moved to the third pipe containing $NaHCO_3$ neutralizer. The next four pipes contained distilled water and the strand was rinsed for a period of time in each of them. The last pipe contained methanol and was used to displace any water that may have remained in the strand. Lastly, the strand was air dried for thirty minutes and visually inspected for the removal of chrome. Figures 4.1.1-4.1.4 are photos of different steps throughout the chrome removal process.



Figure 4.1.1: Ultrasonic Tank with Eight PVC Pipes



Figure 4.1.2: Nitrogen Purge Placed Through Center of the Strand



Figure 4.1.3: Strand Lowered into HCL with Nitrogen Purge

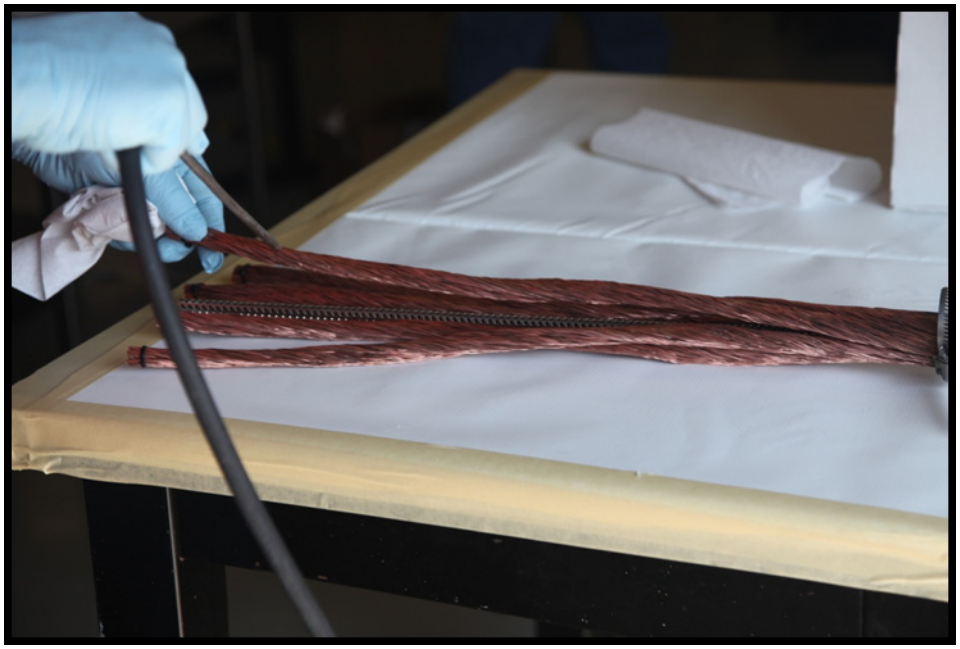


Figure 4.1.4: Drying and Visual Inspection of Chrome Removed from Strand

After each bar had been inspected and determined to be free of chromium a copper sleeve having a thickness of approximately 1.25 mm (.05 in) was placed over the wires and compacted to final diameter of approximately 32 mm (1.25 in). Two different methods of compaction were used to prepare compacted cylindrical bars of lengths ranging from 184 mm (7.25 in) to 317.5 mm (12.5 in).

The first method of compaction was completed utilizing a Val Power hydraulic crimping machine. This can be seen in Figure 4.1.5.



Figure 4.1.5: Val Power Hydraulic Crimper

This method of compaction was used on bars “A” and “B” and produced an unpredictable fold in the sample due to the buckling of the copper sleeve under compaction. The unpredictable fold was seen as a possible source of damage to the CS cable and as a result a second method of compaction was developed. The second method of compaction was then developed and the remaining three bars were compacted using the press and die which can be seen in Figures 4.1.6 and 4.1.7.



Figure 4.1.6: Press



Figure 4.1.7: Die

In order to compact the copper sleeve utilizing the press and die, a two step method was developed. The first step pressed the copper sleeve into an oval using two clamshells. As an addition to the clamshells two pieces of welding wire were laid on the two halves of the clamshell. This was to initiate a fold in the copper sleeve during compaction that would allow the buckling of the copper to react in a predictable manor. The second step involved placing the sleeve in the die seen in Figure 4.1.7 and compacting it until the final diameter of approximately 32 mm (1.25 in) was reached. The clamshell dies are shown in Figure 4.1.8. Disk samples of heights 12.7 mm (0.5 in) and 19 mm (0.75 in) were cut from these bars using the electro discharge machining (EDM) technique. Figure 4.1.9 shows examples of disk samples.

.



Figure 4.1.8: Clamshell with Welding Wire

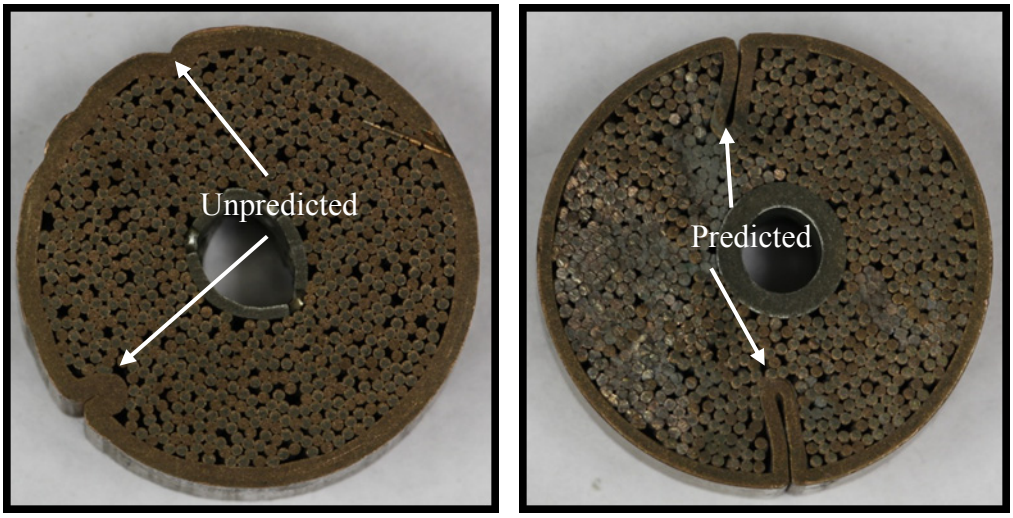


Figure 4.1.9: Predictable vs. Unpredictable Folds

In addition to different heights each section was given a numerical and letter designation to represent which bar the sample came from and from which end. The numbering began at the front of the sample and increased in the direction of compaction. This is demonstrated in Figure 4.1.10.

Due to the differing lengths of the original bars, different numbers of ¾" (19.05 mm) and ½" (12.7 mm) samples were obtained from the bars. Table 4.1.1 shows a summary of the original length of the bars as well as the number of bars obtained from each bars, compaction method, and the number of disk samples from each bar. Figure 4.1.11 shows the two types of thin wall disk samples.

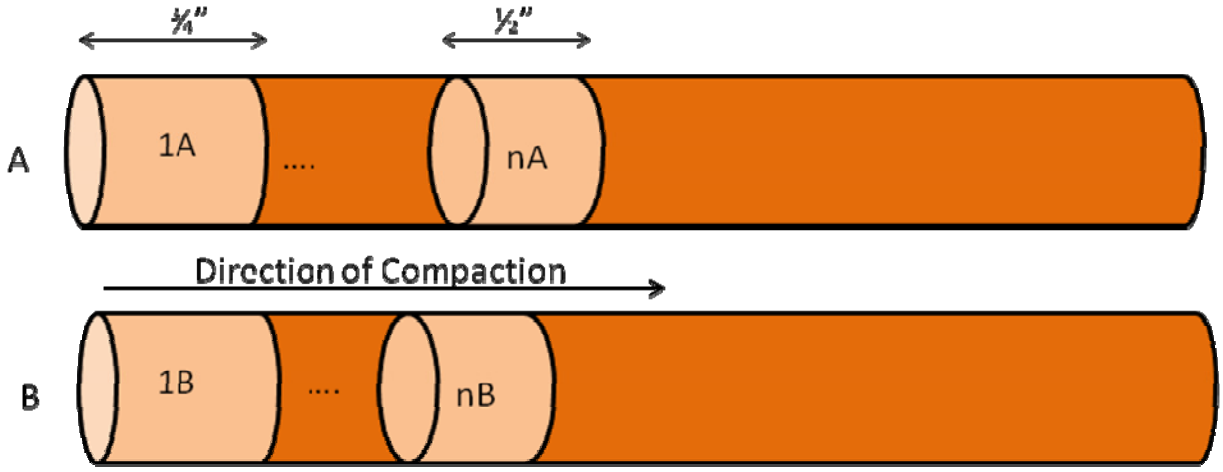


Figure 4.1.10: Marking of the Samples

Table 4.1.1: Sample Summary

Bars	Length (in)	Number of Disk Samples	Compaction Method	Qty: ¾"	Qty: ½"
A	7.25	11	Hydraulic	6	5
B	12.5	18	Hydraulic	9	9
C	10.54	16	Press and Die	8	8
D	11	16	Press and Die	8	8
E	12	19	Press and Die	9	10

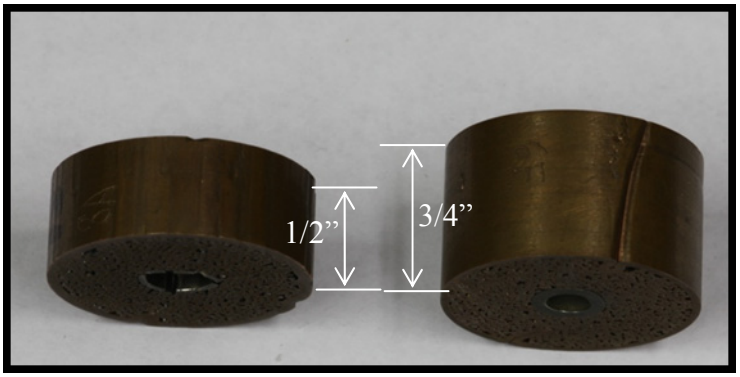


Figure 4.1.11: Samples after Cutting

4.2 Thick Wall Sample Preparation

In addition to the thin walled samples prepared in section 4.1 a small batch of samples were made using a thicker copper sleeve. The sleeve used in the initial sample preparation had a thickness of 1.25 mm (0.05in) while the sleeve used for the new samples had a thickness of approximately 5 mm (0.2in).

The new sample was created from a 483 mm (19 in) piece of the same CS cable used to prepare the thin walled samples. The cable had the foil removed and was acid washed in an ultrasonic bath to remove the chromium just as before. Once a visual inspection was complete and satisfaction was reached that all the chrome had been removed the cable was inserted into the copper sleeve and compacted.

Due to the thickness of the new sleeve the same final outer diameter of the thin walled samples was not going to be possible. Instead, the focus was on achieving the same inside diameter since this was the area being physically tested.

Initially the outer diameter of the sleeve was measured to be 48.25 mm (1.89 in) and had an inner diameter of 37.85 mm (1.49 in). Because the inner diameter would not be able to be measured, once the compaction process was started, a math formula was used based on the area of the sleeve and the principal of conservation of mass. The formula used for the calculation can be seen below.

$$I.D. = \sqrt{O.D.^2 - \frac{4 * V}{\pi * L}}$$

Compaction took place using the Val Power hydraulic crimper mentioned above in Figure 4.1. Small increments of compaction were done and the O.D. was measured along with the length of the sample. The measurements were then input into the above equation to give the final inside diameter. This process was repeated until a final inside diameter of 29.6 mm (1.16 in) was reached.

Once the sample had been compacted it was sent to an outside machine shop to be cut utilizing the same EDM technology used to cut the first set of samples. The samples were cut in 12.7 mm (0.5 in) lengths and were given identification marks starting with the letter "x" and preceded by a number designating the position the sample was taken from the rod. A total of 38 samples resulted from Bar X. A picture of one such sample is shown in Figure 4.2.1 below.

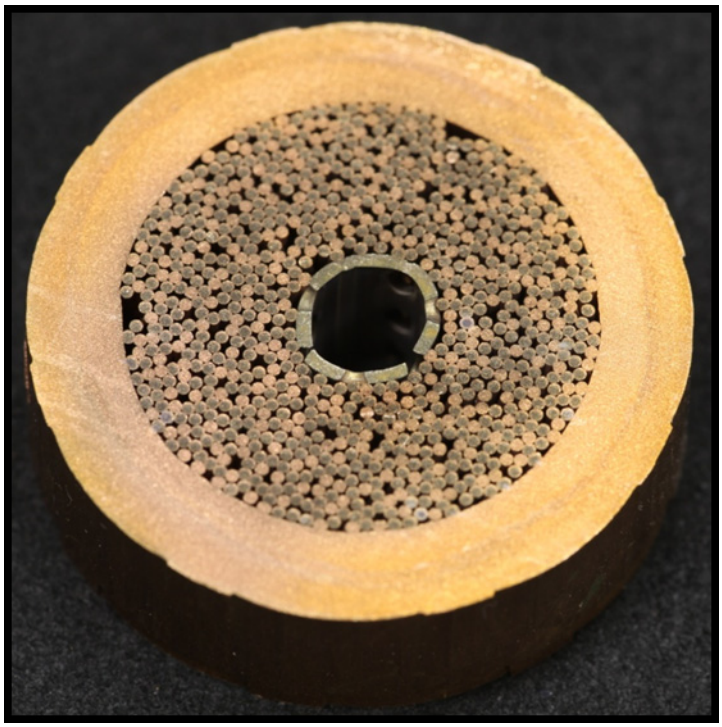


Figure 4.2.1: Bar X Thick Wall Sample After Compaction and EDM

The purpose of creating Bar X was an attempt at creating samples with no folds. As seen with Bars A and B un-predictable folds were created when using the hydraulic crimper. This problem was alleviated by using the press and die method, which created the folds in a predictable manner as seen in Bars C-E. By using a thick wall sleeve the sleeve was unable to fold inward on itself and instead was forced to disperse leaving a relatively uniform wall around the cable. The lack of folds can be best seen in Figure 4.2.1 above.

4.3 Sample Soaking

The purpose of exposing the samples to moisture was to simulate the conditions the actual CS wire may see in the field. The ultimate goal being to find what happens to the quality of the sintering between the strands and the copper sleeve once the wire has been exposed to moisture for a period of a year. In order to accelerate the effect of moisture exposure on the samples, the moisture soaking was done at elevated temperature under constant humidity environments. Because two sets of samples were created two soaking cycles had to be conducted.

The first soaking cycle was conducted for the thin walled disk samples. The soaking periods were divided into three time frames, one week, two weeks, and one month. In addition each time frame had three temperatures at which samples were soaked; 60˚C, 80˚C, and 100˚C. This made for a total of nine different soaking conditions all kept at a constant humidity of 100%.

To ensure the disk samples would be kept at 100% humidity, the samples were placed in specially design glass jars. The jars were filled with water and the samples were placed on a shelf just above the water line. A sealing lid was then placed on the jar and an Omega HX-15 high temperature and relative humidity sensor was placed through the lid to record the temperature and humidity level inside the jar for the duration of the soaking. The jars were also equipped with a vent line that was vented into an adjacent bottle of water to ensure that the pressure inside the jar was maintained at atmospheric. The jars were then placed in scientific ovens calibrated to maintain constant temperature. The photograph of the setup for the soaking process is shown in Figure 4.3.1.

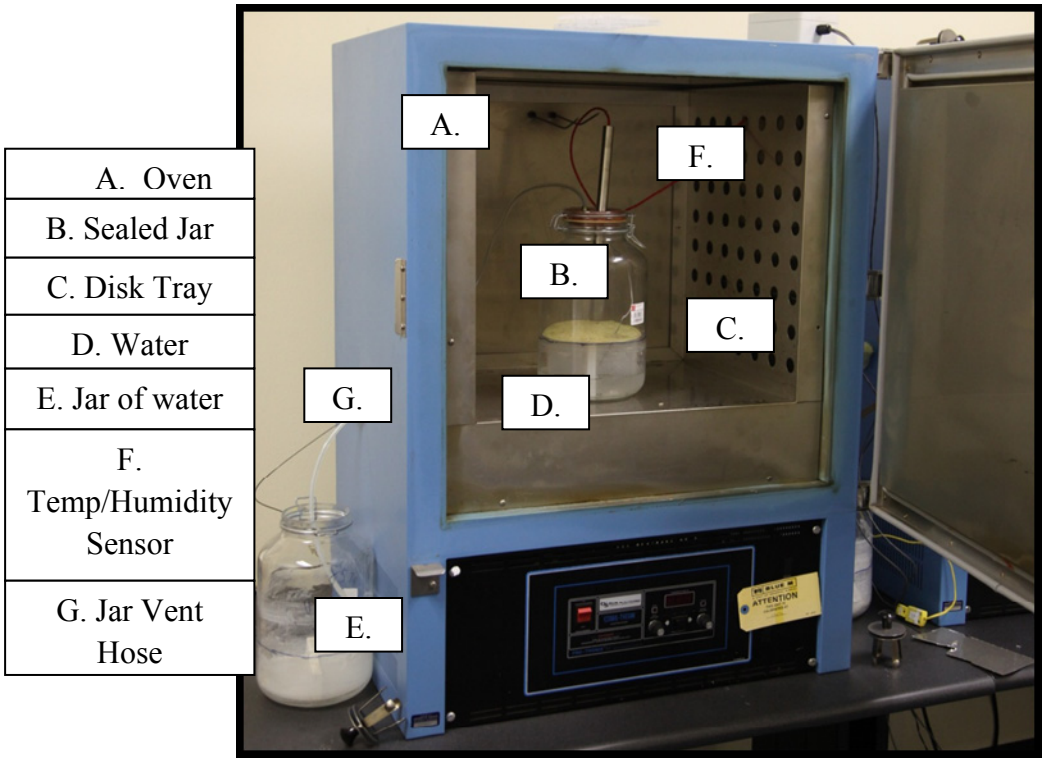


Figure 4.3.1: Soaking Setup

Each soaking time frame contained nine disk samples taken from different bars. A table of the soaking process including which samples were soaked in each time frame can be seen in Tables 4.3.1, 4.3.2, and 4.3.3.

Table 4.3.1: Sample Soaking 1 Week

60 Degrees	80 Degrees	100 Degrees
12c	8b	16e
15e	9c	12d
2c	13b	4e
11c	3e	16b
6d	7d	18b
9d	15d	5d

Table 4.3.2: Sample Soaking 2 Weeks

60 degrees	80 Degrees	100 degrees
17b	5e	15b
18e	2e	7b
2b	11e	13e
14b	11b	9e
10e	6b	4b
1e	16c	8e

Table 4.3.3: Sample Soaking 1 Month

60 Degrees	80 Degrees	100 Degrees
9a	7c	10c
5c	10a	14c
3a	11a	6a
6c	8c	1c
4a	4c	7a
2a	3c	13c

In addition to soaking several samples were kept un-soaked for comparison of data later in the testing.

The next soaking cycle was conducted for the thick walled samples. The cycles were conducted in the exact same manner as above with the notable exception of the amount of soaking cycles.

For the thick walled samples a decision was made to lessen the amount of variables going into the samples and only run two temperature ranges and two time frames. The second soaking cycle consisted of 28 disk samples being soaked, four left un-soaked and un-sintered, and six disk samples were un-soaked and sintered. Table 4.3.4 below is a breakdown of each disk sample was soaked.

Table 4.3.4: Thick Walled Sample Soaking Periods

Soaked/ Sintered					
80C		100C			
2 weeks	4 weeks	2 weeks	4 weeks	Un-soaked Sintered	Un-soaked Un-sintered
19x	12x	14x	32x	2x	35x
20x	27x	28x	1x	29x	36x
5x	21x	13x	34x	10x	37x
18x	9x	15x	31x	30x	38x
17x	24x	11x	16x	6x	
8x	23x	4x	22x	3x	
7x	33x	25x	26x		

During the soaking process of both the thin wall and thick wall samples temperature and humidity measurements were recorded. This was to ensure that the samples were indeed soaked at the desired temperature and humidity designated for the procedure. The temperature and humidity was simultaneously recorded using Omega HX15 temperature and humidity sensors capable of collecting data from - 40→180˚C and 0→100% relative humidity with outputs ranging from 4→20mA. A sample of these recordings is shown in Figures 4.3.2 and 4.3.3 below.

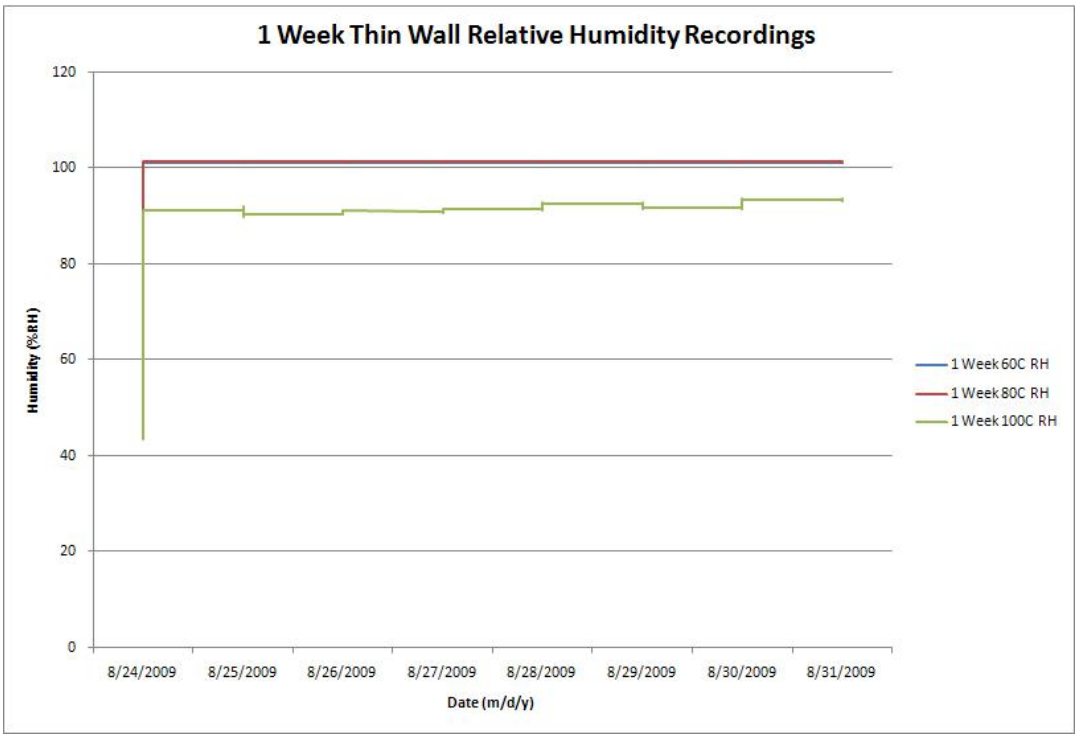


Figure 4.3.2: 1 Week Thin Wall Humidity Recordings Measured by Omega Sensors

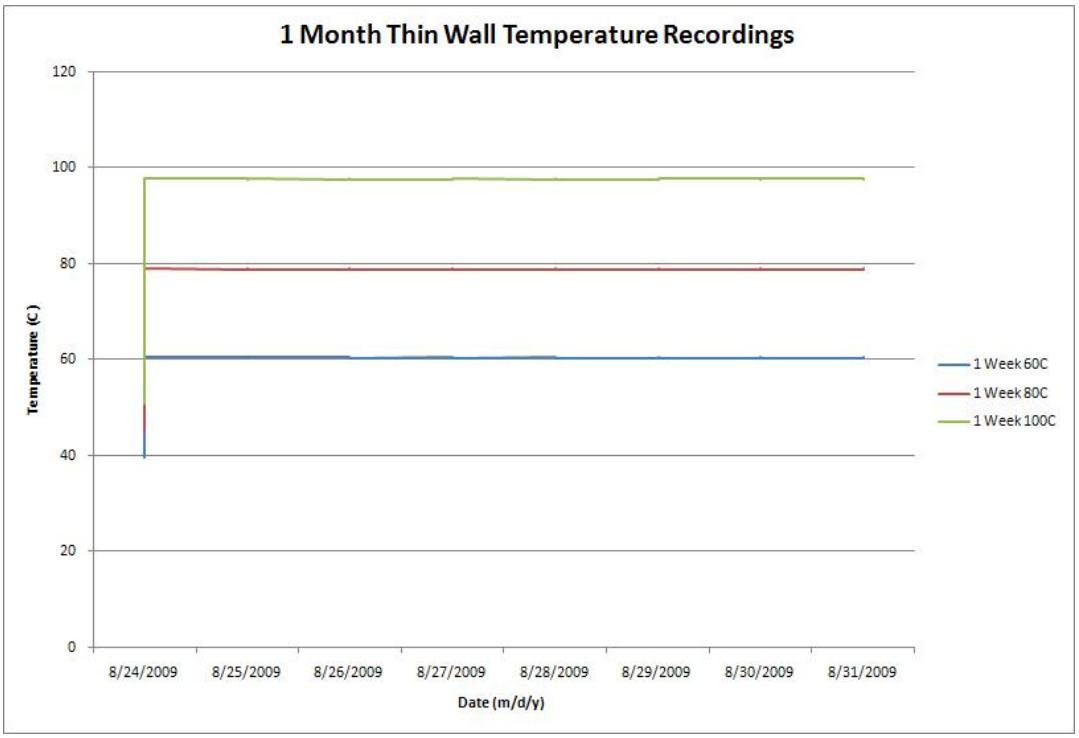


Figure 4.3.3: 1 Week Thin Wall Temperature Recordings Measured by Omega Sensors

During the soaking of the samples near 100˚C the jars on two of the time frames sprung leaks causing minor fluctuations in the humidity levels inside the jars. These levels can be found on the remaining graphs located in the appendix portion of this report.

In addition to soaking disk sample 16c was polished using a multistep process starting with 200 grit paper then continuing with 320, 400, 640, 800, and 2400 grits. Between each step the disk sample was visually inspected to ensure that a flat surface was being achieved and that the scratches from the previous step had been removed. After that a 9 micron polish was applied to a polishing pad and the sample was polished for approximately ten minutes.

Sample 16c was polished so that microscopic photos of the cables structure could be seen and photographed throughout the soaking process. Pictures of sample 16c before soaking can be seen in Figures 2.1.7 a-c on pages 24 and 25 earlier in this report. (Note: scale pictures may be found in appendix). After aging the only noticeable difference in the sample was color detected by visual inspection as seen in figures 4.3.4-4.3.7 below.

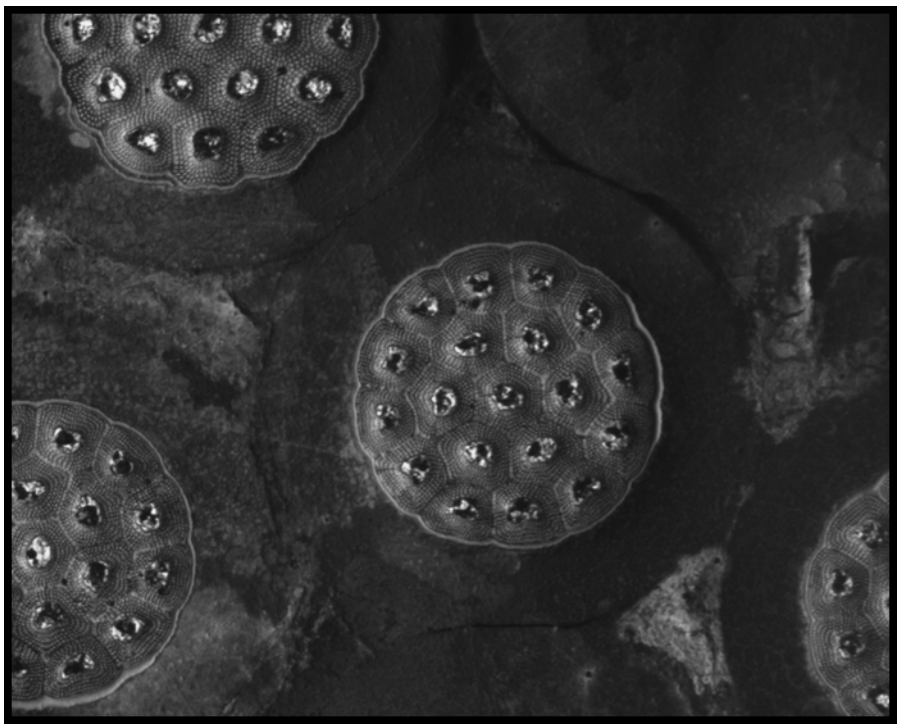


Figure 4.3.4: Sample 16c After Soaking 50x

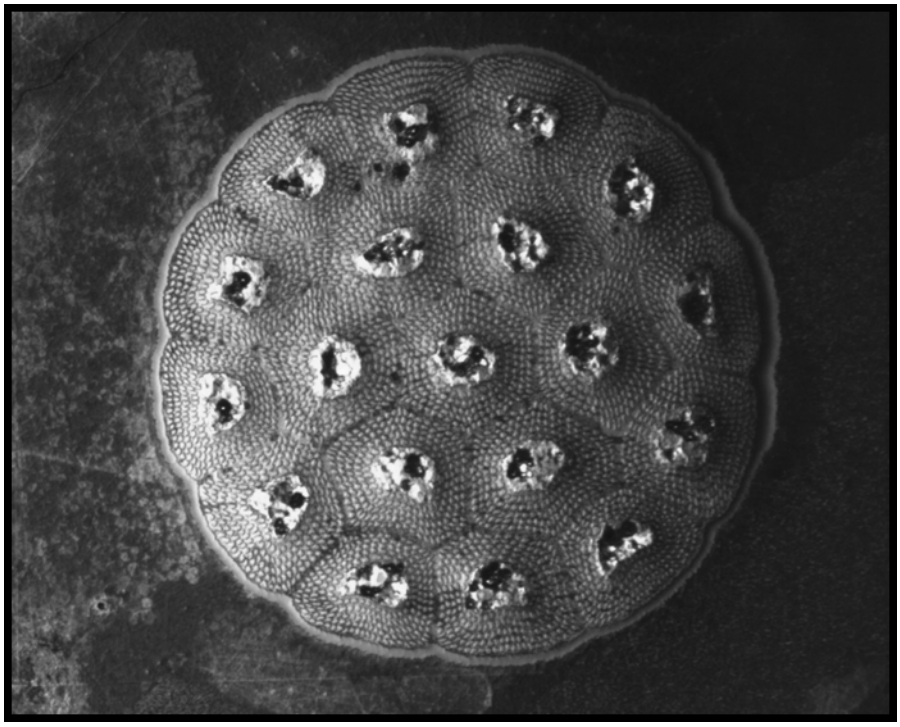


Figure 4.3.5: Sample 16c After Soaking 100x

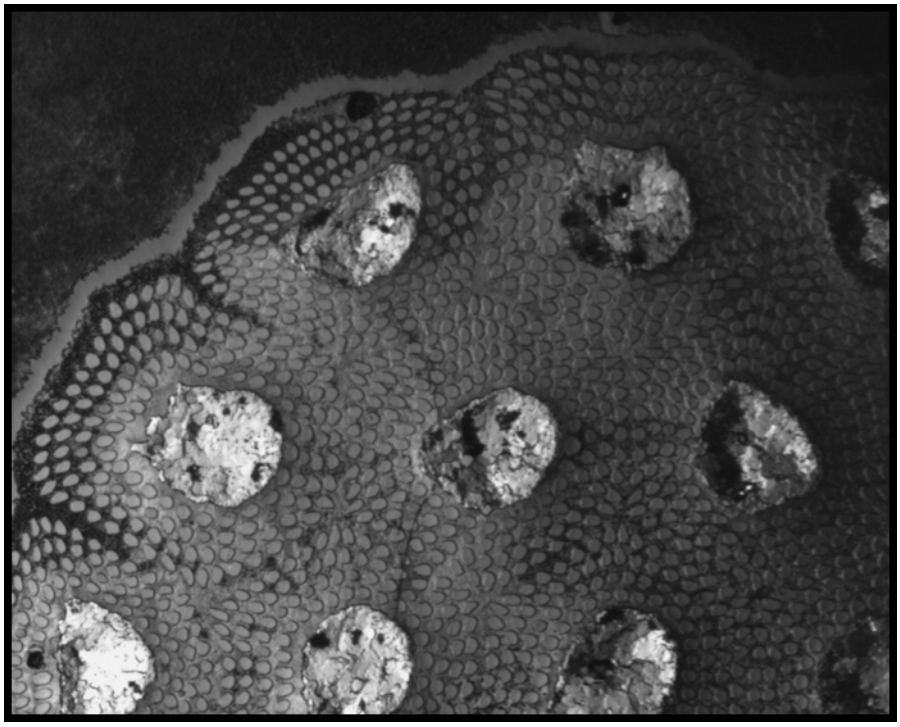


Figure 4.3.6: Sample 16c After Soaking 200x

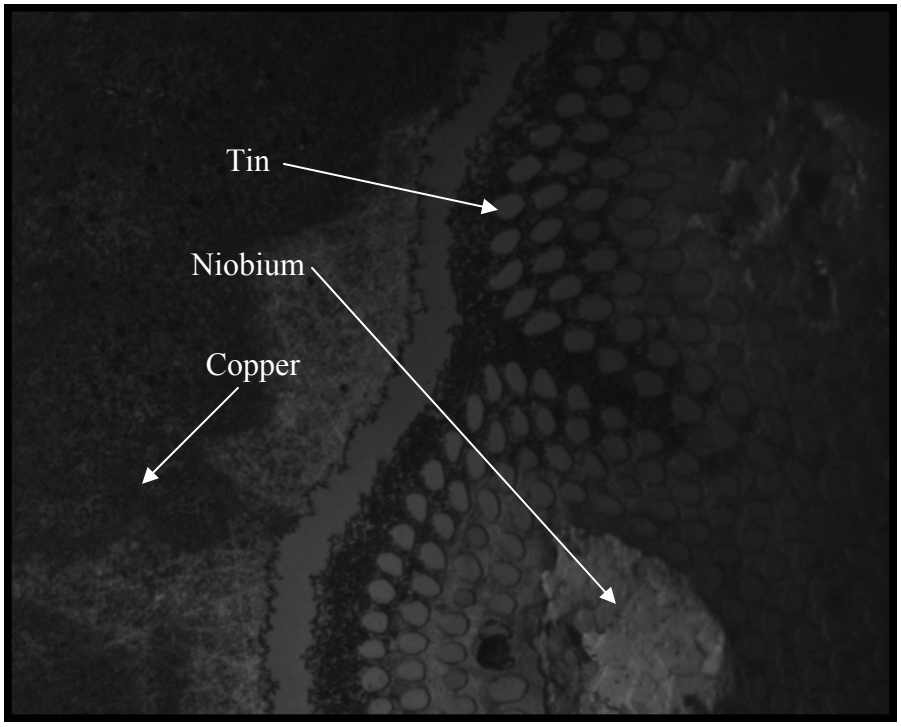


Figure 4.3.7: Sample 16c After Soaking 500x

Again, the change in color before and after soaking is demonstrated in 4.3.8 below.

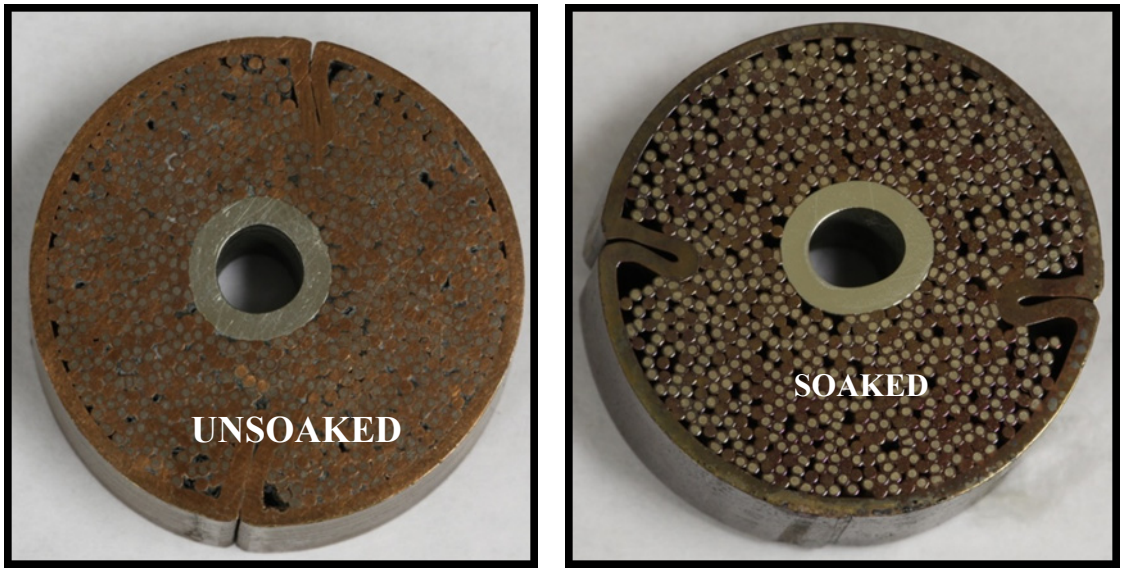


Figure 4.3.8: Visual Discoloration of Soaked Samples

The change in color is due to the oxidation of the copper. Two main types of oxidation occur during the soaking process. The red color is the formation of Cuprous oxide while copper carbonate and copper chloride have a distinct green color.

4.4 Sample Sintering

The sintering process for both the thin walled disk samples and the thick walled samples was very similar. The major difference between the two processes was that the thin walled samples were sintered in a tube furnace while the thick walled samples were sintered in a box furnace. Both sets of samples were placed in a retort that had argon flowing through them during the sintering process. A picture of this retort can be seen in Figure 4.4.1. The following section highlights the processes for each set of samples.

Sintering for the thin walled samples took place in a custom built pipe oven manufactured from stainless steel and capable of temperatures in excess of 650˚C. The samples were sintered using a precise temperature-time profile. A summary of this profile is given in Table 4.4.1.

Table 4.4.1: Thin Wall Sample Ramp Rate and Heat Cycles

Range (˚C)	Rate (˚/hr)	Time to Ramp (hr)	Hold Time (hr)
0-210		20	50
210-550	5	68	1
550-650	2	50	100



Figure 4.4.1: Thin Wall Sample Retort

During sintering the samples see very high temperatures and as such it is important that atmospheric air not be present in the oven. The presence of air can cause oxidation within the metal. Another consideration is that the samples may not be completely clean of oils and sediment that may catch fire during the sintering process. To ensure that the samples stayed in an inert environment a special retort was designed to place the samples in.

The retort was designed out of stainless steel and was 1092 mm (43 in) long by 38 mm (1.5 in) in diameter. Each end was fitted with a cap that once the samples were placed inside would be welded onto the retort. The end caps were welded into place to ensure an air tight environment for the samples. Each end cap was fitted with a compression fitting that would allow for the connection of inert argon gas to be run through the retort during sintering. This would ensure that any vapors released from the sintering process would be removed and not allowed to react with the samples. Pictures of the end caps with compression fitting can be seen in Figure 4.4.2.

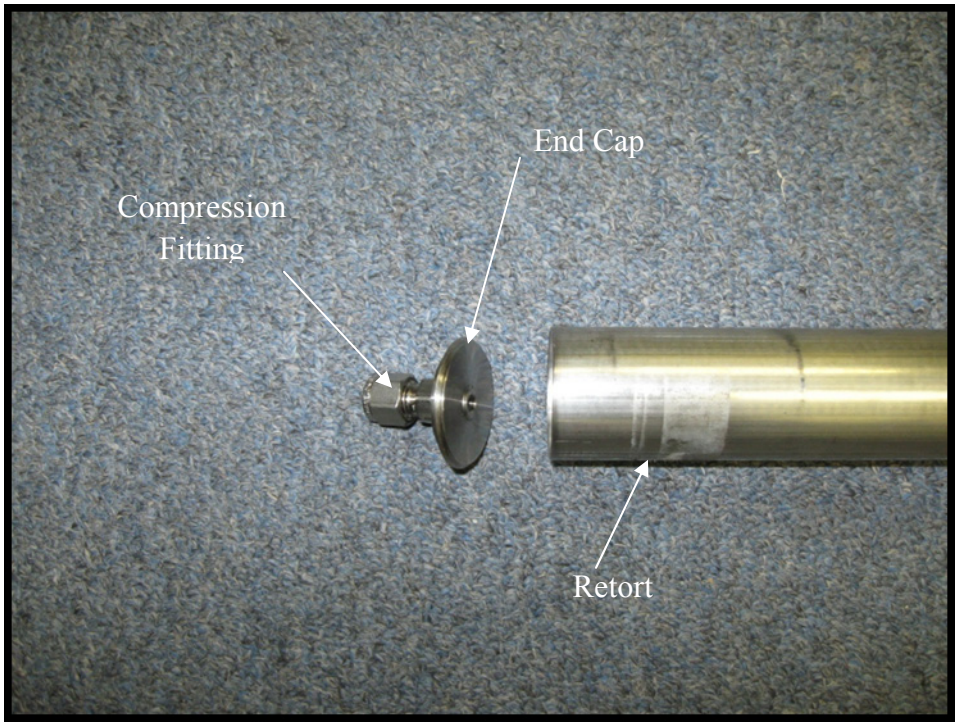


Figure 4.4.2: Thin Wall Retort End Cap and Compression Fitting

Precaution was taken so that the disk samples would not sinter to one another once placed in the retort. A stainless steel welding wire was bent into triangular clips and placed between each disk sample to prevent them from touching each other as they were placed in the retort. A picture of the clips can be seen in Figure 4.4.3 and a picture of the clips between each disk sample can be seen in Figure 4.4.4.



Figure 4.4.3: Stainless Clips

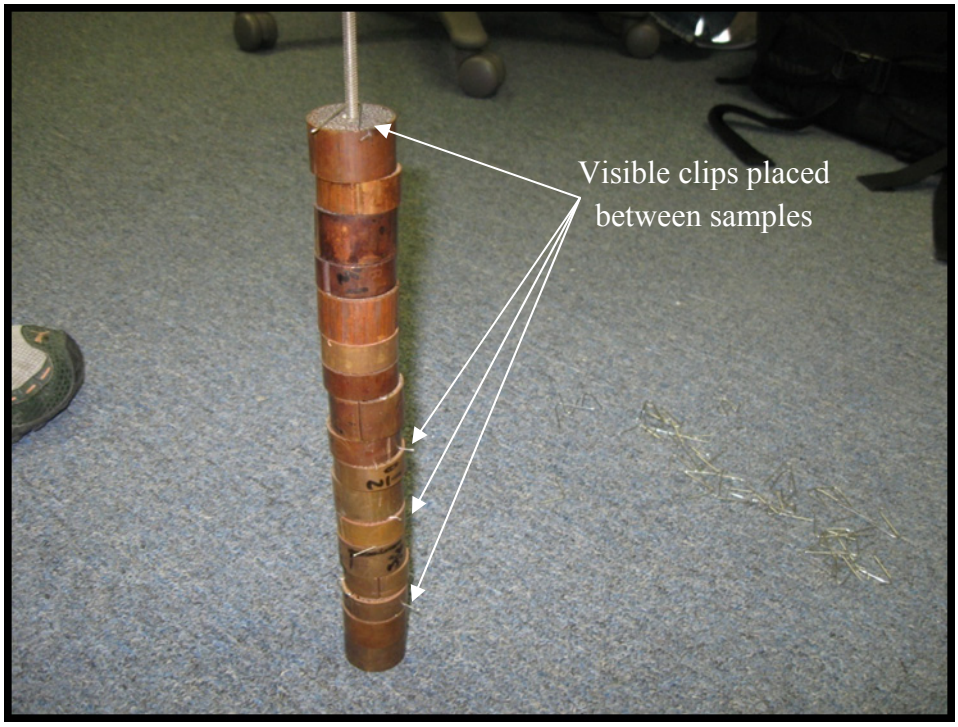


Figure 4.4.4: Clips Placed Between Samples

The disk samples were placed in the retort in a random fashion with the exception of the un-soaked disk samples which were placed at the beginning of the retort. The un-soaked thin walled disk samples were placed at the front of the retort to ensure that clean argon would be flowing over them and to ensure that they would not be exposed to any residue possibly coming from the soaked disk samples. Figure 4.4.5 shows the complete stack of disk samples before being placed in the retort.



Figure 4.4.5: Complete Stack of Thin Wall Disk Samples

Once the disk samples were placed in the retort the additional space left in the retort was accounted for by a spring (see Figure 4.4.6). The spring was placed in the end of the retort to ensure that the disk samples did not move and the only spaces between them was the one created by the clips.

Once the disk samples and spring had been placed inside the retort the end cap was then TIG welded onto the retort and the entire assembly was then placed inside the tube oven. As mentioned early a special tube oven was constructed for the sintering of these disk samples. A picture of the tube oven may be seen in Figure 4.4.7.



Figure 4.4.6: Spring

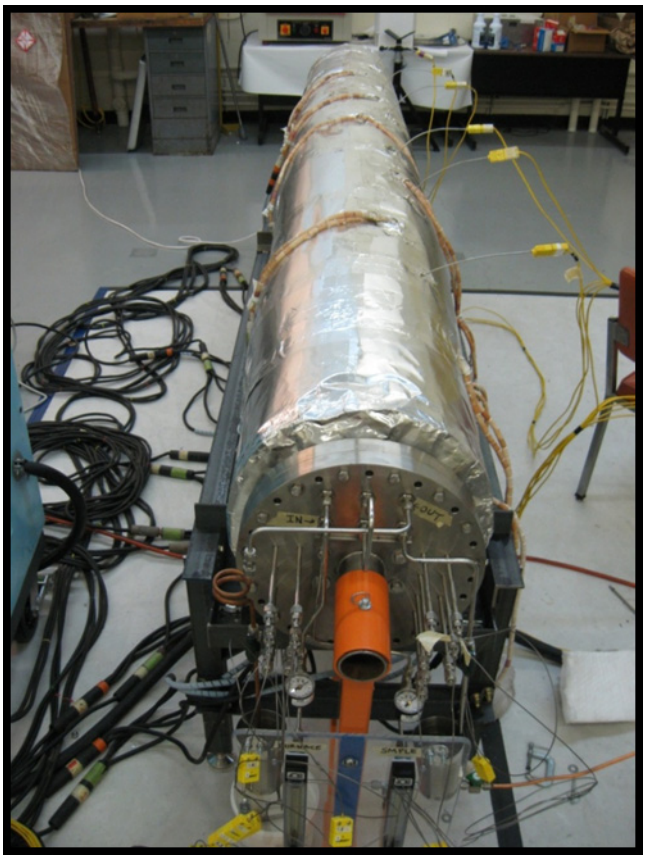


Figure 4.4.7: Stainless Tube Oven

The tube oven measures approximately 3.3 m (130 in) long by 336.5 mm (13.25 in) in outside flange diameter. To ensure proper heating of the disk samples the assembly was placed on a rack on the inside of the oven which can be seen in Figure 4.4.8.

The argon supply lines were then hooked to the retort with the inflow tube first making a complete pass through the oven and then hooking to the retort at the back of the oven. This was done to ensure that the argon was heated to the oven's temperature before being supplied to the disk samples. The argon return line was connected to the back of the retort at the front of the oven. A picture of this can be found in Figures 4.4.9 and 4.4.10. The inflow is highlighted by the green arrows and the outflow is highlighted by the red.

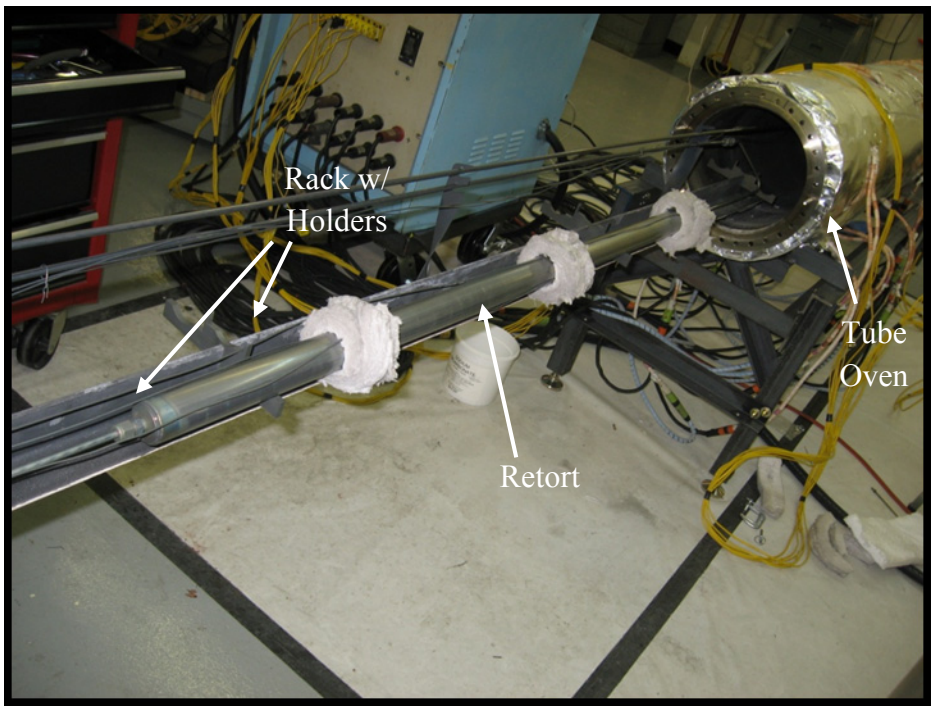


Figure 4.4.8: Retort on Rack

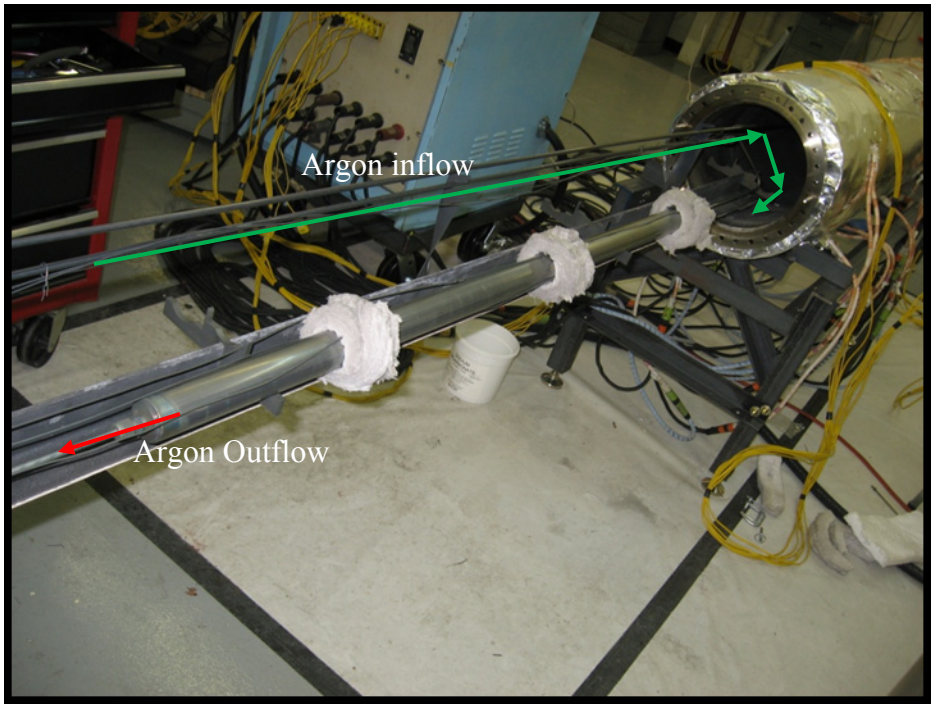


Figure 4.4.9: Argon Gas Flow to Retort

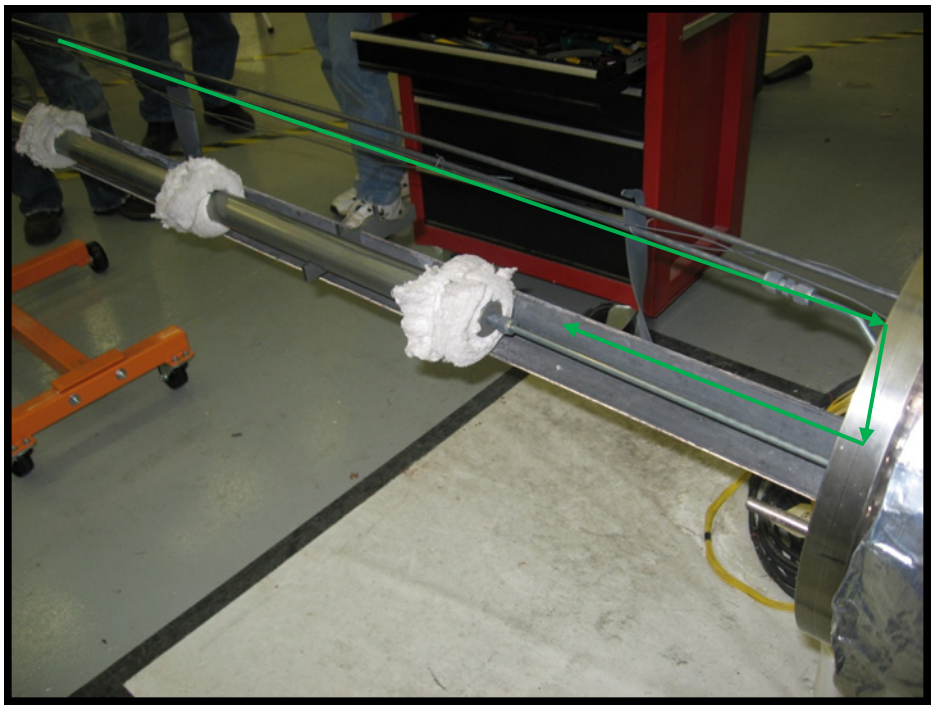


Figure 4.4.10: Argon Inflow

Once the assembly was connected and placed in the oven the sintering process began following the prescribed method as outlined in Table 4.4.1 earlier in Section 4.4 of this report.

The process for sintering the thick wall samples was very similar to the thin wall samples with the notable differences being the retort and the oven. The retort the samples were sintered in measured 628.65 mm (24.75 in) long by 47.63 mm (1.875 in) O.D. and can be seen in Figure 4.4.11



Figure 4.4.11 Thick Walled Sample Retort

Like the thin walled sample retort, it too was constructed of stainless steel and contained a compression fitting and end cap as shown in Figure 4.4.11.

The samples were placed in such a manner such that the un-soaked samples received the clean incoming flow of argon just as the thin walled samples had. Again in replicating the thin walled samples sintering process each sample had a metal spacer placed between it and the next sample; this was to ensure that the samples did not sinter together.

Unlike the thin walled samples the thick walled samples were sintered in a custom built carbon steel box oven also capable of temperatures in excess of 650˚C. The box oven measured 800 mm x 1530 mm x 304.8 mm (31.5” x 60.25” x 12”) (inside dimensions) and contained the same argon fittings and thermocouple fittings that the tube oven had. A picture of the box oven can be seen in Figure 4.4.12

Like the thin walled samples the same prescribed sintering process was used and can be seen in Table 4.4.1 above.

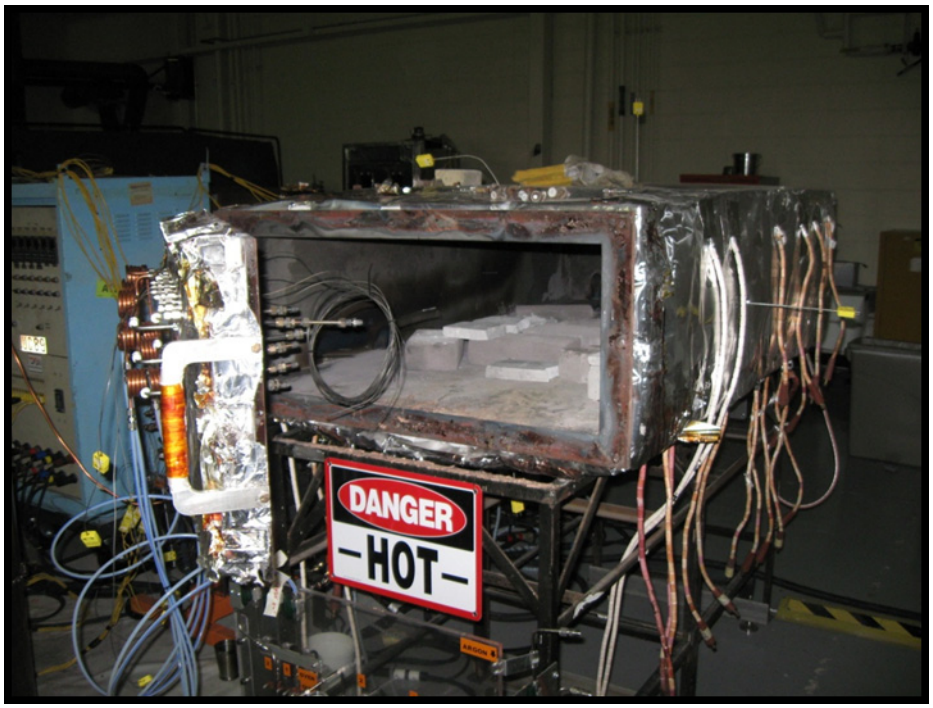


Figure 4.4.12: Box Oven Used for Sintering Thick Wall Samples

Chapter V

MECHANICAL TESTING

5.1 Thin Wall Testing Procedure

In order to push the coil pack from its copper sleeve a special press and die were machined from carbon steel. The press was designed such that the copper sleeve of the bar would sit on the inside edge of the die. In addition, the backside of the die was tapered so that the copper strands being pressed from the disk sample would not interfere with the inside of the die during the experiments. The press was machined with two notches on opposing faces such that the press would not interfere with the folds in the sleeve of the disk sample. Pictures of the press and die are shown in Figures 5.1.1 and 5.1.2.

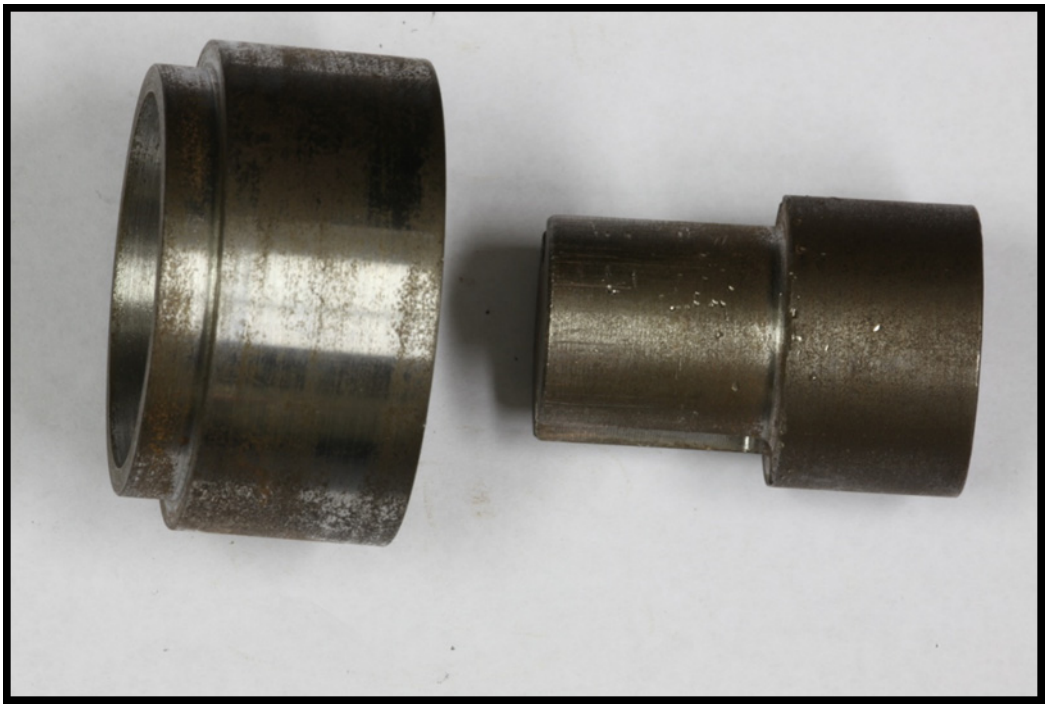


Figure 5.1.1: Press and Die

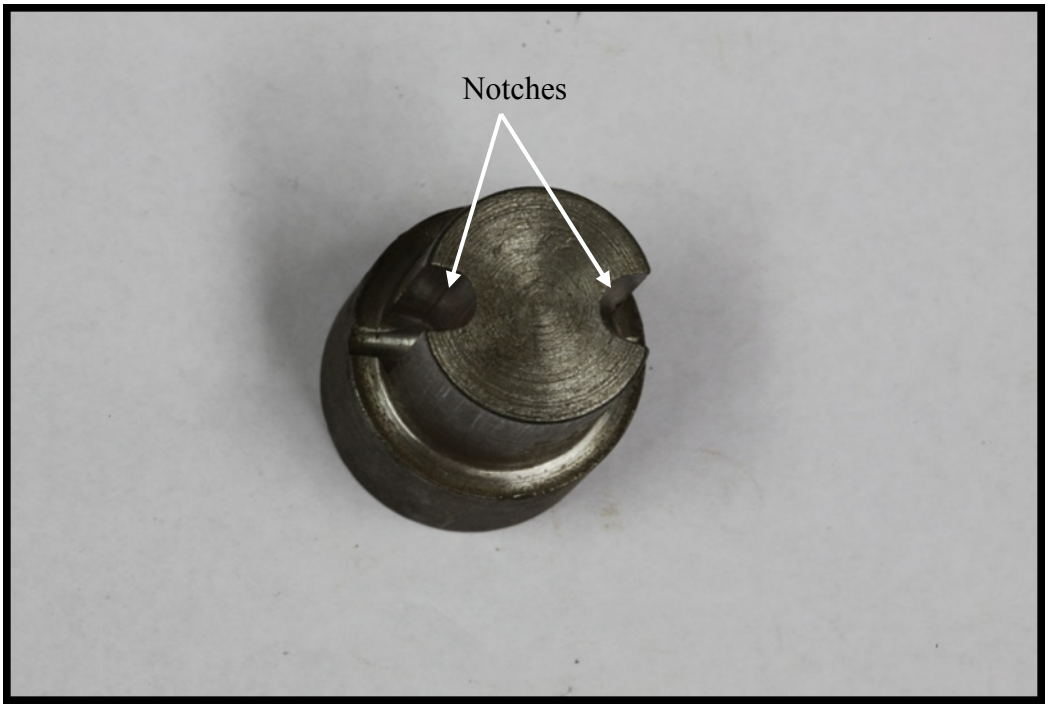


Figure 5.1.2: Notches Cut into Press

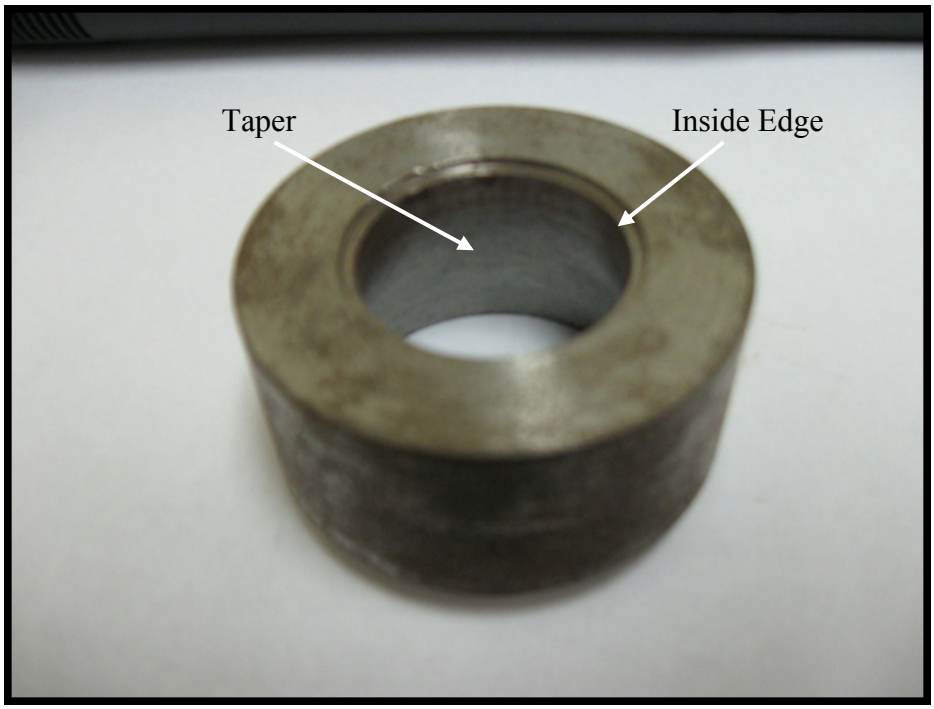


Figure 5.1.3: Die Inside Edge and Taper

Testing of the disk samples was conducted at the University of Tennessee utilizing a MTS machine fitted with a 50,000 lb load cell. To test, the die was placed in the hydraulic actuator of the MTS machine and the disk sample was then set on top of the die in the inside edge shown in Figure 5.1.3. The press was then set on top of the disk sample with careful attention to the alignment of the notches and folds. Once the setup was stacked inside the MTS machine the hydraulic actuator was then raised until the top of the press just touched the bottom of the load cell, Figures 5.1.4 and 5.1.5. The strain rate was held constant at 0.0095 mm/sec (0.00037 in/sec) and data was collected every half second during the experiments.

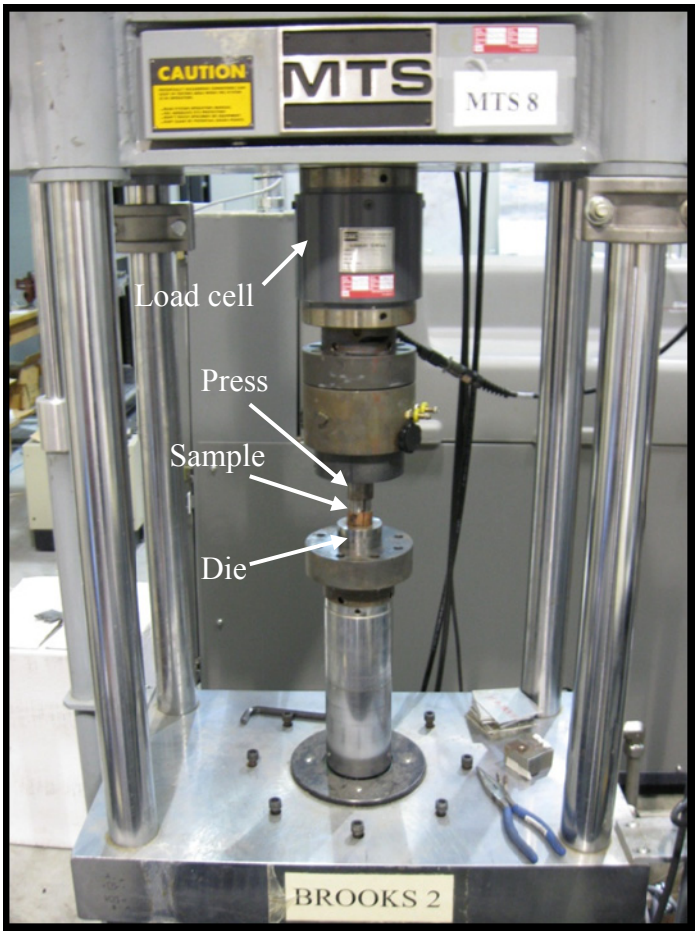


Figure 5.1.4: MTS Testing Setup

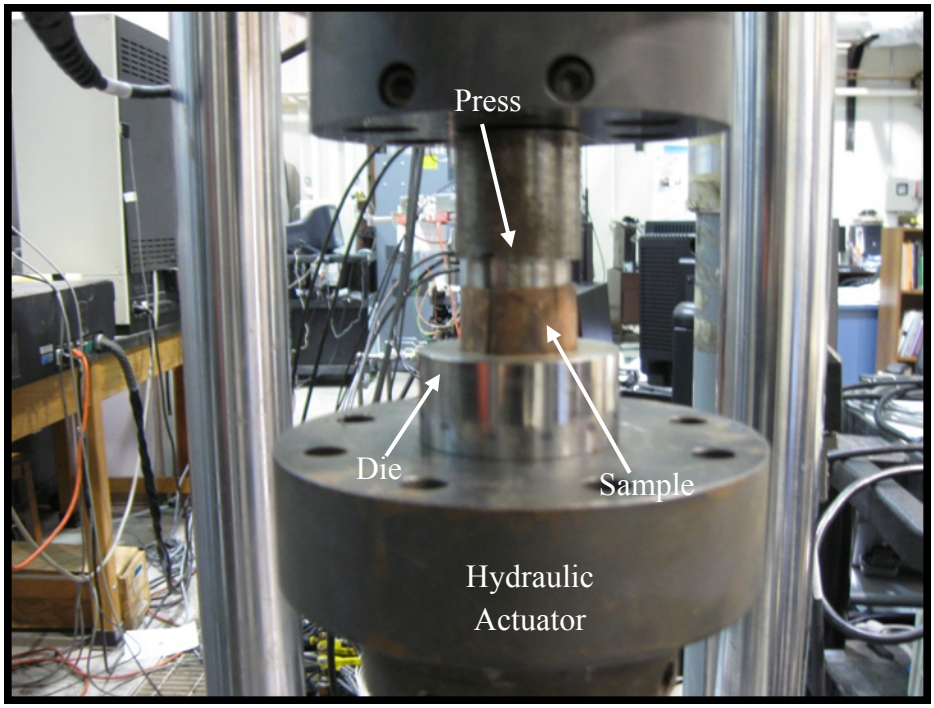


Figure 5.1.5: Close-up of Disk sample Testing Setup

A test run of a few thin walled disk samples was conducted to ensure that the testing procedures were accurate and after a few minor modifications to the press to reduce the overall diameter and deepen the notches, testing proceeded with a more of the thin walled samples. Once a few thin wall samples had been pressed a discrepancy was noticed in the data believed to have been caused by the bulging of the outer sleeve of the sample. This caused the fabrication of a collar which would be placed around the sample during pressing. This would ensure that the wall of the sample did not bulge. Results of this change are discussed in Chapter VI of this report. Pictures of the collar can be seen in Figure 5.1.6 and 5.1.7.



Figure 5.1.6: Rigid Clamping Collar for Thin Wall Samples

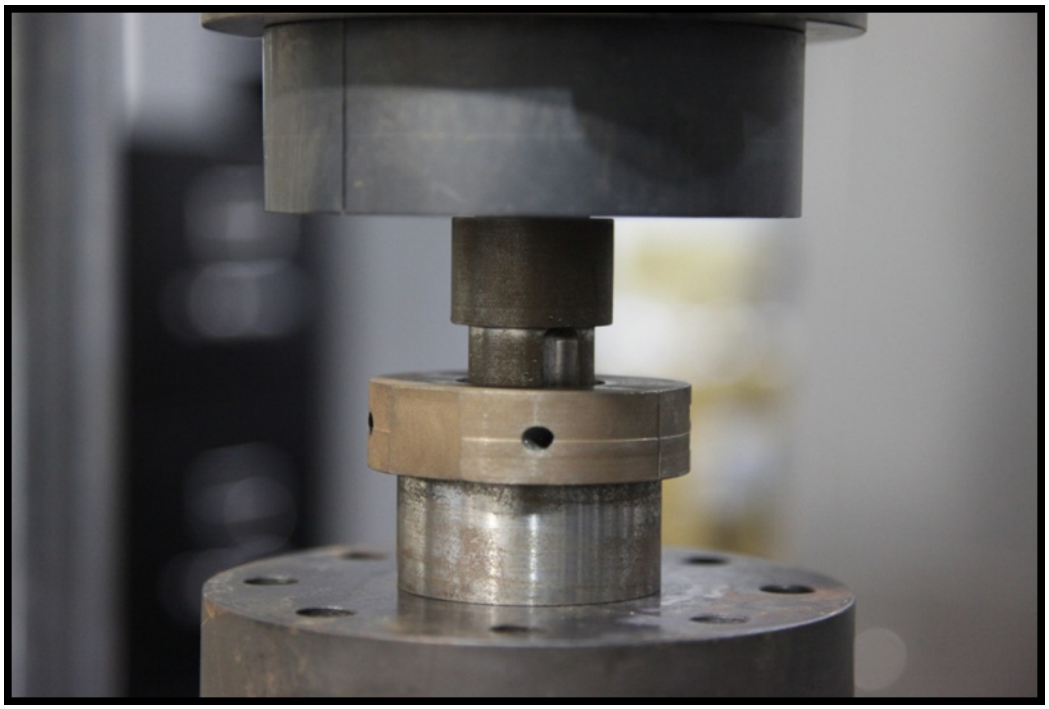


Figure 5.1.7: Rigid Clamping Collar Installed During Testing of Thin Wall Sample

Once the clamping collar was installed the discrepancy in the data disappeared and the collar was used for testing the remainder of the thin wall samples.

5.2 Thick Wall Testing Procedure

Following the same methodology of the thin walled sample testing a press and die were made from carbon steel. The larger thick wall samples required that new testing equipment be fabricated to accommodate the changes in the sample dimensions. A new press was machined without the notches cut into it due to the lack of folds in the new thick wall samples. A new die and rigid clamping collar were fabricated as a result of the thick wall samples larger O.D. The new press and die as well as the new rigid clamping collar can be seen in Figure 5.2.1.

The thick wall samples were tested in the same manner as the thin wall samples. Pressing of the samples was performed on the same MTS machine located on UT campus and used the same pressing rates as well as data sampling rates.

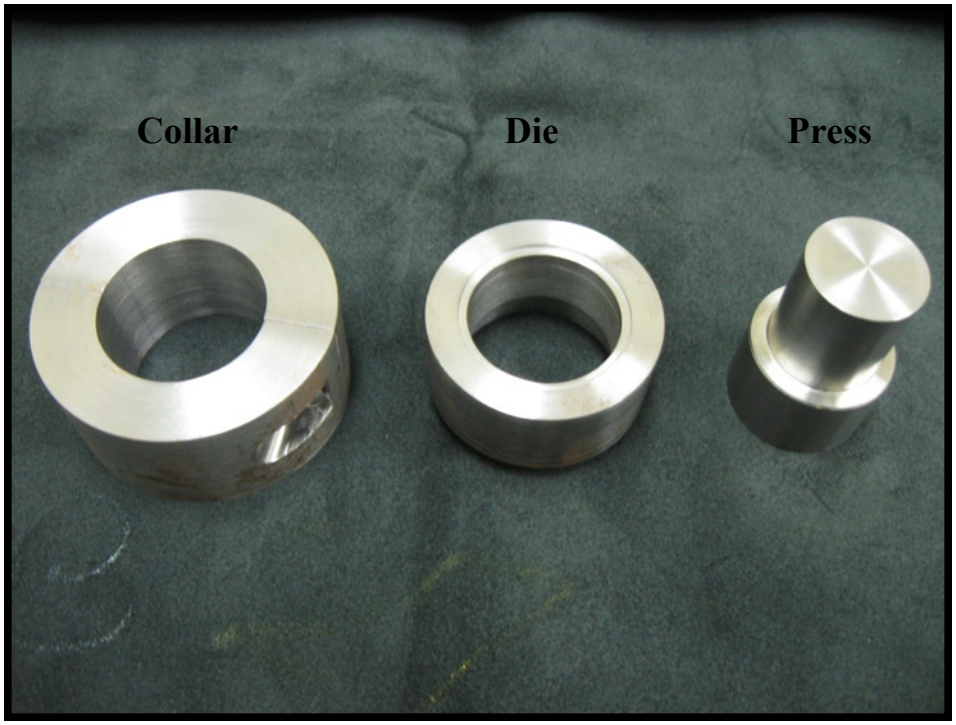


Figure 5.2.1: Press, Die, and Collar for Thick Wall Samples

Chapter VI

RESULTS AND DISCUSSION

6.1 Thin Wall Samples Results and Discussion

In this research, a total of 118 (both thin and thick wall) disk samples were tested for the peak load. Out of these, 37 thin wall samples were first pushed using the press and die (shown in Figure 5.1.1) described above. During the testing it was discovered that the copper sleeve deformed in a manner to invalidate the results. As a result, the press and die design was modified and a rigid collar was clamped to prevent the out of plane deformation of the collar sleeve. The new press, die and collar method of testing was used for the remainder of the tests for both the thin wall and thick wall samples. The details of the collar design were discussed in Chapter V. First the test results of the thin wall disk samples that were tested without the use of the collar will be discussed.

Figure 6.1.1 shows representative load versus time plots for 19 mm (0.75 inches) disk samples that were pushed without the collar. These disk samples were soaked for a period of one week at different temperatures.

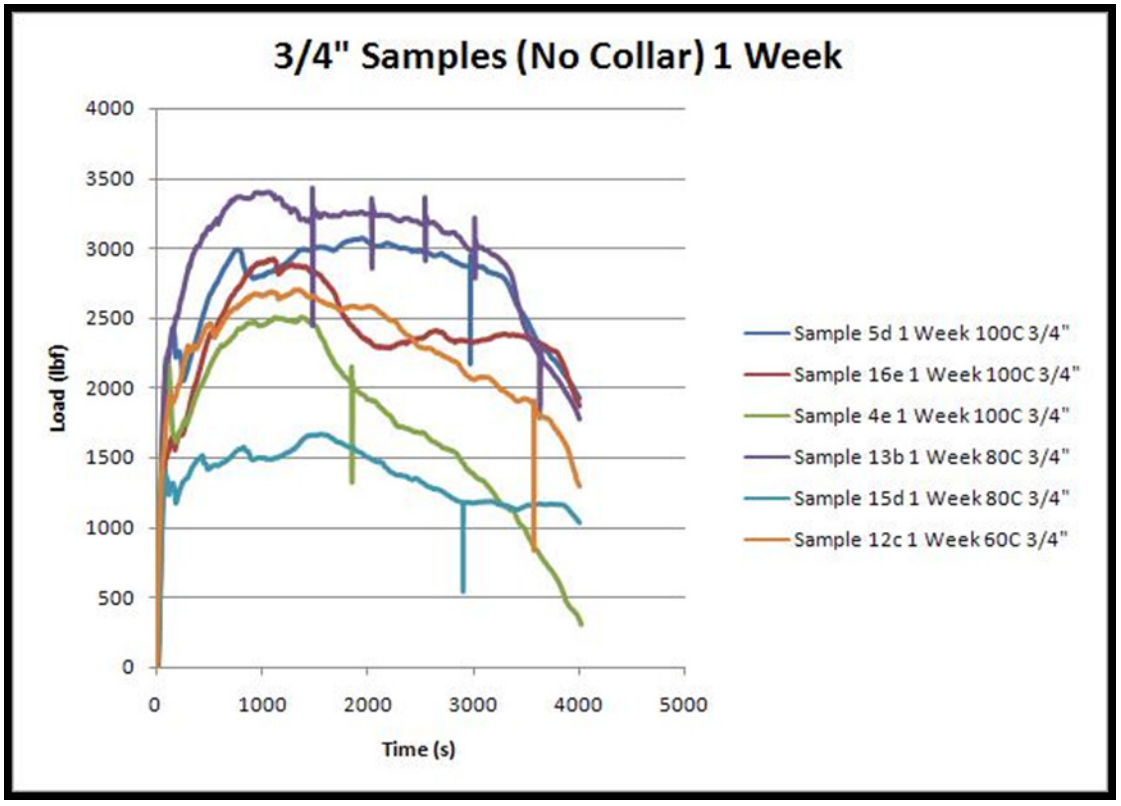


Figure 6.1.1: Thin Wall Disk Samples Pressed w/o Collar Demonstrating Stick Slip

Several interesting features are noted from Figure 6.1.1. The vertical spikes in the curves are believed to be stick slip between the wire coil pack and the copper sleeve. The second feature is the apparent randomness of the data itself. During testing it was expected that the higher temperature soaking period would require a lower force than the lower temperature soaked disk samples, however, there is no consistency between the temperature at which the disk sample was soaked and the force required to push the wire coil out of the copper sleeve. The inconsistency of this data is believed to be due to the presence of folds (see Figures A14-A50 in Appendix) and the variation in their geometry and orientation from specimen to specimen. These folds were produced during the compaction process. The change in orientation with respect to the loading axis is likely to produce large fluctuation in the data. The tests done without the collar produced bulging of copper sleeve during loading. As the sleeve bulges the wires break loose from the sleeve instead of being sheared away as the testing was designed to do.

In order to prevent the bulging and distortion of the copper sleeve during loading a rigid clamping collar (Figures 5.1.6 and 5.1.7) was designed and clamped to the outside of the copper sleeve of the disk sample.

Once the collar was clamped to the disk sample the bulge was eliminated and the spikes in the data curves disappeared. A comparison between the load versus time curves obtained with and without the clamped collar around the sleeves can be seen in Figures 6.1.2 and 6.1.3.

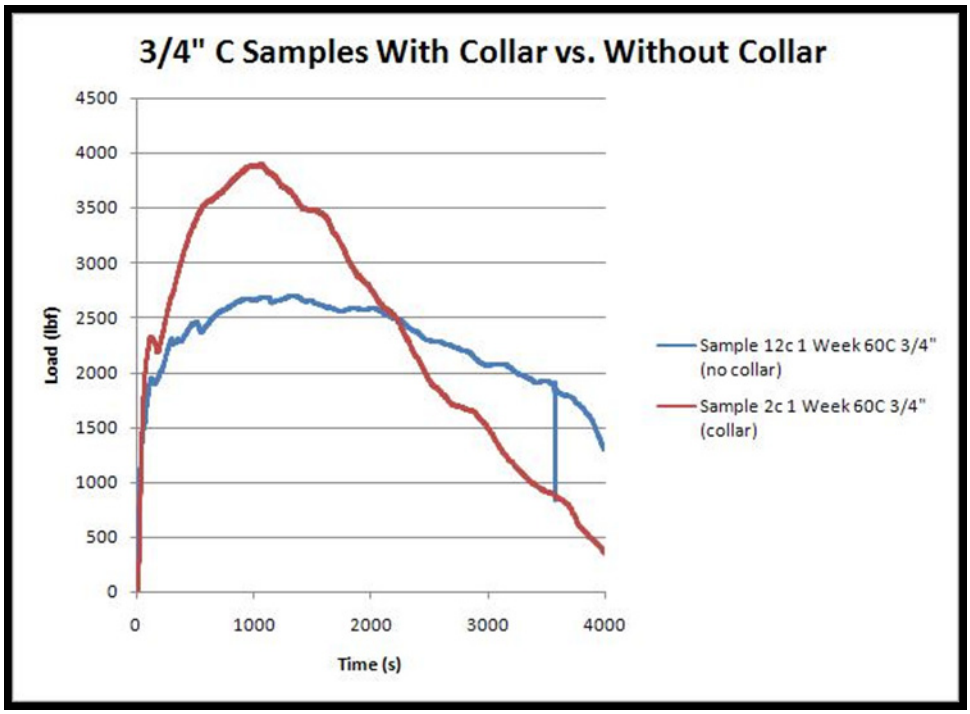


Figure 6.1.2: ¾" Disk sample Comparison of Collar vs. No Collar

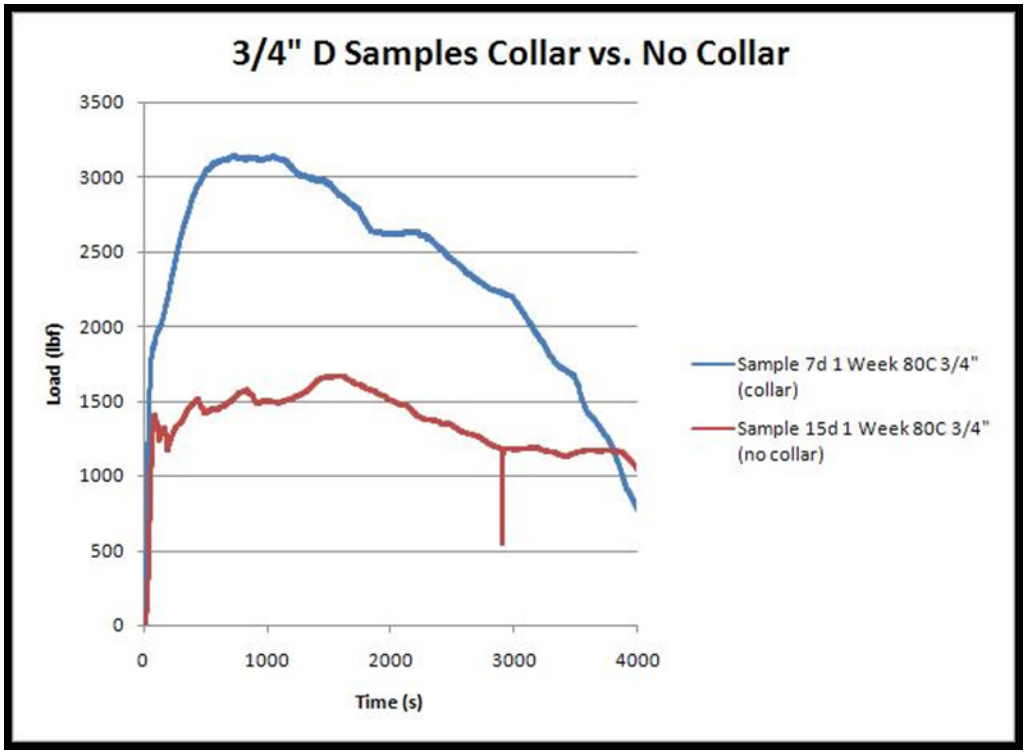


Figure 6.1.3: ¾" Disk sample Comparison of Collar vs. No Collar.

Notice also the difference in the appearance of the curve as well as the maximum load reached. The curve with the collar is much smoother and reaches a higher load than that with the no-collar disk sample.

The testing of the remaining 38 thin wall disk samples from this point forward continued with the collar in place around each disk sample before being placed in the testing machine.

Once the testing was complete several anomalies were noted and required that the data from several thin wall disk samples be discarded from the comparison. These anomalies involved several different factors and will be briefly discussed in the following section.

6.2 Thin Wall Sample Data Elimination

The "A" bar was the first bar compacted by the hydraulic crimper. The majority of the disk samples machined from "A" bar were placed in the one month soaking time frame with a few remaining disk samples making it into the soaked-unsintered and unsoaked-unsintered categories. The problem with the "A" bar was that during the preparation of the sample the chrome had not been completely removed. The removal of the chrome is crucial for the sintering of the copper and as a result the strands did not

sinter when placed in the heat treatment. This discovery was not made until the disk samples had been tested and a visual inspection performed to note that the wires had not bonded with one another. Figure 6.2.1 shows a picture of disk sample 10a in which the loose wires can be seen with a dark chrome coating. Additional photographs shown in appendix show the same the same feature with disk samples taken from "A" bar.

Due to the failure of the chrome removal, the data collected from the "A" disk samples was discarded from the comparison. The only conclusion from this data was that the lack of chrome removal prevents strands from being sintered.

During the testing of the disk samples a few were crushed due to the deformation of the sleeve of the disk sample. All the disk samples had different fold geometry and fold alignment, which made the alignment of the pressing apparatus difficult. Disk samples 2e, 11b, and 3e were crushed in the testing process due to the sleeve becoming wedged in between the press and the die. Pictures of the failed disk samples are shown in Figures 6.2.2-6.2.4.



Figure 6.2.1: Disk sample 10a No Chrome Removal



Figure 6.2.2: Disk sample 2e



Figure 6.2.3: Disk sample 11b

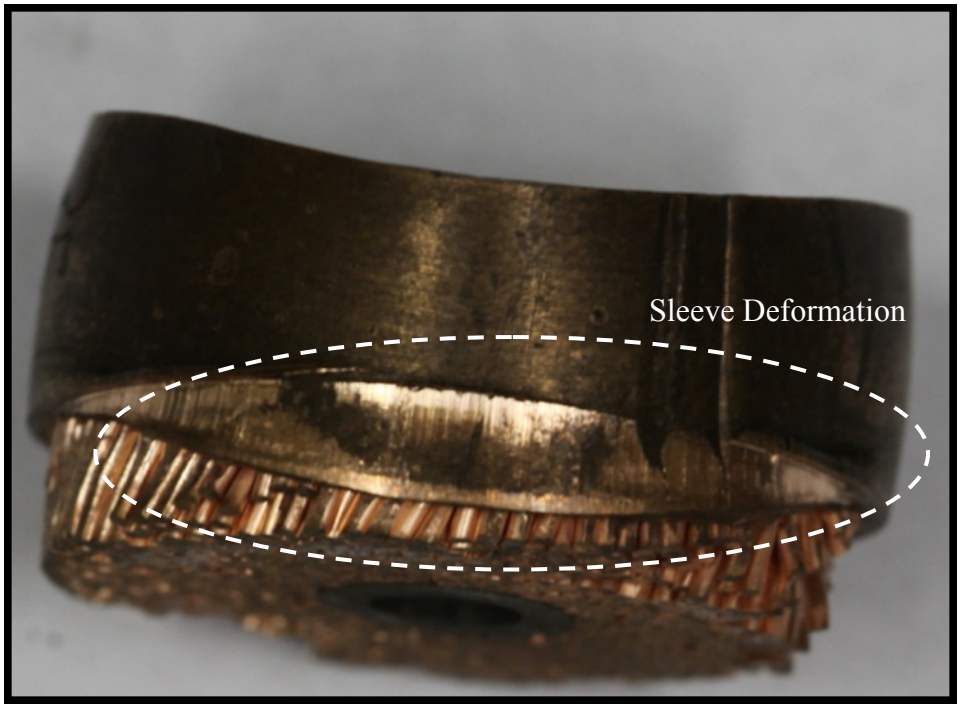


Figure 6.2.4: Disk sample 3e

The load-time curves from these three samples are shown in Figure 6.2.5. Due to the nature of the failure during testing, differing loads were reached for each disk sample with the third disk sample, 3e, being stopped before the completion of the test. The data from these three disk samples was therefore eliminated from the comparison. In addition, data from disk samples 14c, 10c, 9e, and 9d had to be eliminated due to corruption of the data collection system resulting from power failure.

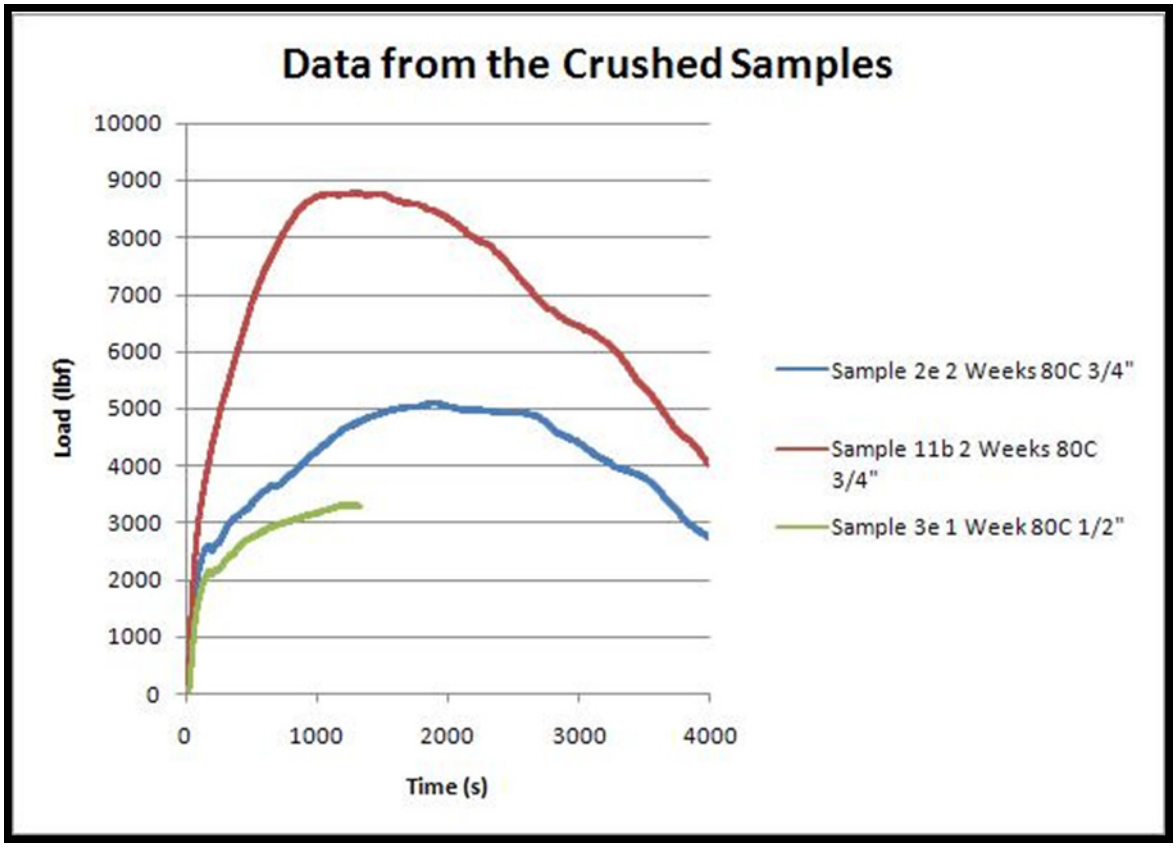


Figure 6.2.5: Crushed Disk sample Data

6.3 Analysis of Thin Wall Results

This section discusses only the data of the disk samples that were tested with the clamping collar. The data was divided into the following four groups:

- 19mm (¾") Collar Soaked-Sintered
- 19mm (¾") Collar Soaked-Unsintered
- 12.7mm (½") Collar Soaked Sintered
- 12.7mm (½") Collar Soaked-Unsintered

For each of these groups there were four cases – 0 week soak (unsoaked), one week soaked, two weeks soaked, and one month soaked. For each of these cases, there were three temperature conditions – soak at 60^{o}C, soak at 80^{o}C, and soak at 100^{o}C.

However, due to the elimination of some of the data several categories were absent in the final comparison. The peak loads for all the specimens tested (with collar) are shown in Figures A1-A13 in the appendix. The only observation from the data from individual disk samples is that there is a large variation in the peak load values for seemingly identical specimens subjected to identical moisture soaking conditions.

Normally, for small size disk samples such as the one used in this study (½"and ¾", Figure 4.1.7), the natural data scatter would be expected to be much smaller unless there are some other variables at play.

The average peak load values are shown as a function moisture soaking conditions in Figures 6.3.1 – 6.3.4. For cases where there were multiple disk samples for the same condition, the standard deviation in the data is displayed by error bars. The purple bar located on the left side of the graph is the average of control disk samples that were not soaked for any period of time or temperature. The control disk samples remained in a cardboard box at room temperature and were not exposed to any accelerated soaking environment.

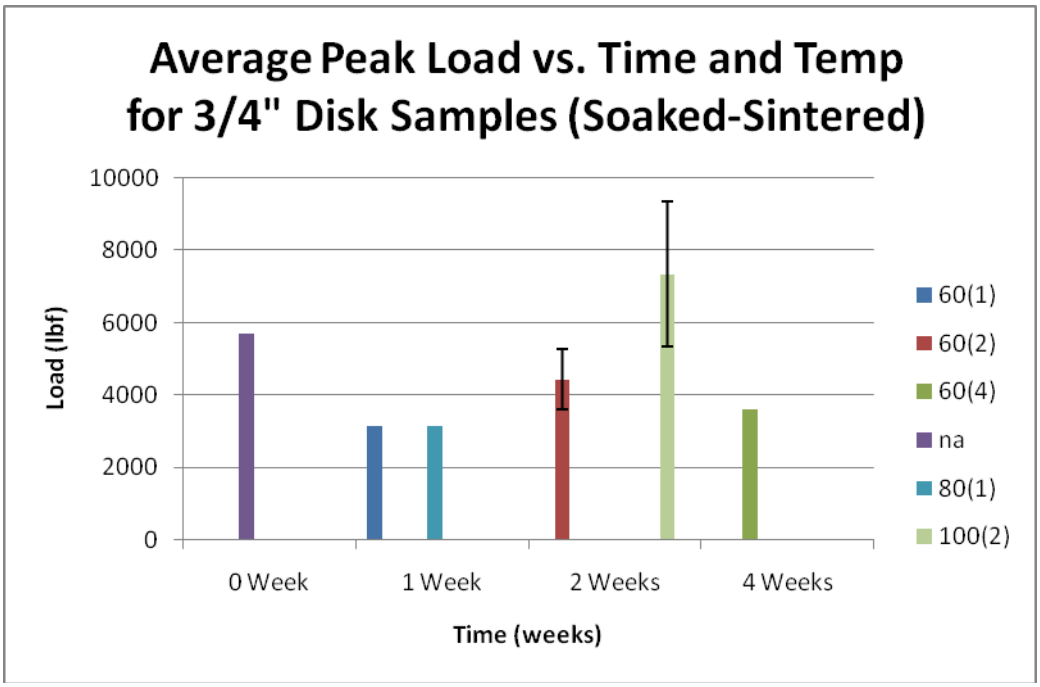


Figure 6.3.1: Soaked and Sintered ¾" Disk samples. The numbers in parenthesis are the aging period in weeks.

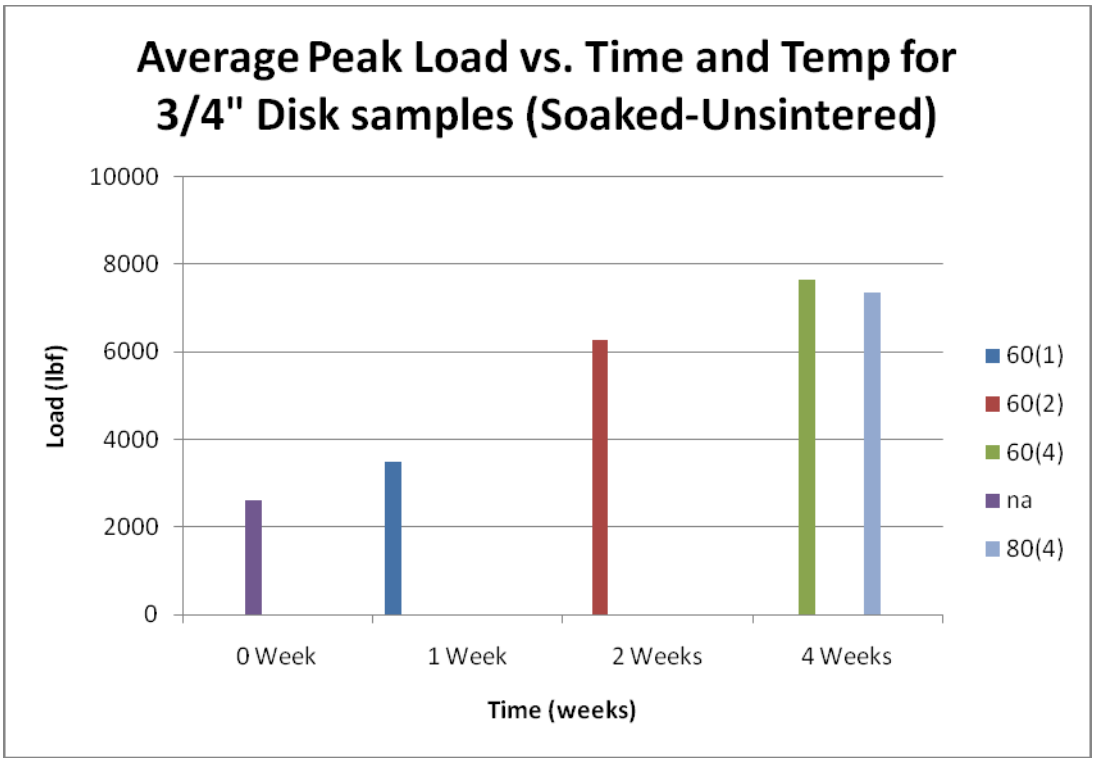


Figure 6.3.2: Soaked and Unsintered ¾" Disk samples. The numbers in parenthesis are the aging period in weeks

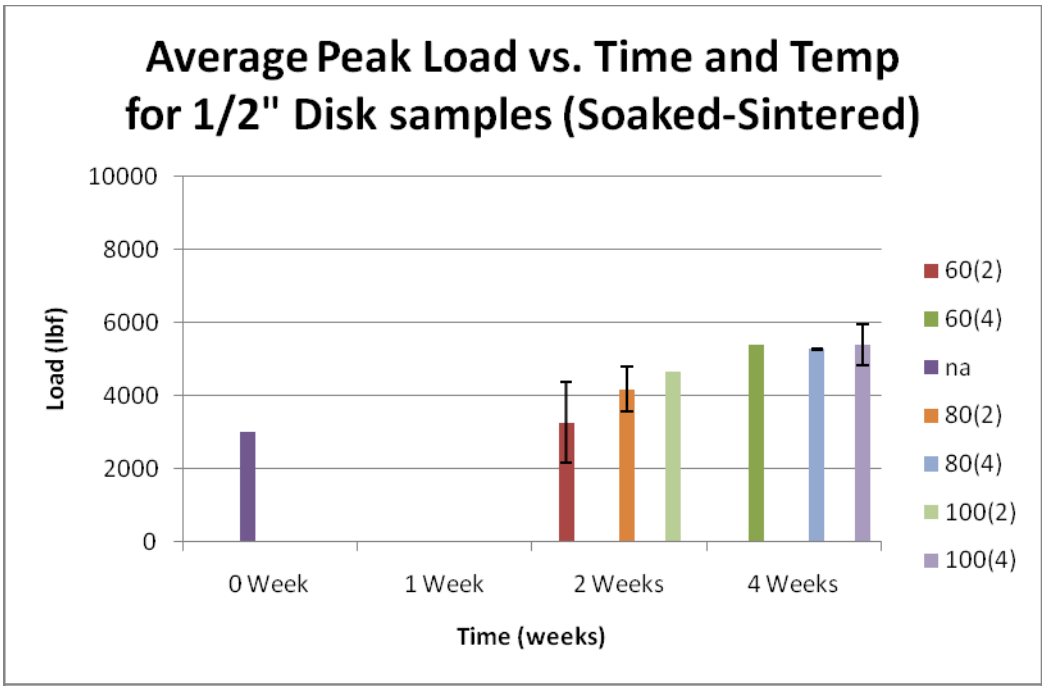


Figure 6.3.3: Soaked and Sintered ½" Disk samples. The numbers in parenthesis are the aging period in weeks.

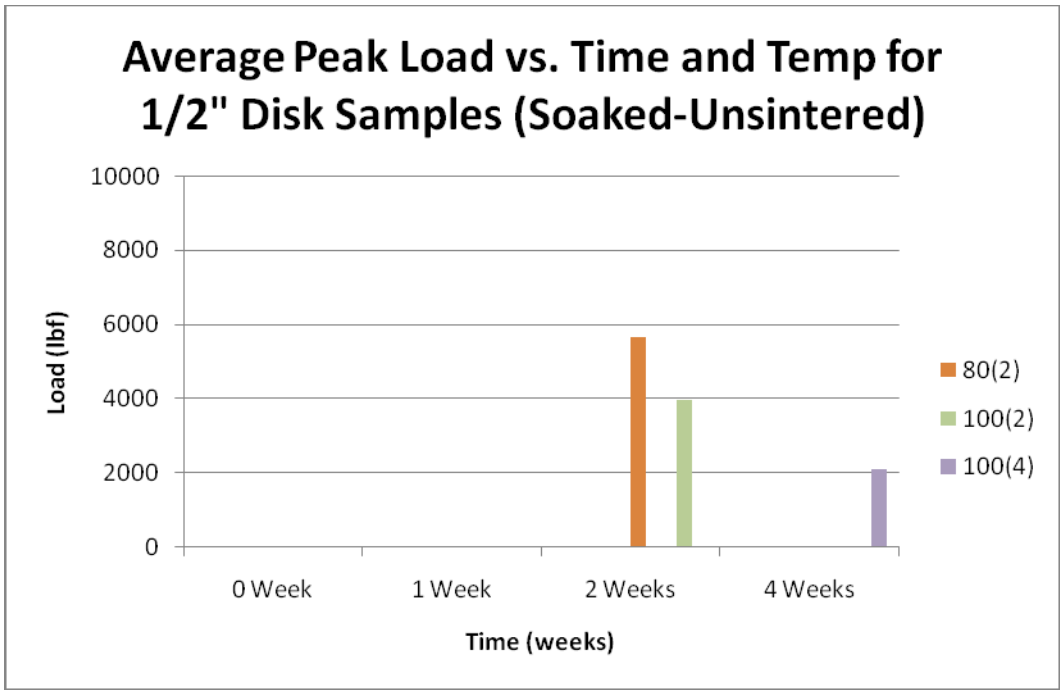


Figure 6.3.4: Soaked and Unsintered ½" Disk samples. The numbers in parenthesis are the aging period in weeks.

From the bar charts shown in Figures 6.3.1 – 6.3.4, there does not appear to be any correlation between the recorded peak load and the soaking conditions. This does not, however, mean that soaking has no effect on sinter quality. In addition to the variables related to the soaking conditions there were some other unintentional and uncontrolled variables. These variables were the random occurrence and orientation of folds in copper sleeve, the size and depth of the folds, and the compaction methods used. The size and depth of the folds varied from disk sample to disk sample. In addition, bars "A" and "B" were compacted by a different method than bars "C", "D", and "E". As a result bars "A" and "B" had un-predictable folds that became larger or smaller or changed orientation throughout the sample. The compaction method is also believed to have played a role in the amount of force required to separate the wire coil from the sleeve. The most significant of these variables is believed to be the orientation of the fold with respect to the loading axis. Schematic in Figure 6.3.5 shows the effect of the fold orientation. If the fold is not parallel to the loading axis, there will be a component, P_N, of the applied force that will be acting normal to the fold axis. This force will cause the strands to dig into the fold and cause the distortion of the fold rather than producing a shearing effect between the strands and the sleeve.

Based on these observations, it is difficult to identify any quantitative relationship between moisture soaking condition and the sinter quality. However, from the appearance of failed specimens, it is clear that there was some level of sintering both among the strands as well as between the strands and the copper sleeve in all thin wall disk samples regardless of their moisture soaking conditions. In all the thin wall sintered specimens (except the ones from bar A in which chrome did not appear to have been removed properly), groups of strands were bonded together (see Figures A14- A18, A25-A44, A47-A52, A62-A78, A81, A84, A86, A88 in Appendix).

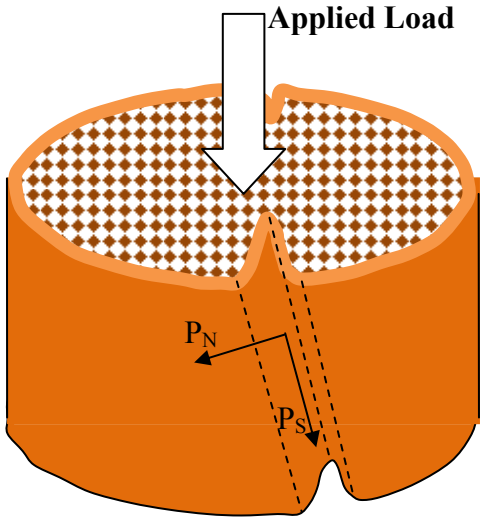


Figure 6.3.5: Effect of the fold orientation with respect to the loading axis.

In addition, the exposed inside portions of the copper sleeves had some strands stuck to the sleeve (see Figures A31, A37, A43, A49, A70, A75) suggesting some level of sintering between strands and sleeve.

6.4 Analysis of Thick Wall Results

Due to the inconsistencies in the results obtained with the mechanical tests of the thin wall samples, thick wall specimens were tested in an attempt to find a correlation between soaking and sintering quality without the interference of the folds. Thirty eight thick wall samples were tested and elimination of only one data point was necessary.

Disk sample 31x was soaked at 100˚C for a period of four weeks. The data from disk sample 31x was eliminated from the comparison due to an accidental over write caused by an incorrect file name. However the data was plotted and can be seen for reference in figure 6.4.1.

Similar to the thin wall samples, load vs. time was recorded and the max force was taken from each sample. Figure 6.4.1 is a plot created with the data from the testing

of the samples soaked for four weeks at 100˚C. Similar plots for the remaining Sample X groups can be found in the Appendix.

Looking at the plots it appears that there is a wide spread between the lowest force recorded and the highest force recorded. One interesting correlation between the two is that during visual inspections of the samples, those with the lower force had the copper wire removed as a single bundle from the sleeve and in a very clean manner. This is in contrast to a sample with a higher recorded force where several strands were left still attached to the sleeve wall. This phenomenon is illustrated in Figure 6.4.2 with samples 1x and 32x, which can be found on the plot in Figure 6.4.1.

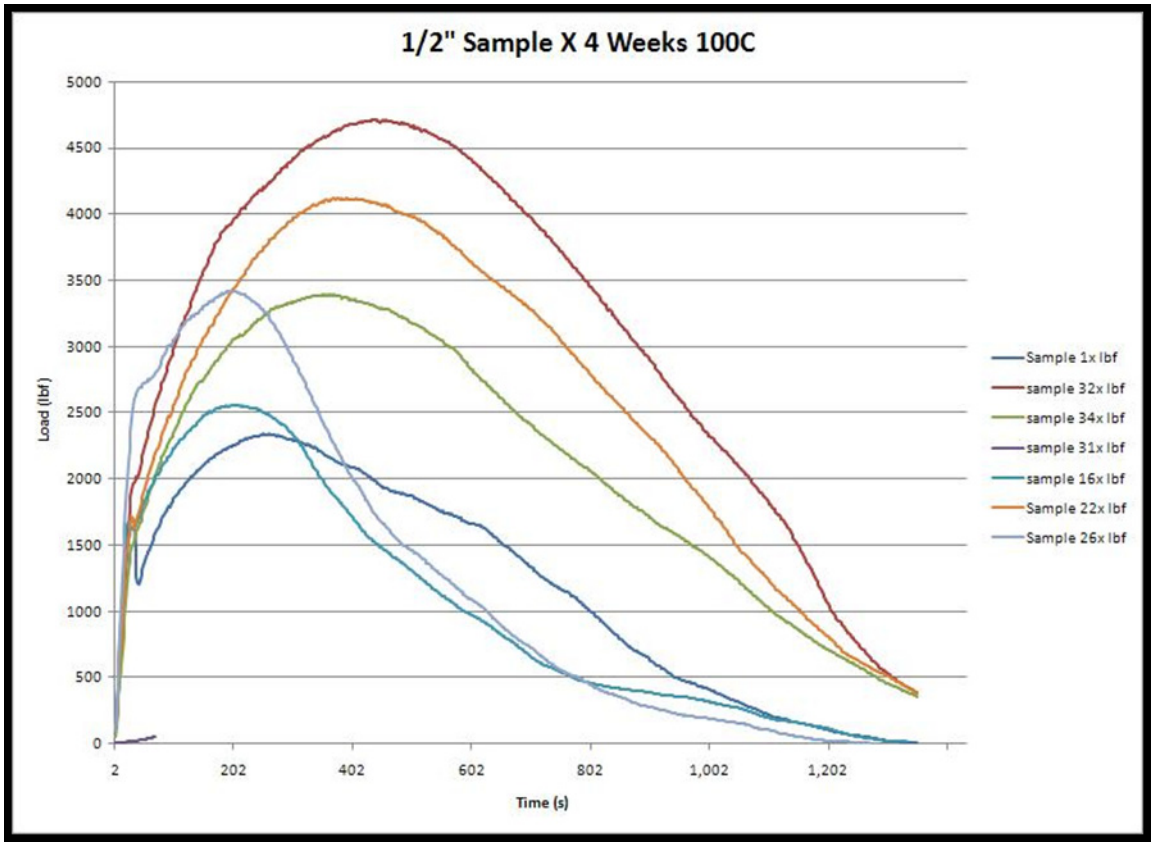


Figure 6.4.1: ½" Sample X Four Weeks 100˚C

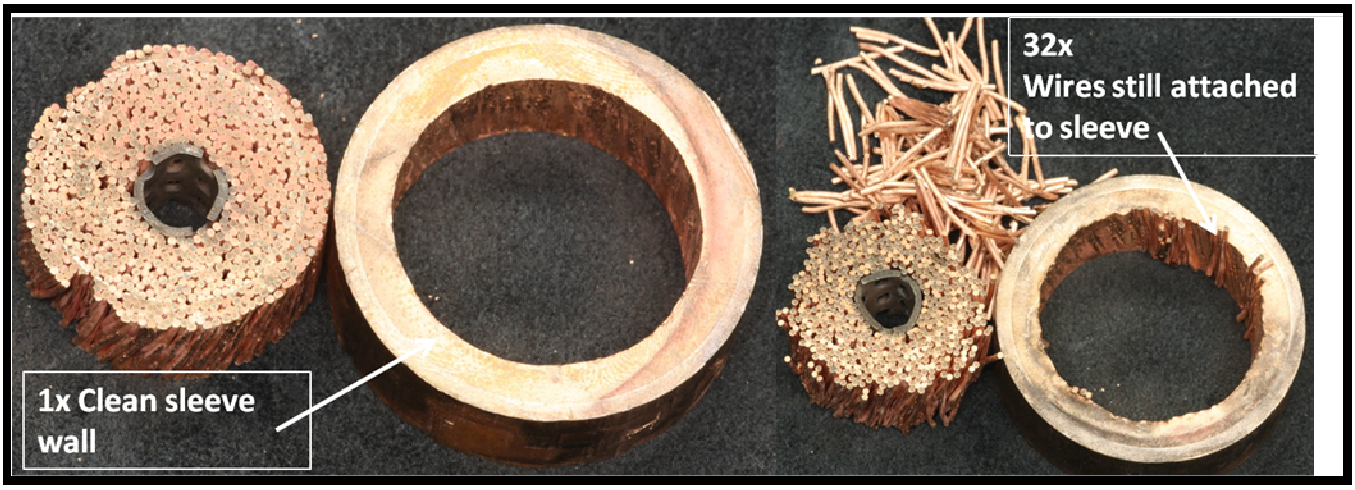


Figure 6.4.2: Sample 1x (low load) Clean Sleeve vs. Sample 32x (high load) Wires in Sleeve

Similar occurrences happened throughout the different soaking periods with each batch of disk samples showing similar results, the high load samples still had strands of CS cable attached to the sleeve while the low load samples had clean walled sleeves.

Next, to further compare results the highest load from each sample was taken and averaged along with the other samples from its soaking period. The data was the graphed on a bar chart seen in Figure 6.4.3. As with the thin wall samples the standard deviation was calculated (using excel) and plotted in the form of error bars on each of the bars. The peak average load as well as the standard deviation can be seen in Table 6.4.1.

Table 6.4.1: ½" Sample X Average Peak Loads and Standard Deviation

	US-UnSin	US-Sin	2 weeks 80C	4 weeks 80C	2 weeks 100C	4 weeks 100C
Avg Peak Load (lbf)	2621.7 (11.66 kN)	2423.1 (10.78kN)	3141.7 (13.97 kN)	3188.3 (14.18 kN)	3430.4 (15.26 kN)	3422.6 (15.22 kN)
Std. Dev (lbf)	1002.3 (4.46 kN)	214.6 (.95 kN)	989.8 (4.41 kN)	808.2 (3.60 kN)	615.8 (2.74 kN)	902.3 (4.01kN)

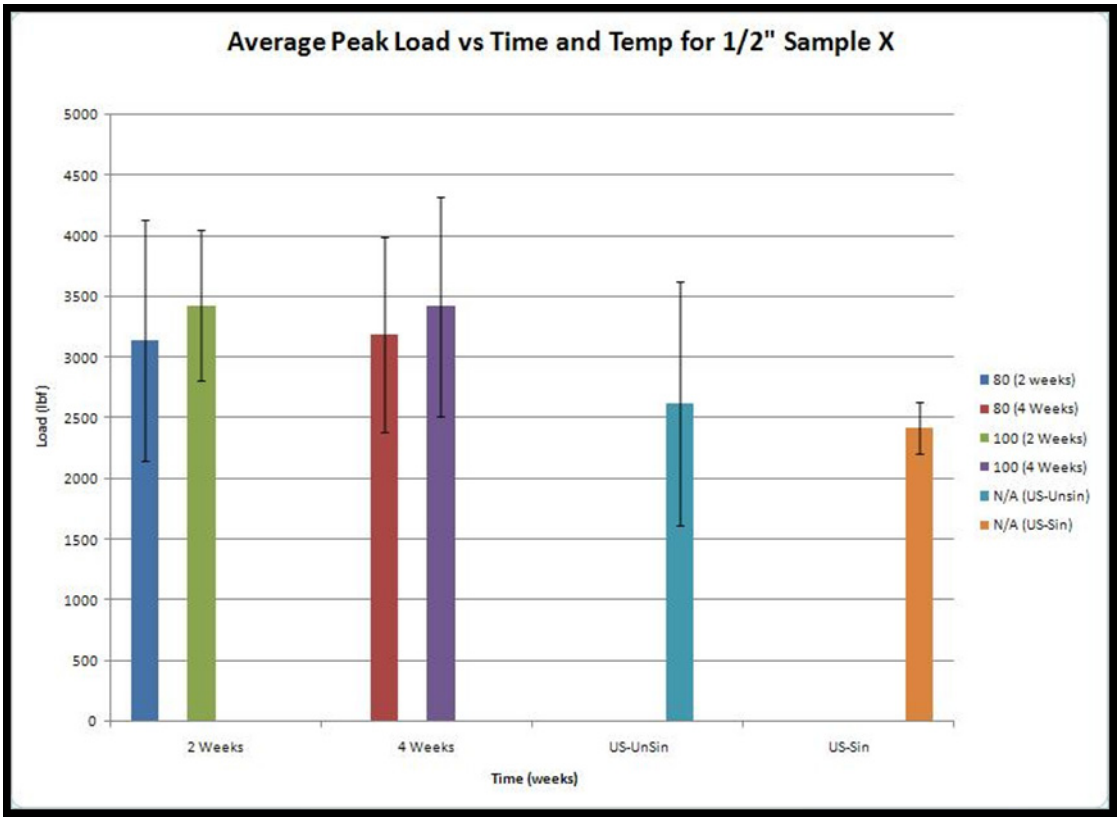


Figure 6.4.3: ½" Sample X Average Peak Loads vs. Time and Temperature

Based on the average maximum load, the samples soaked for two weeks both at 100˚C and 80˚C has a1.33 kN (300 lb) difference between the two. This is consistent with the samples soaked at 80˚C and 100˚C for four weeks. The difference between the two week samples and the four week samples soaked at the same temperatures is less than 0.18 kN (40 lbs) in both cases. All four soaking time frames showed an increase in strength over that of the un-soaked sintered and the un-soaked un-sintered samples. However, the un-soaked-sintered samples were 0.89 kN (200 lb) weaker than the un-soaked un-sintered samples.

As discussed earlier, the belief that some level of oxidation increases the sintering quality appears to be the case with the thick wall samples. Oxidation of copper up to certain thicknesses had properties that increase the strength while too thick of an oxide layer may weaken the sintered part. It appears from the data that the level of oxide formation and strength varies more on temperature and not on time.

To document the change of the disk samples from before soaking to after pressing, pictures were taken at four different stages: before soaking, after soaking, after sintering, and after pressing. These photos can be seen in the appendix with a representation of disk sample 1x seen below in Figure 6.4.4.

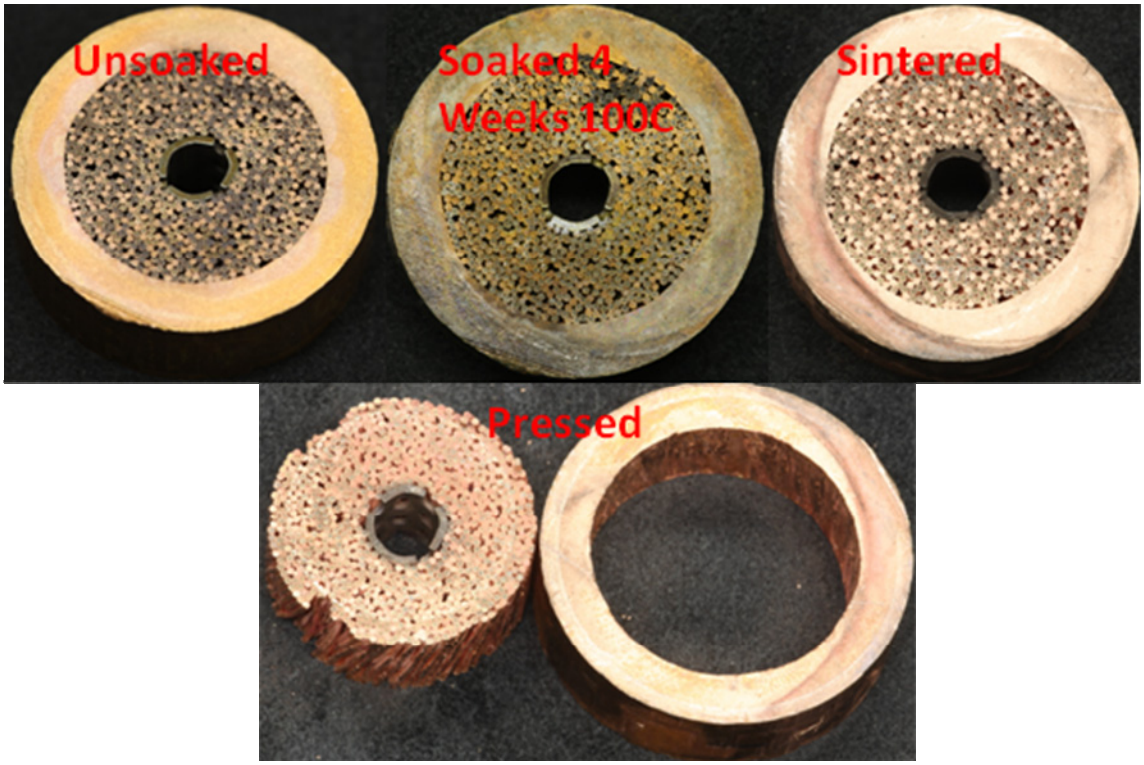


Figure 6.4.4: ½" Sample 1x Pictures of Each Stage of Testing

As seen in Figure 6.4.4 the only noticeable visual difference in the sample during the testing periods is a change in coloration. Change in coloration is most noticeable in the after soaking picture and the after sintering picture. The "soaked" photo shows coloration due to the oxidation of the copper. As discussed earlier different forms of copper oxide has different colors. After sintering much of the copper oxide has been reduced and turned back into copper hence the return of the natural coloring and appearance.

Like the thin wall samples, temperature and humidity levels were recorded within the thick wall sample jars during the soaking period. Figure 6.4.5 displays those recordings versus time. The peak noted on the graph is the change over from the two week 80˚C samples to the two week 100˚C samples. During this time the ovens were shut off and the jars were opened in order to swap the samples. Once the oven was re-started the jar began to leak causing the humidity level to drop from 100% to around 80% within the jar. However, once the soaking period had begun nothing could be done about the leak. Looking at the data, the leak in the jar did not seem to affect the quality of the sintering.

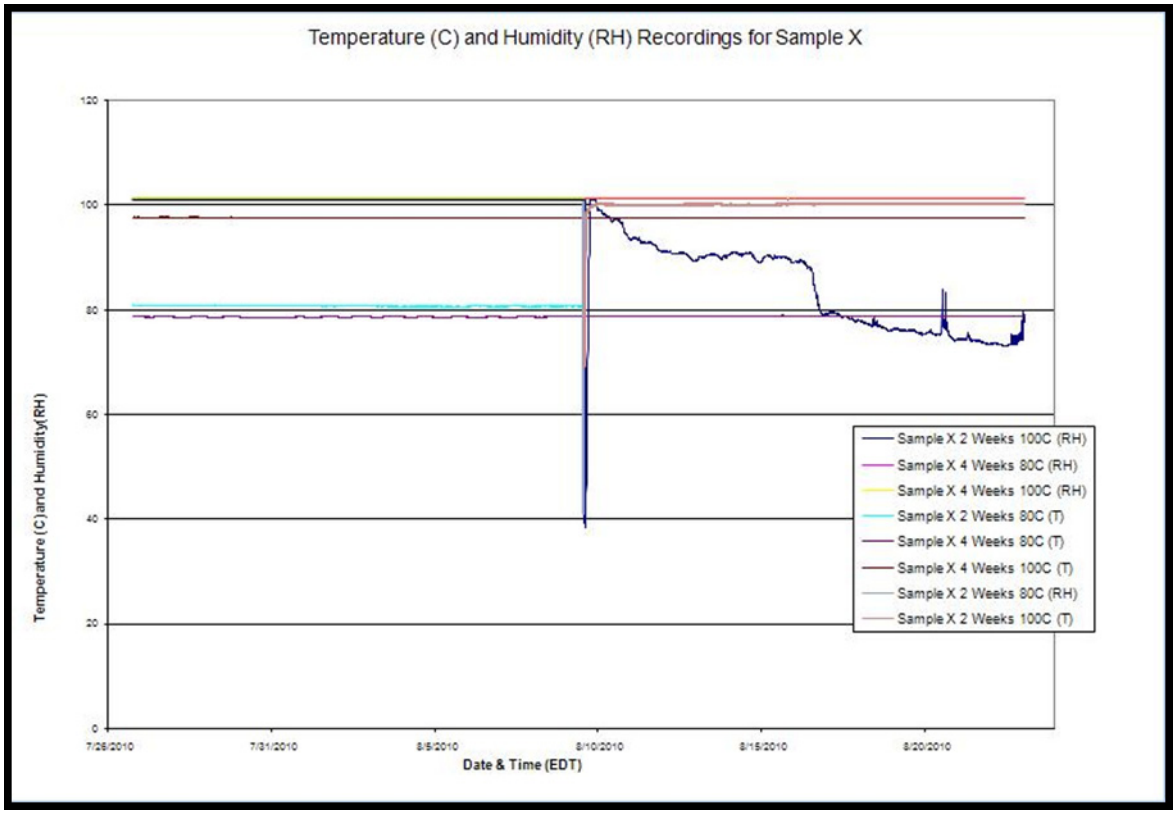


Figure 6.4.5: Sample X Temperature and Humidity Recordings

Chapter VII

CONCLUSIONS AND RECOMMENDATIONS

7.1 Conclusions

This research was initiated to answer the question, "Does prolonged exposure of the superconducting strands to moisture affect the quality of sintering among the individual strands and between the strands and the sleeve?" The data generated during the initial testing of the thin walled samples failed to answer this question. If there was any correlation, the random occurrences of the folds in the copper sleeve and their orientation with respect to the loading axis are believed to have masked that. Although no consistent trends emerged between the moisture soaking conditions and the maximum force needed to push the coiled wires from the copper sleeve, the visual observation of failed disk samples did indicate some level of sintering in all disk samples (both soaked and un-soaked).

The thick walled samples did appear to show some correlation between soaking and the strength of the sintering. It appears that for the 2 week versus 4 week soaking periods and 80 ^{o}C versus 100 ^{o}C soaking temperature, the time does not have as much of an effect on the strength as temperature does. This is consistent with the data that shows samples aged for two weeks vs. four weeks at the same temperature had loads that varied by less than forty pounds. However samples that were aged at 80˚C versus 100˚C had loads that varied by almost 300 pounds. Quality of sintering was also demonstrated in samples that took a higher force to separate the cable from the sleeve. Samples with a low recorded peak force had smooth sleeve walls while samples with a higher recorded load had several strands of cable still attached to the sleeve wall. While more testing would need to be done to confirm these results, it appears that soaking can have a positive effect on the strength of the sintering.

7.2 Recommendations for Future Work

In order to answer the fundamental question, "Does moisture exposure prior to sintering affects the quality of sintering" experiments need to be designed such that other than the moisture and temperature conditions all other variables within the sample are eliminated. One such specimen design is to sandwich the strands between two rectangular copper plates as shown below in Figure 7.2.1. This sandwiched sample can be exposed to accelerated soaking and then sintered under pressure (as shown in Figure 7.2.1). This would be similar to the one expected during the compaction of copper sleeve on the coil pack. Such a sample design will be free of all the variables other than the moisture conditions.

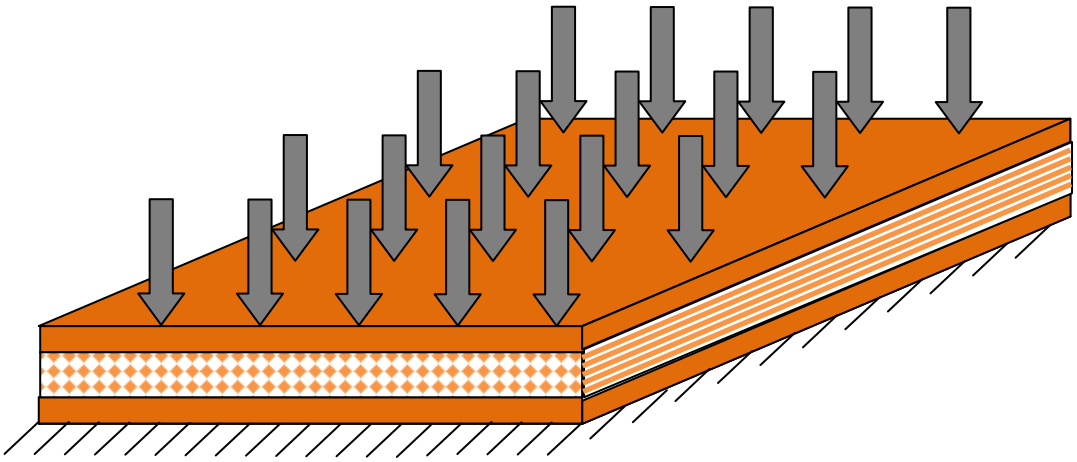


Figure 7.2.1: Suggested specimen design for establishing a quantitative relationship between moisture condition and sinter quality.

After sintering, the shear strength between the copper plate and strands can be determined using the common lap shear test method, Figure 6.2.2. This shear strength is expected to provide a quantitative relationship between moisture soaking condition and sinter quality.

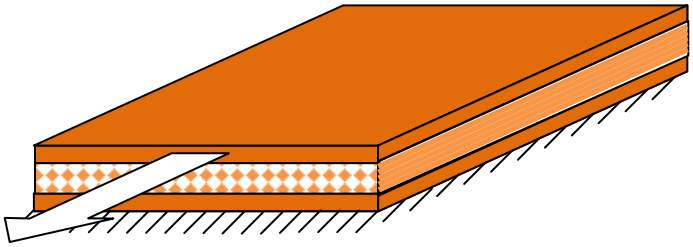


Figure 7.2.2: Lap shear test

In addition to lap shear test, monitoring of the buildup of the oxide layer should be conducted to note any correlation between the thickness of the oxide layer and the recorded peak load. As noted earlier, some levels of oxide may increase the sintering process and thereby increase the strength, while too much of a build up can have adverse effects and hinder the sintering process. Another useful piece of information may be exactly what kinds of oxides are formed at each temperature or soaking period. Therefore if one oxide is found to increase the strength while another decrease it, special provisions can be made to allow the one while preventing the latter.

A final recommendation would be to soak and sinter longer samples of CS cable and measure the current through the samples as compared to a control sample. This would answer how soaking affects the conductivity of the cable.

REFERENCES

1. William H. Danforth, Founder. (2010). Retrieved from http://nestlepurina.com/Danforth.aspx
2. A Short History of Energy (in the U.S.). (2008). [Total U.S. Energy Consumption 2008]
   Retrieved from http://www.thewatt.com/node/153
3. Energy Matters. (1998). [Fusion: The Energy of the 21st Century]. Retrieved from http://library.thinkquest.org/20331/types/fusion/problems.html
4. ITER, The Way to New Energy. (2010). [Magnets] Retrieved from http://www.iter.org/mach/Magnets
5. Davis, Joseph R. (2001). *Copper and Copper Alloys.* Materials Park, OH.: ASM International.
6. Thumler, F. and Oberacker, R. (1993). *Introduction to Powder Metallurgy.* Carlton House, London.: Institute of Materials.
7. National High Magnetic Field Laboratory. (1995-2010) [Making Superconducting Magnets] Retrieved from http://www.magnet.fsu.edu/education/tutorials/magnetacademy/superconductingmagnets/page4.html
8. University of California for the Department of Energy. (2003). [Chromium]. Retrieved from http://periodic.lanl.gov/elements/24.html
9. Owens, Frank J. and Poole Jr., Charles. (1996). *The New Superconductors*. New York, N.Y.: Plenum Press.
10. Chemistry Comes Alive. (1999). [Oxidation and Reduction of Copper]. Retrieved from http://jchemed.chem.wisc.edu/JCESoft/CCA/CCA3/MAIN/REDOXCU/PAGE1.HTM

APPENDIX

Figures A1 – A13 are the peak load values for individual disk samples. Figures A14 – A88 are the photographs of disk samples after the completion of the push tests. These photographs show samples from every category included in this report.

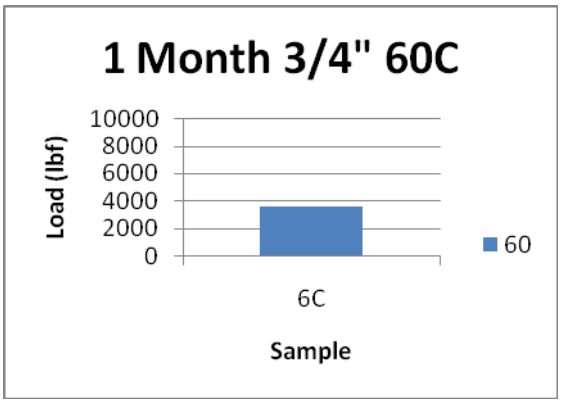


Figure A1:

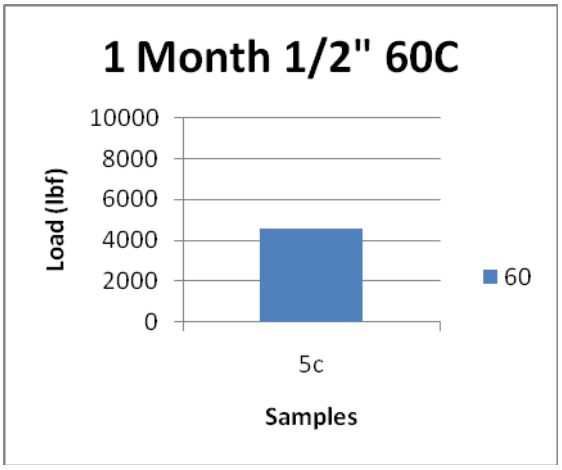


Figure A2:

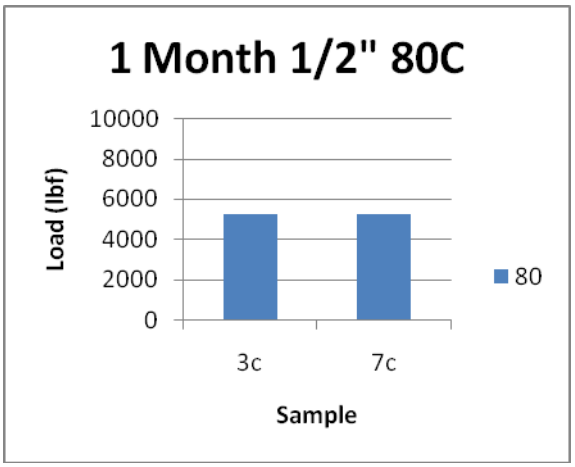


Figure A3:

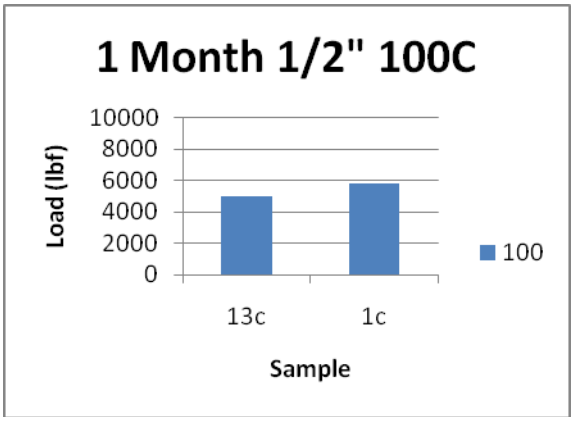


Figure A4:

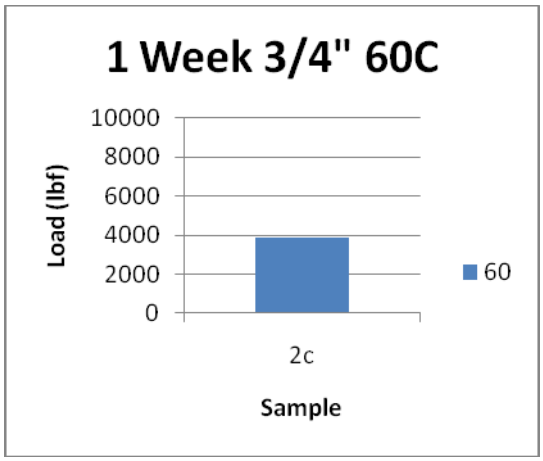


Figure A5:

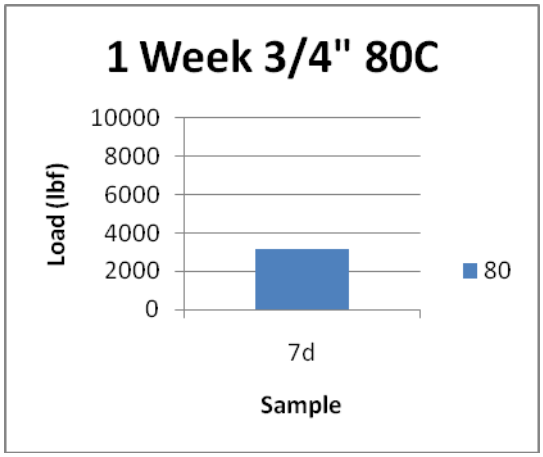


Figure A6:

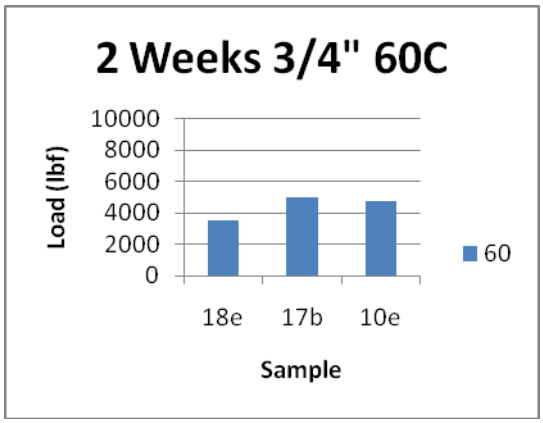


Figure A7:

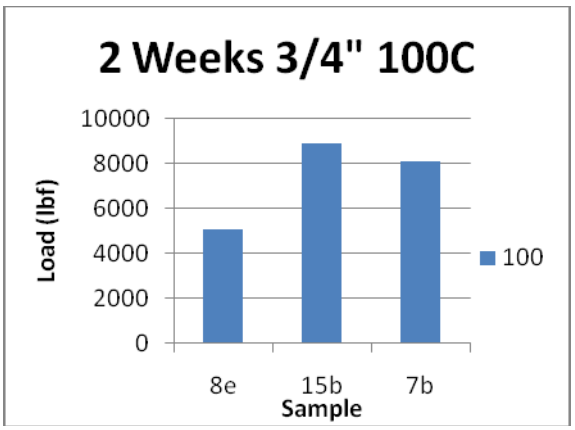


Figure A8:

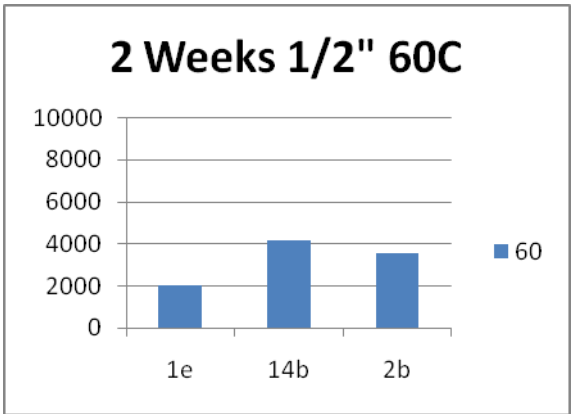


Figure A9:

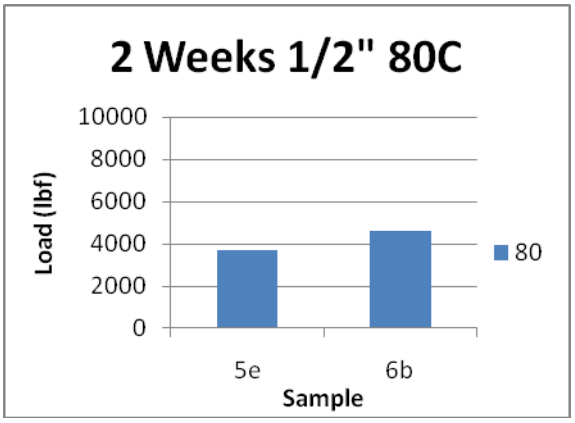


Figure A10:

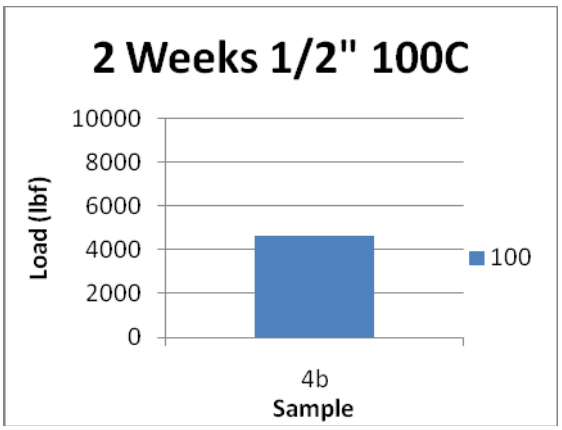


Figure A11:

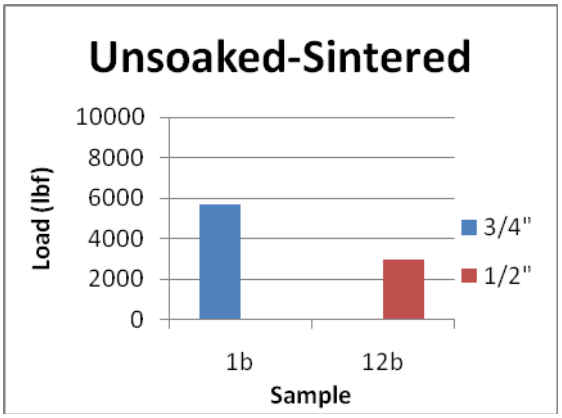


Figure A12:

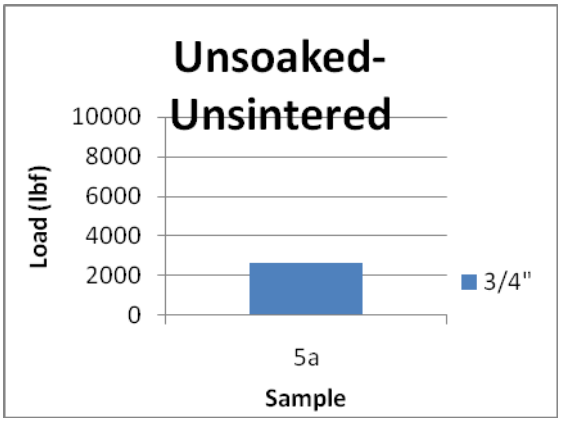


Figure A13:

Figures A14-A88 are pictures of every thin walled sample tested during the research. Each disk sample is segregated by soaking period and method tested.

Thin Walled Samples Pressed with no Collar:

Unsoaked-Sintered



Figure A14: Sample 16D



Figure A17: Sample 1D



Figure A15: Sample 4D



Figure A18: Sample 3D



Figure A16: Sample 10D

Soaked-Unsintered

1 Week 60˚C



Figure A19: Sample 14E

1 Week 80˚C



Figure A20: Sample 15C



Figure A21: Sample 1A

1 Week 100˚C



Figure A22: Sample 7E

Unsoaked-Unsintered



Figure A23: Sample 17E



Figure A24: Sample 12E

Soaked-Sintered

1 Week 60˚C

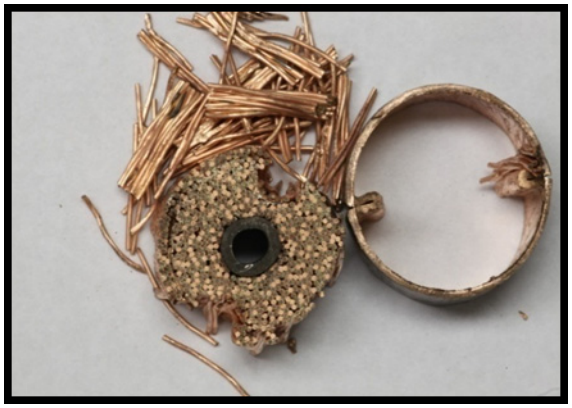


Figure A25: Sample 12C



Figure A26: Sample 15E



Figure A27: Sample 11C



Figure A28: Sample 6D



Figure A29: Sample 9D

1 Week 80˚C



Figure A30: Sample 8B



Figure A31: Sample 9C

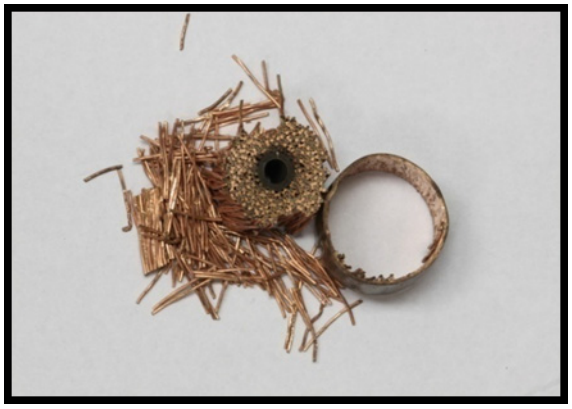


Figure A32: Sample 13B



Figure A33: Sample 3E



Figure A34: Sample 15D

1 Week 100˚C



Figure A35: Sample 16E



Figure A36: Sample 12D



Figure A37: Sample 4E



Figure A38: Sample 16B



Figure A39: Sample 18B



Figure A40: Sample 5D

2 Weeks 80˚C



Figure A41: Sample 2E



Figure A42: Sample 11E

2 Weeks 100˚C



Figure A43: Sample 13E



Figure A44: Sample 9E

4 Weeks 60˚C



Figure A45: Sample 9A



Figure A46: Sample 3A

4 Weeks 80˚C



Figure A47: Sample 8C



Figure A48: Sample 4C

4 Weeks 100˚C



Figure A49: Sample 10C



Figure A50: Sample 14C

Thin Walled Samples Pressed with Collar:

Unsoaked-Sintered



Figure A51: Sample 1B



Figure A52: Sample 12B

Soaked-Unsintered

Figure A55: Sample 5B

1 Week 60˚C



Figure A53: Sample 13D

2 Weeks 80˚C



Figure A56: Sample 14D

1 Week 100˚C



Figure A54: Sample 2D

2 Weeks 100˚C



Figure A57: Sample 10B

2 Weeks 60˚C



4 Weeks 60˚C



Figure A58: Sample 3B

4 Weeks 80˚C



Figure A59: Sample 11D

4 Weeks 100˚C



Figure A60: Sample 8D

Un-Soaked-Un-Sintered



Figure A61: Sample 5A

Soaked-Sintered

1 Week 60˚C



Figure A62: Sample 2C

1 Week 80˚C

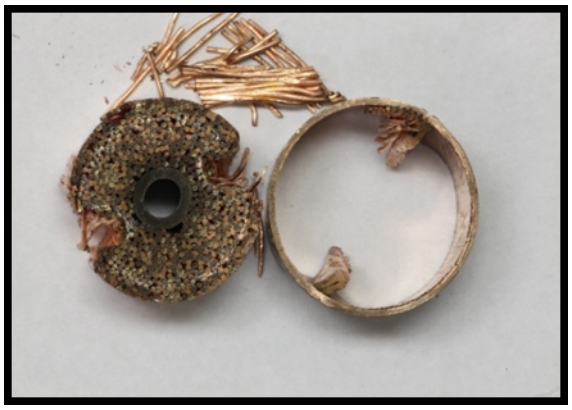


Figure A63: Sample 7D

2 Weeks 60˚C



Figure A64: Sample 17B



Figure A65: Sample 18E



Figure A66: Sample 2B



Figure A67: Sample 14B



Figure A68: Sample 10E



Figure A71: Sample 11B



Figure A69: Sample 1E



Figure A72: Sample 6B

2 Weeks 80˚C



Figure A70: Sample 5E

2 Weeks 100˚C



Figure A73: Sample 15B



Figure A74: Sample 7B



Figure A75: Sample 4B



Figure A76: Sample 8E

4 Weeks 60˚C



Figure A77: Sample 5C



Figure A78: Sample 6C



Figure A79: Sample 4A



Figure A80: Sample 2A

4 Weeks 80˚C



Figure A81: Sample 7C



Figure A82: Sample 10A



Figure A83: Sample 11A

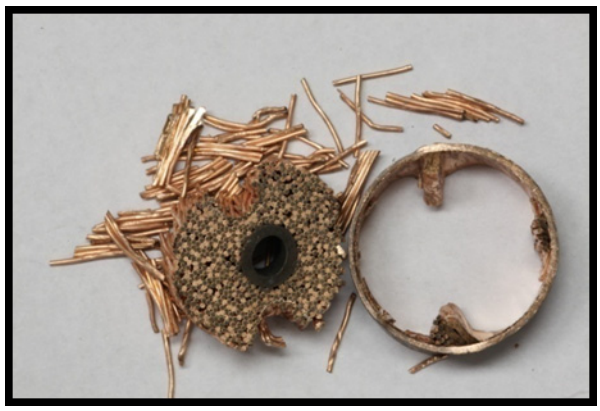


Figure A84: Sample 3C

4 Weeks 100˚C



Figure A85: Sample 6A



Figure A86: Sample 1C



Figure A87: Sample 7A



Figure A88: Sample 13C

Scales for Microscope Photo

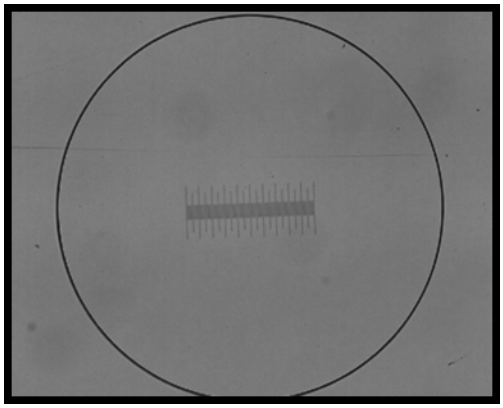


Figure A89: 1mm at 25x

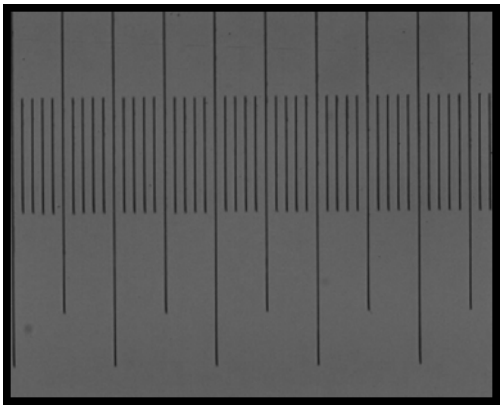


Figure A92: 1mm at 200x

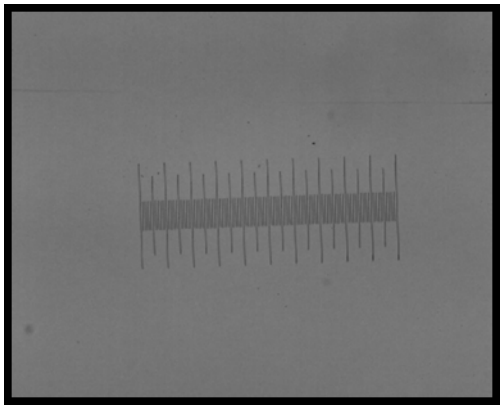


Figure A90: 1mm at 50x

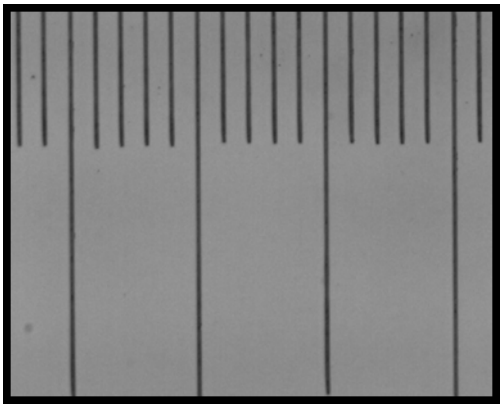


Figure A93: 1mm at 500x

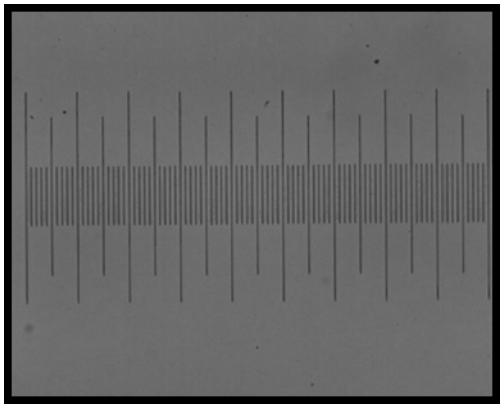


Figure A91: 1mm at 100x

Temperature and Humidity Recordings:

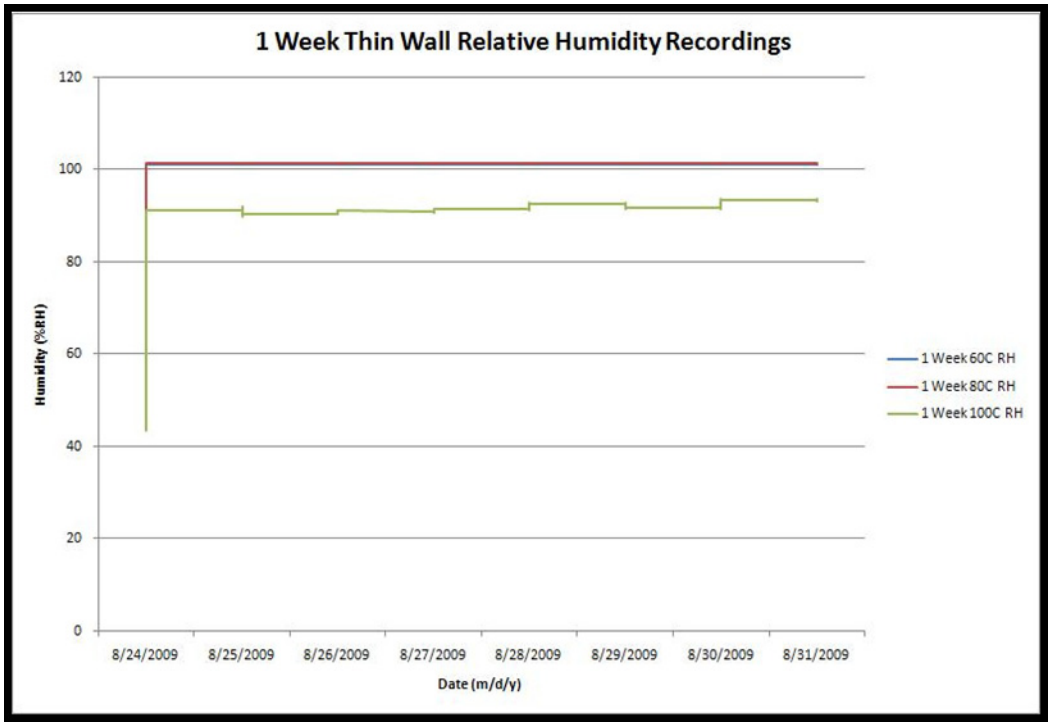


Figure A94: 1 Week Thin Wall RH

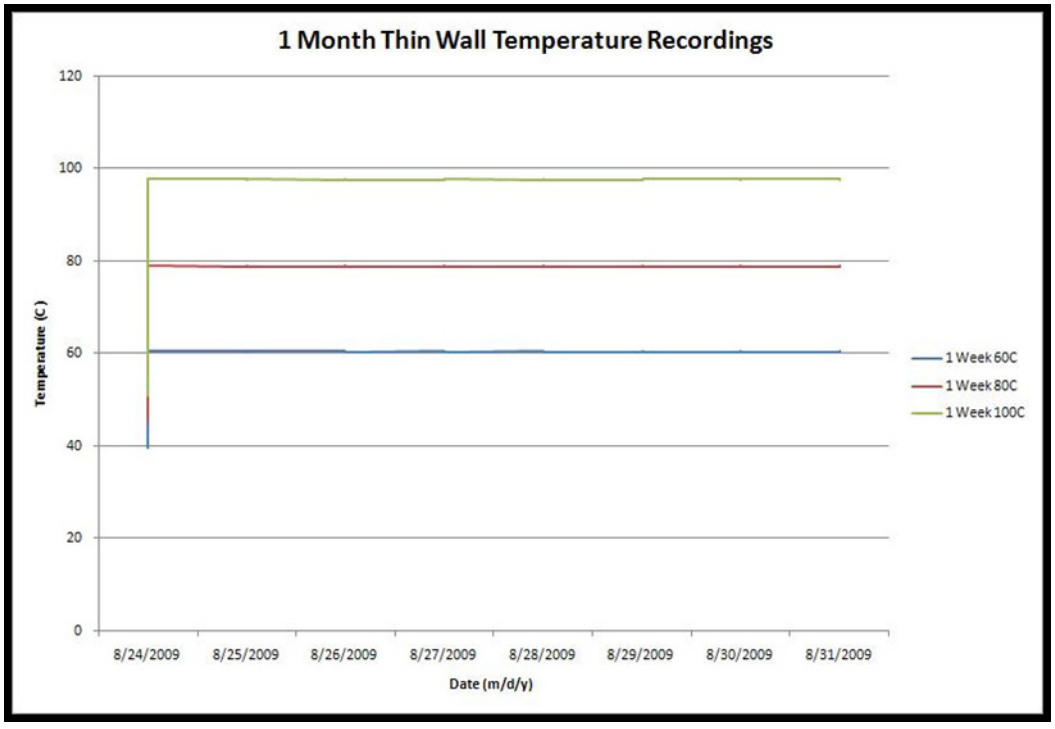


Figure A95: 1 Week Thin Wall Temperature

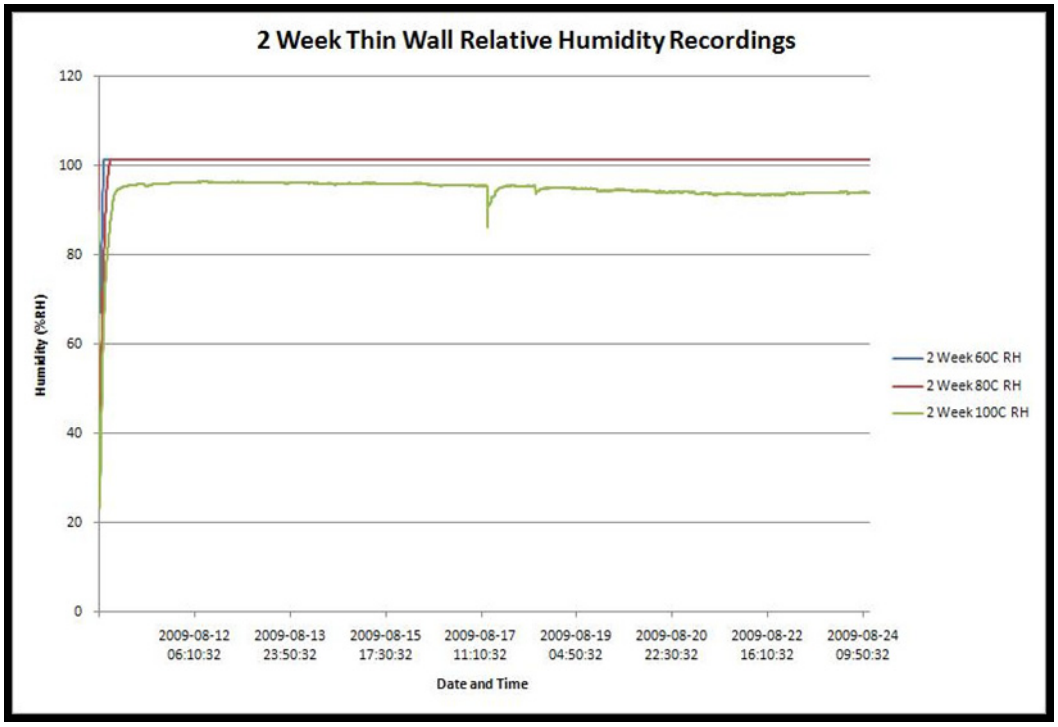


Figure A96: 2 Week Thin Wall RH

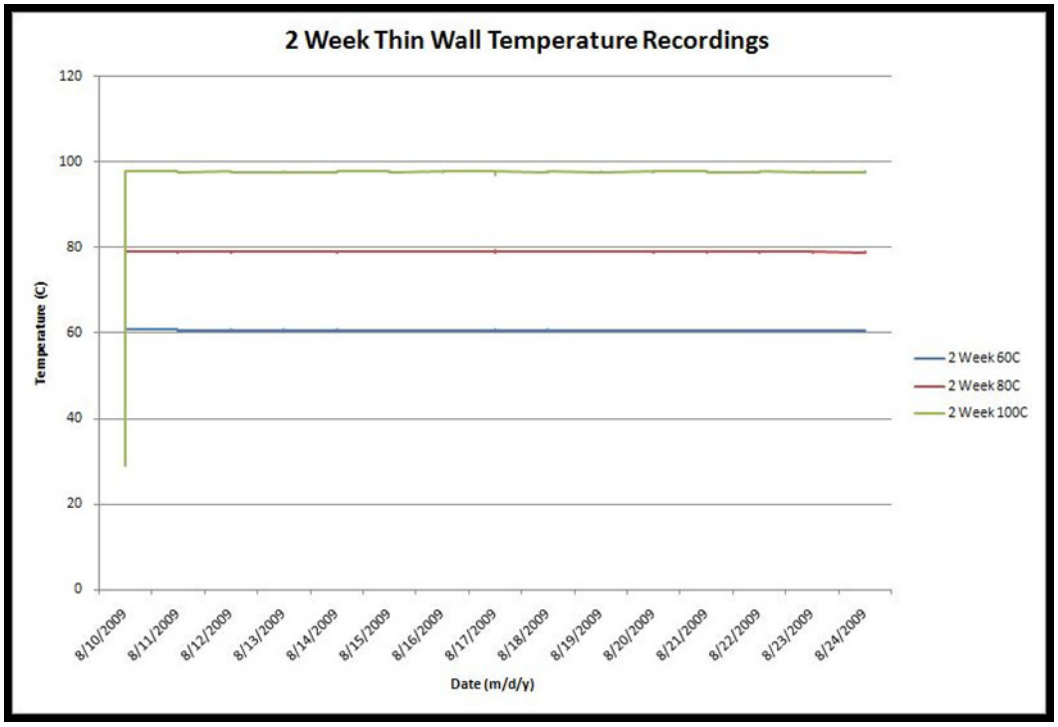


Figure A97: 2 Week Thin Wall Temperature

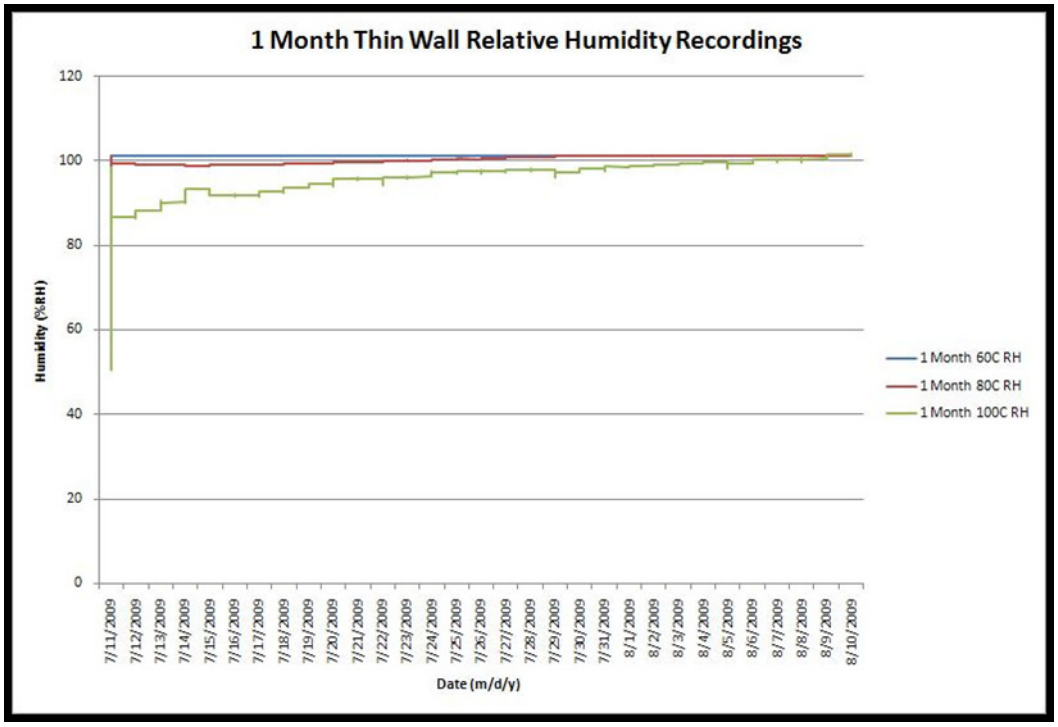


Figure A98: 1 Month Thin Wall RH

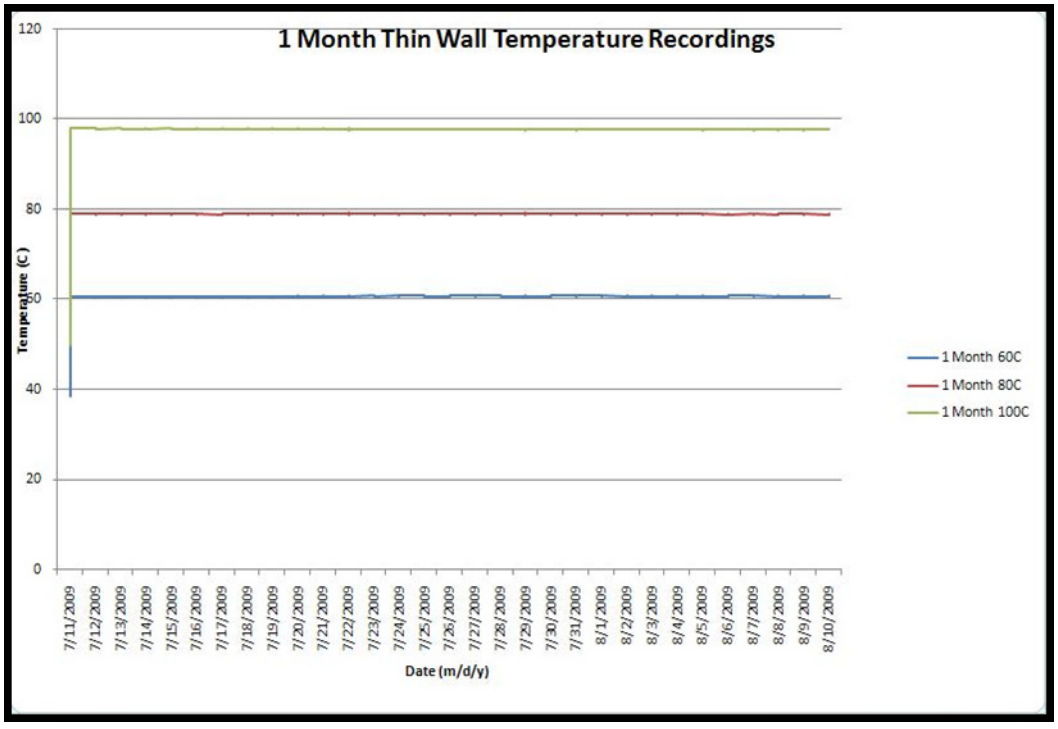


Figure A99: 1 Month Thin Wall Temperature

Thick Walled Sample X Pictures:

Pictures are arranged by soaking group and in the order of: un-soaked, soaked, sintered, pressed.

Un-Soaked Un-Sintered

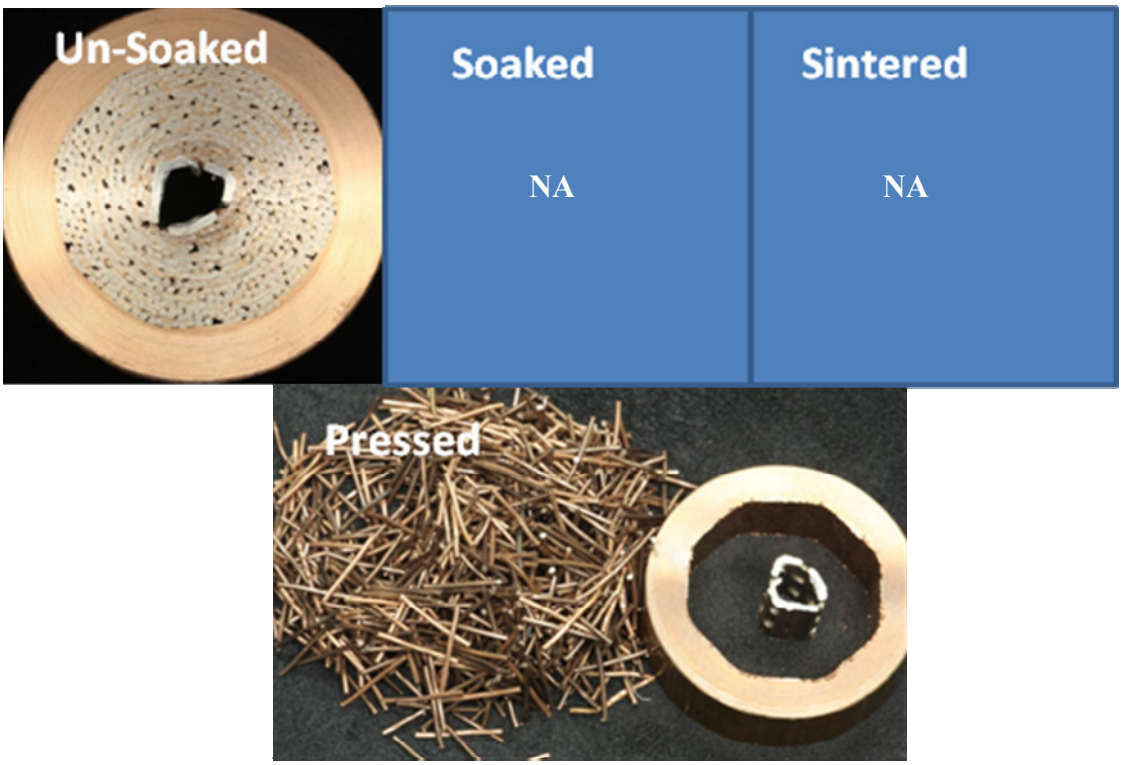


Figure A100: Sample 35X

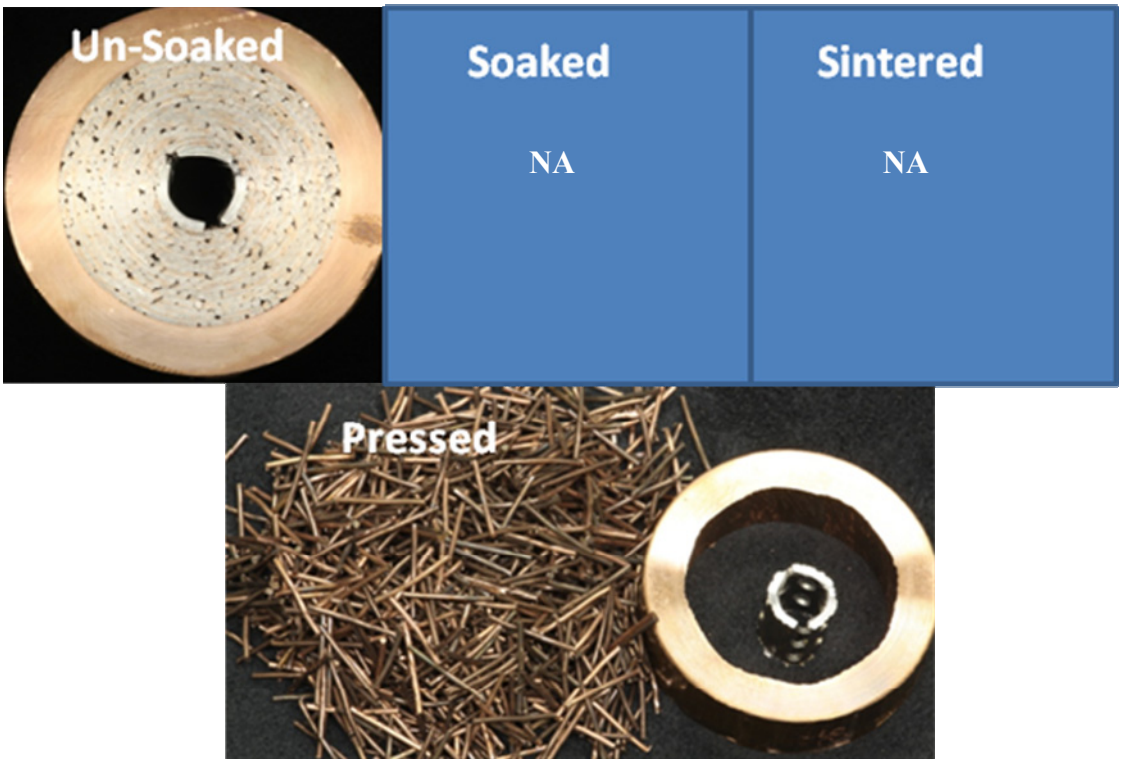


Figure A101: Sample 36X

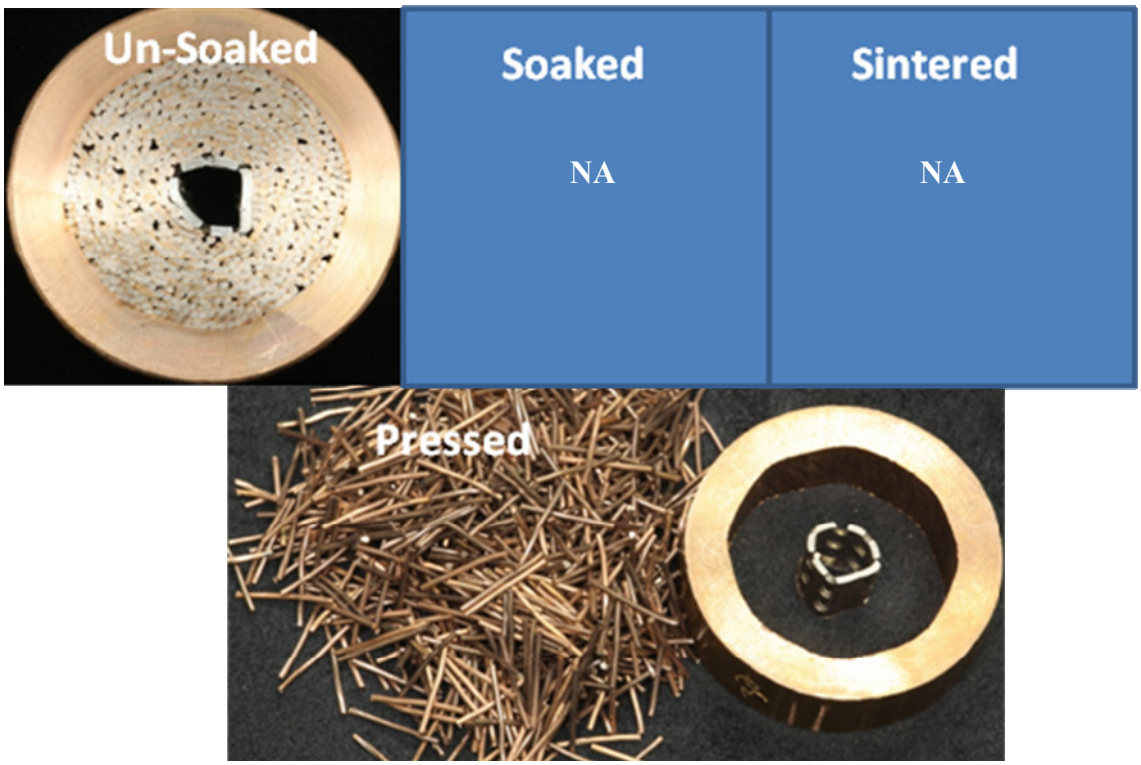


Figure A102: Sample 37X

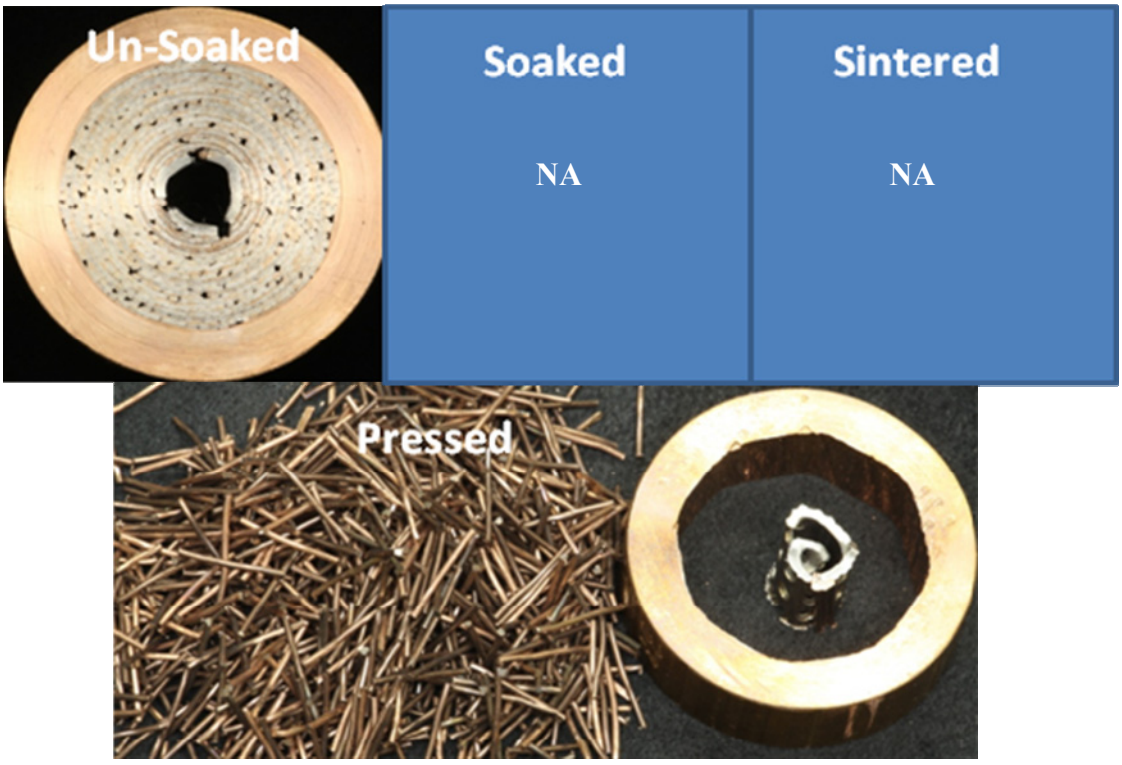


Figure A103: Sample 38X

Un-Soaked Sintered

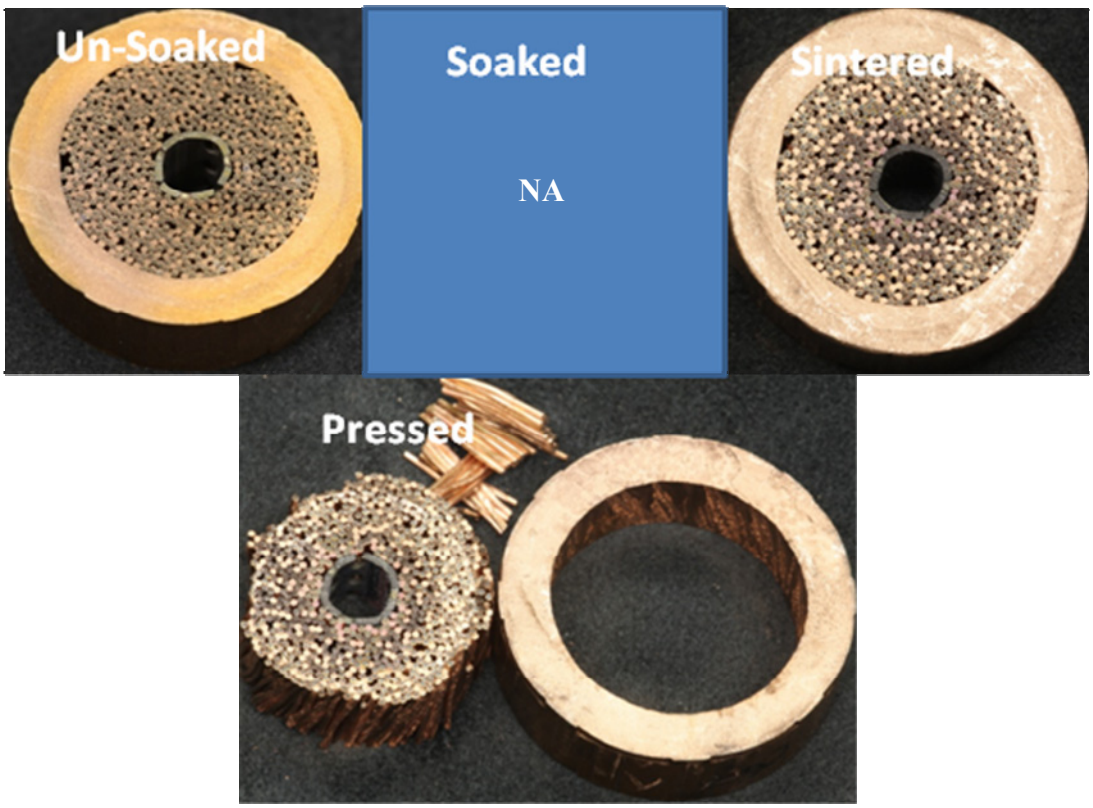


Figure A104: Sample 2X

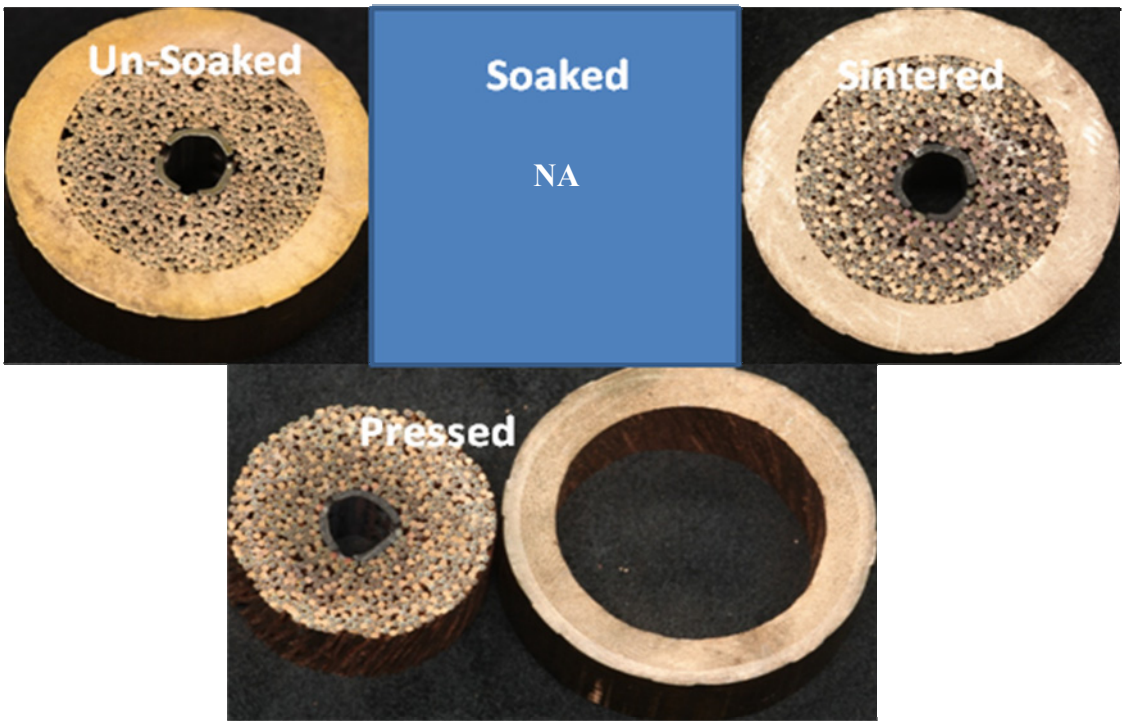


Figure A105: Sample 3X

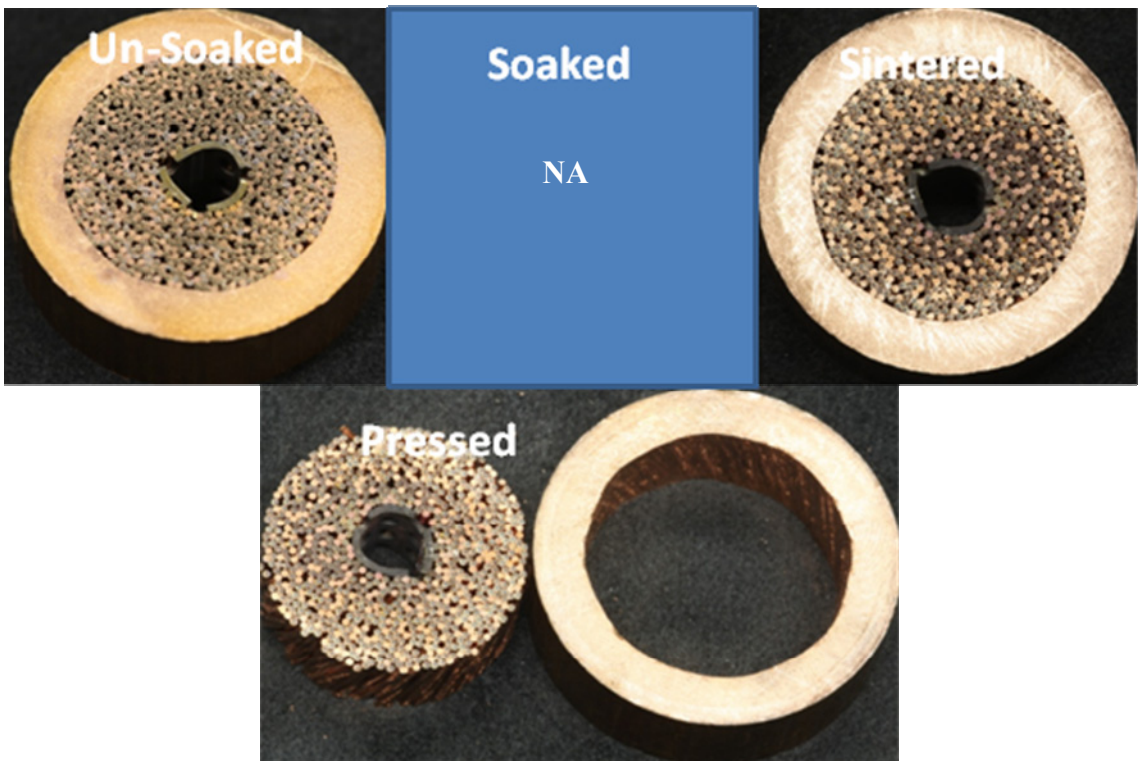


Figure A106: Sample 6X

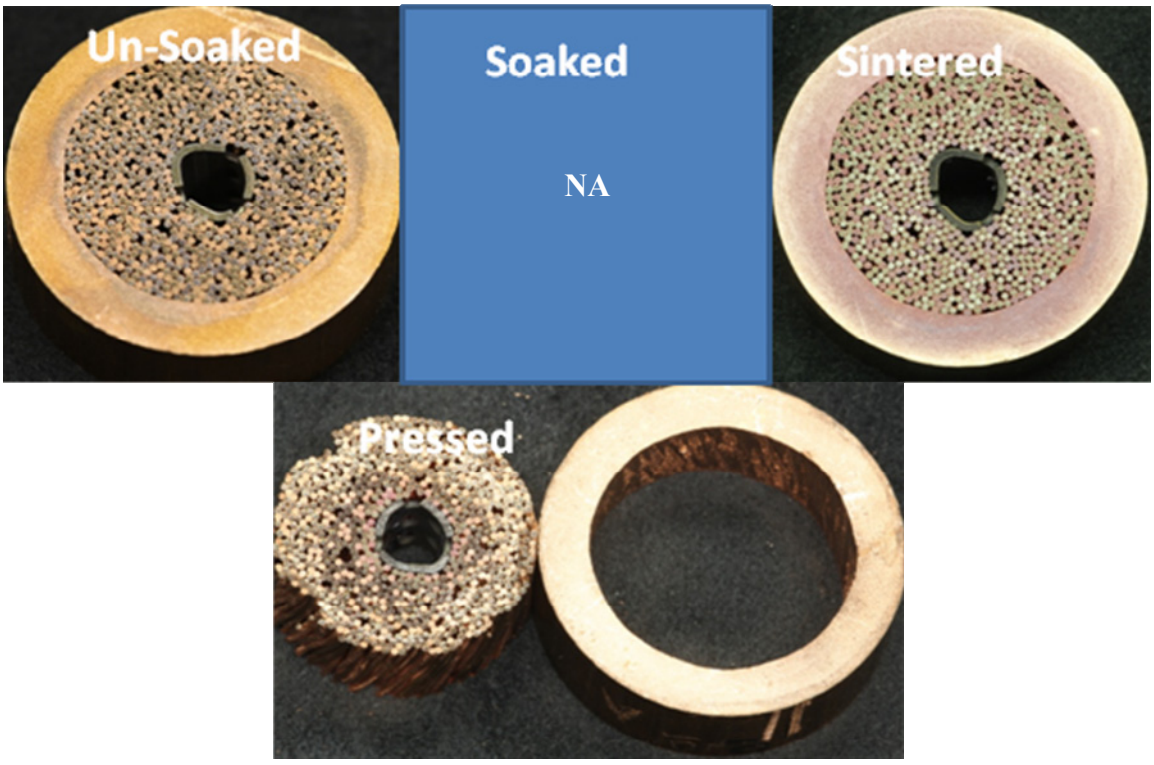


Figure A107: Sample 10X

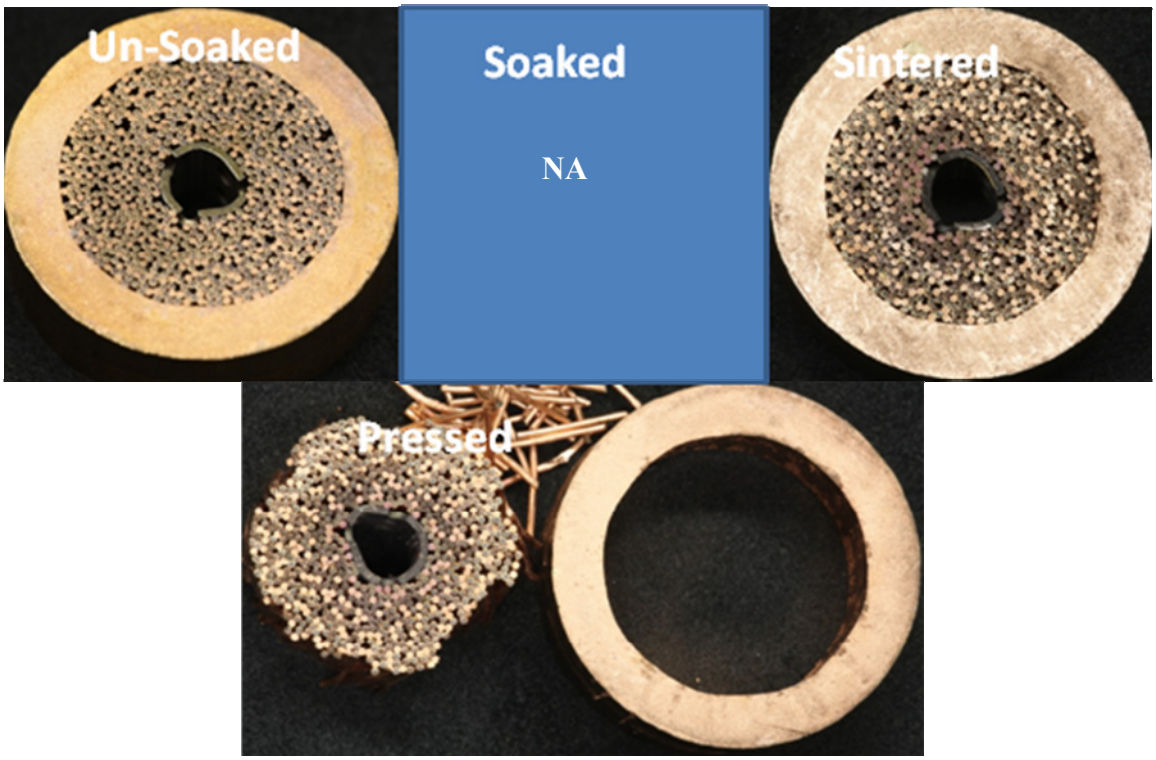


Figure A108: Sample 29X

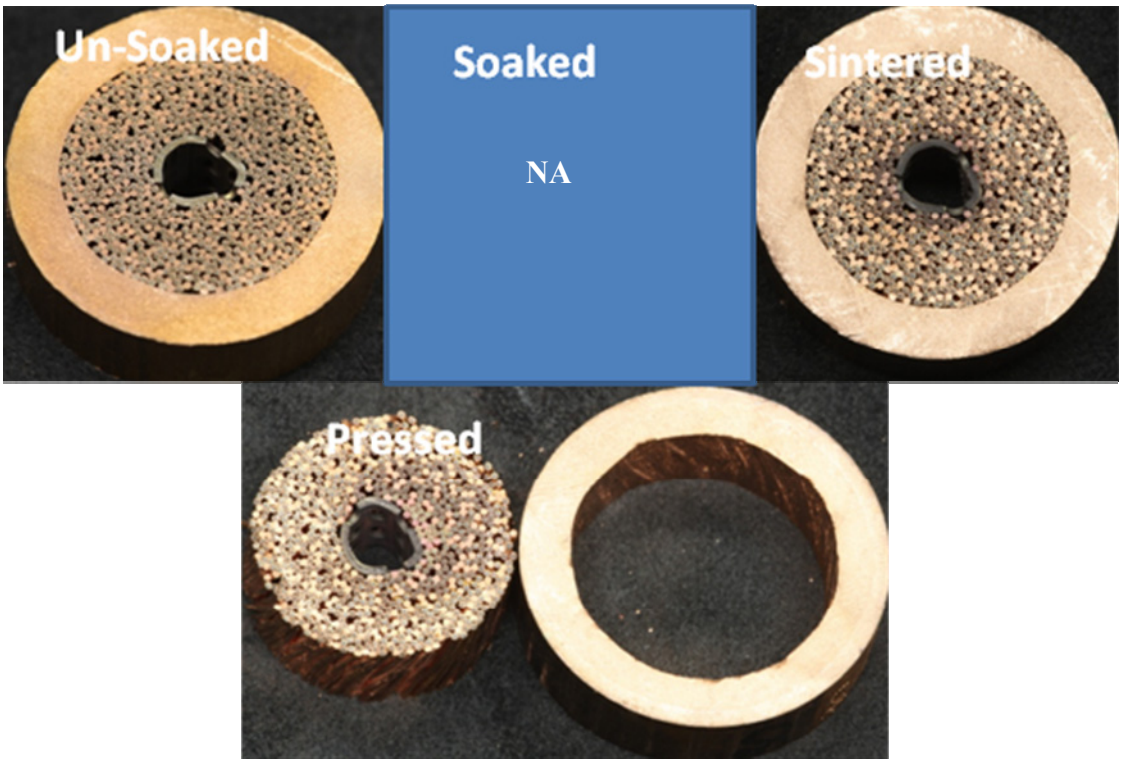


Figure A109: Sample 30X

Two Weeks 80˚C

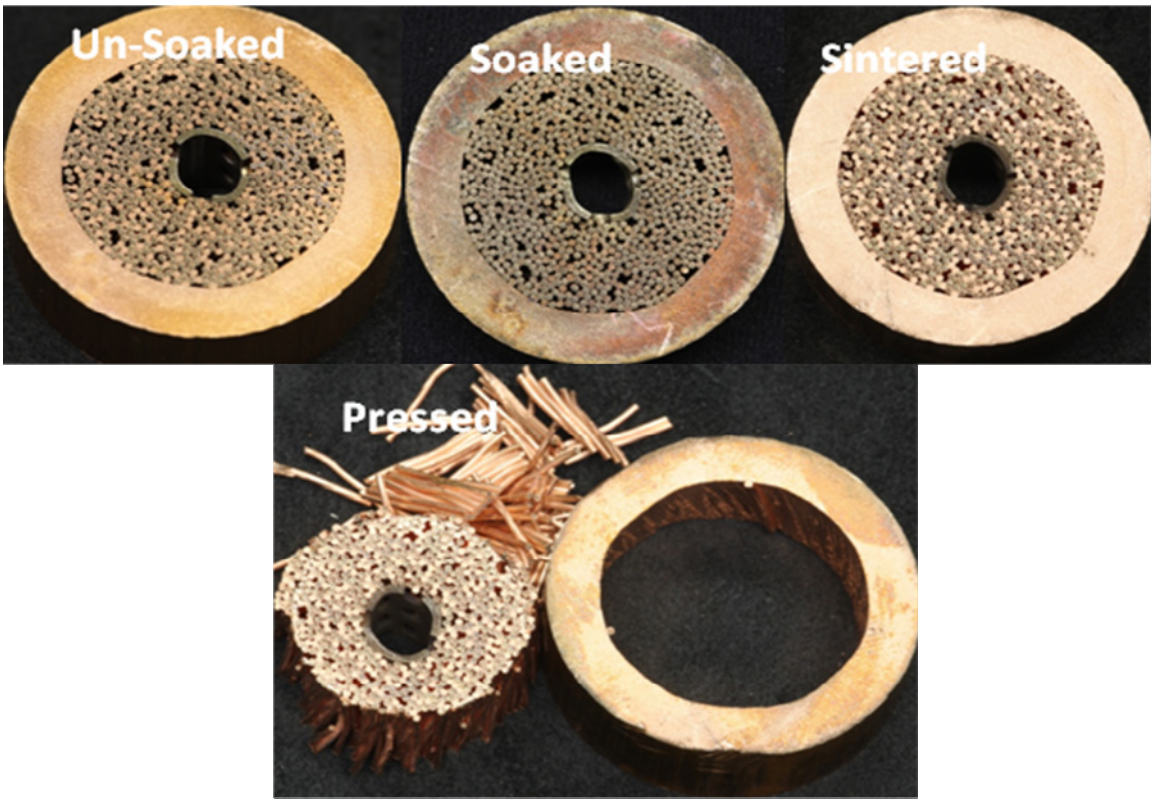


Figure A110: Sample 20X

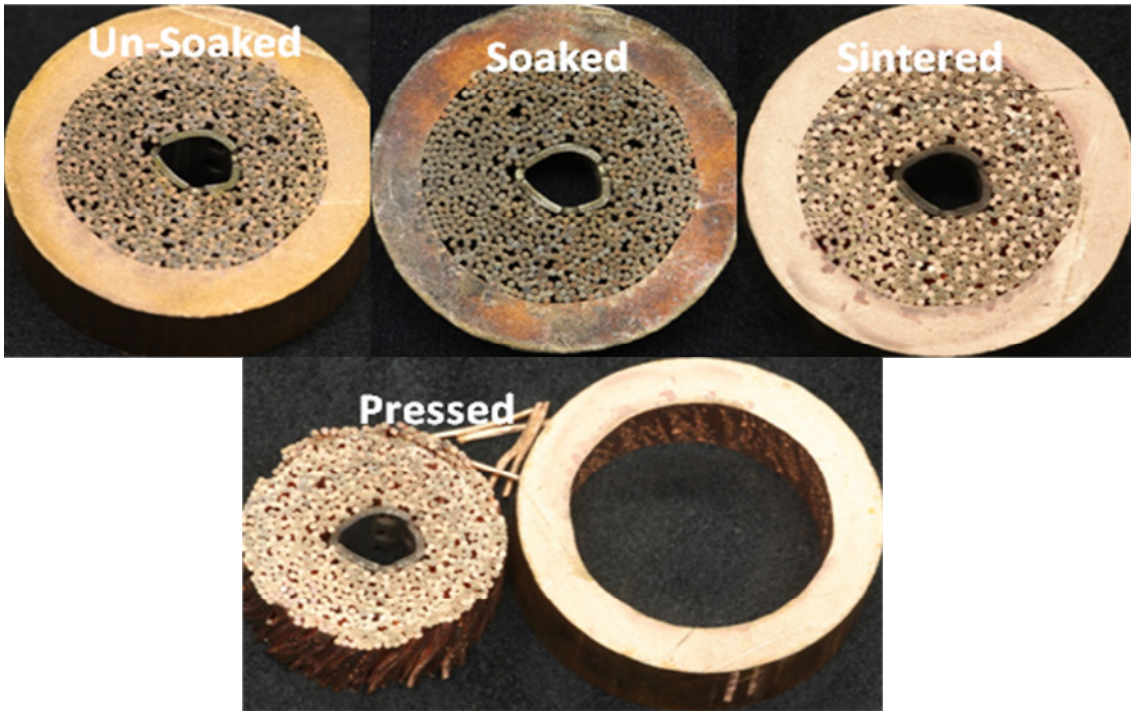


Figure A111: Sample 8X

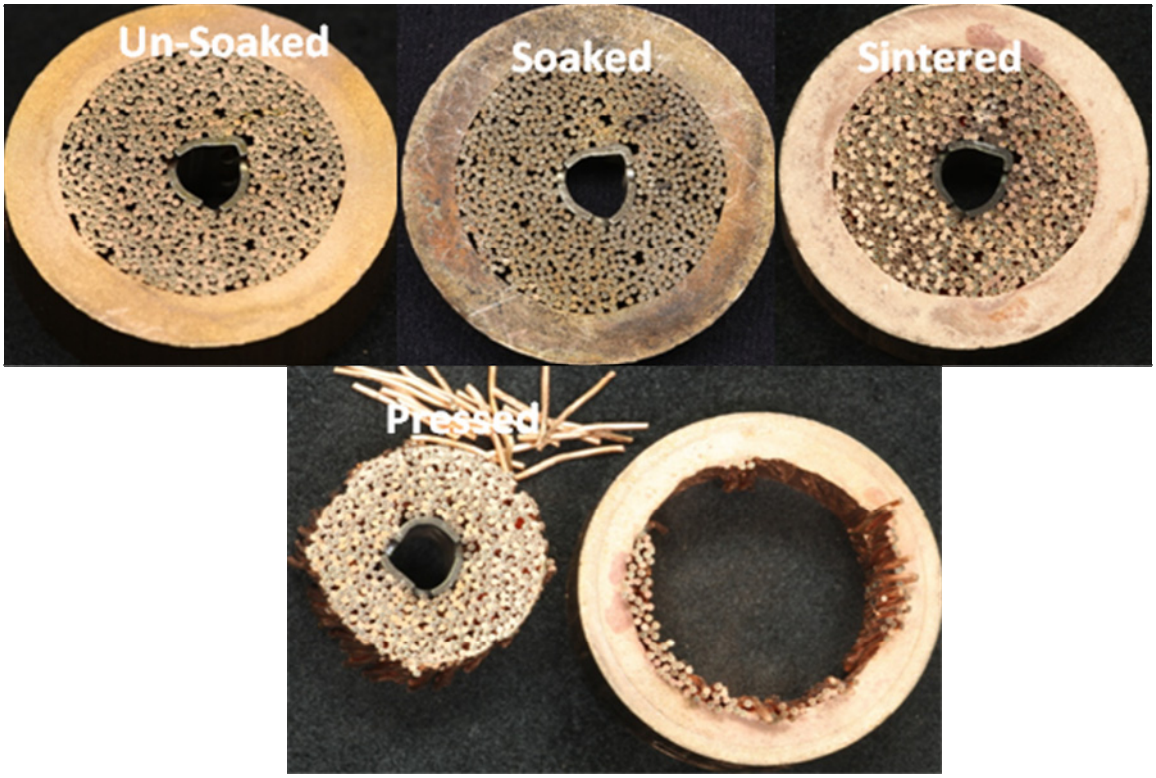


Figure A112: Sample 17X

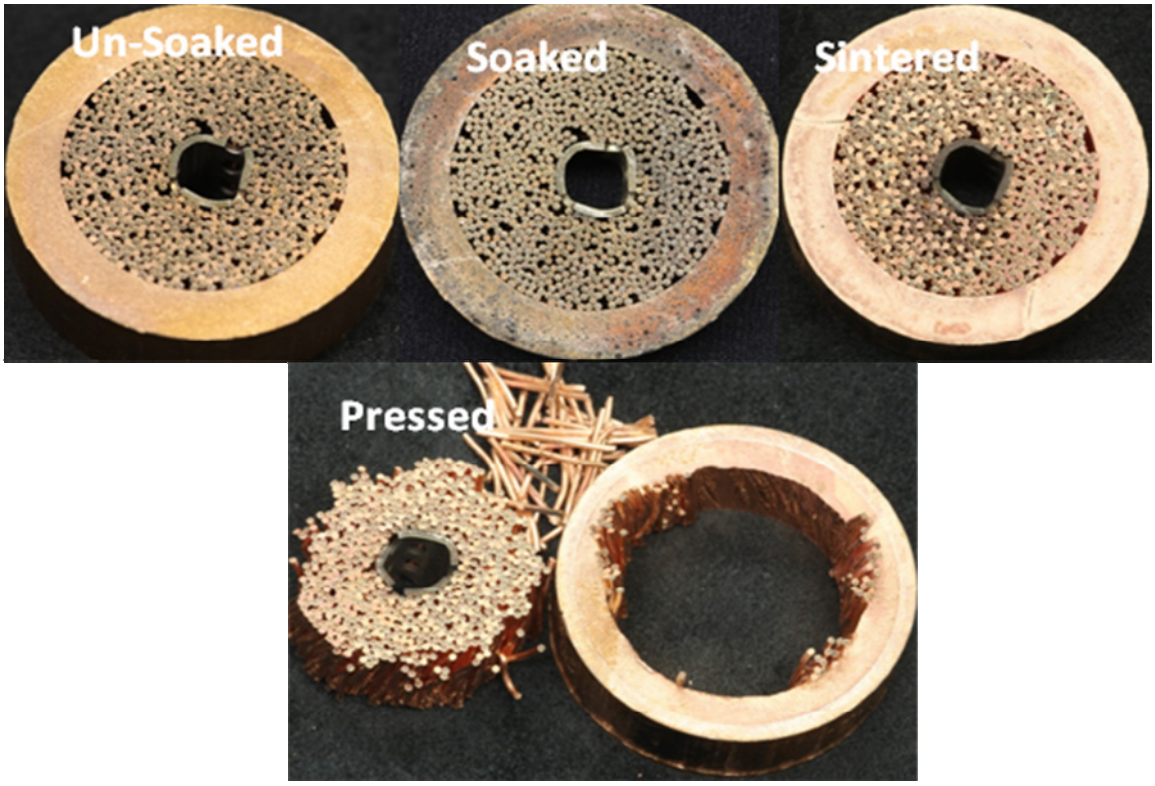


Figure A113: Sample 18X

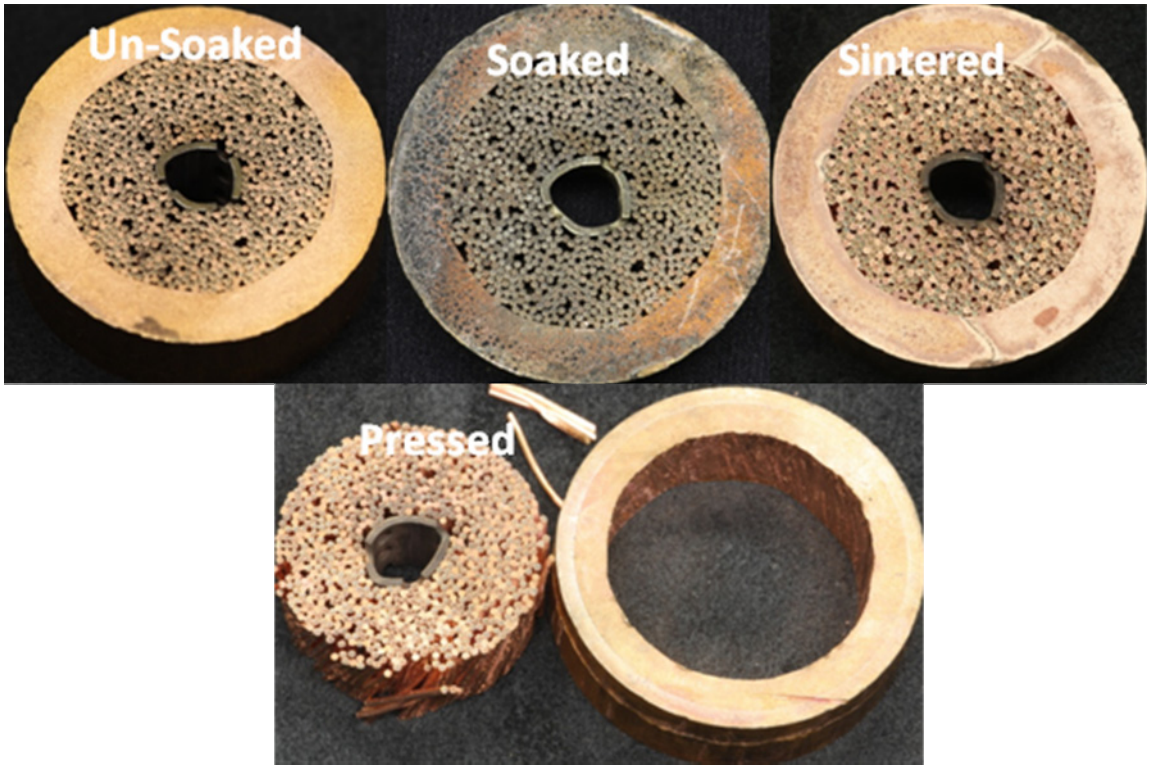


Figure A114: Sample 7X

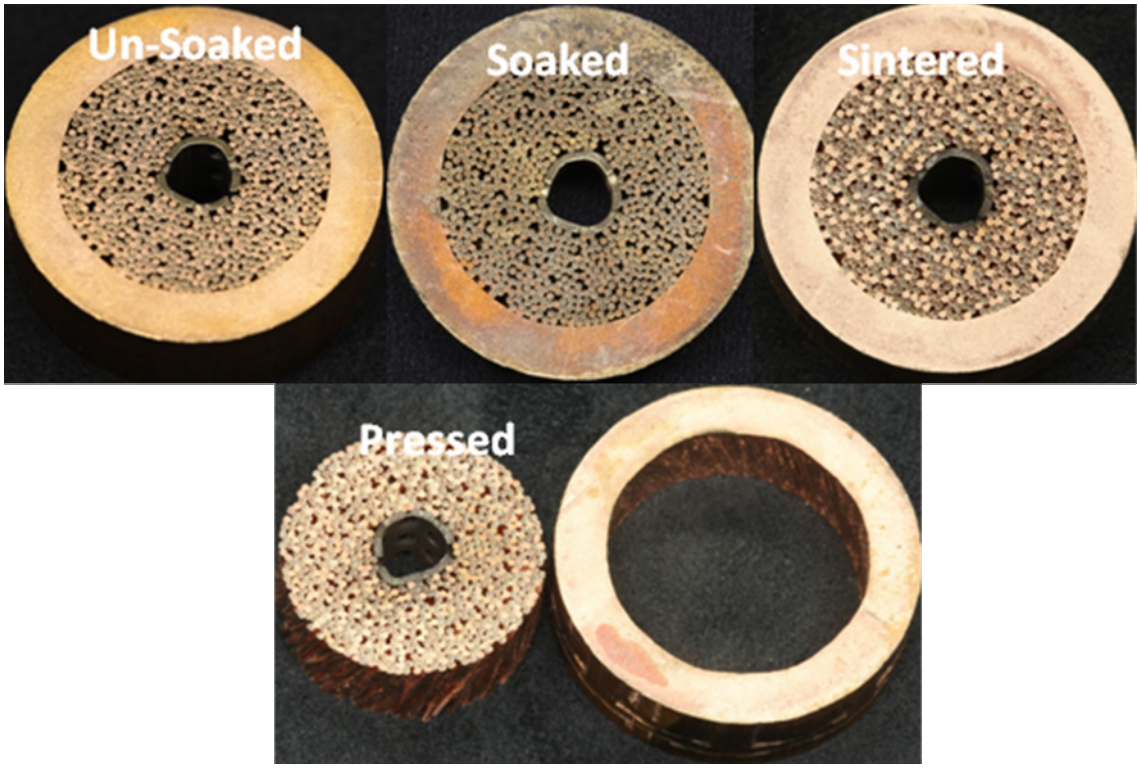


Figure A115: Sample 5X

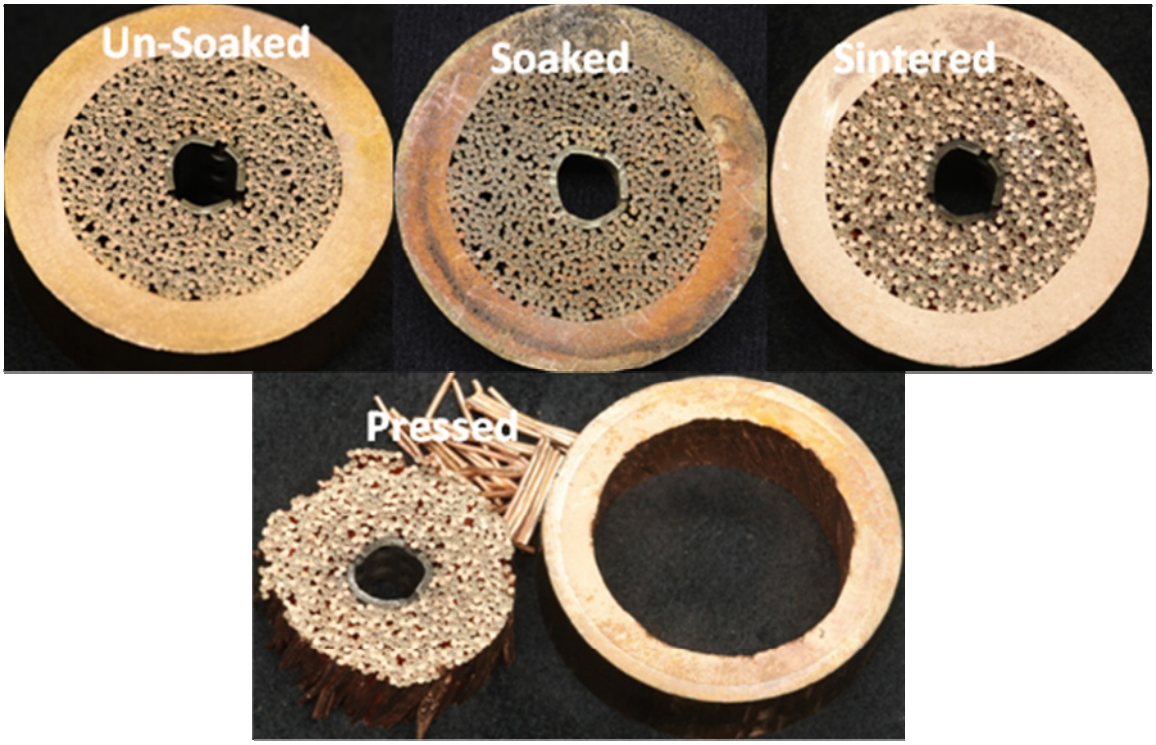


Figure A116: Sample 19X

Two Weeks 100˚C

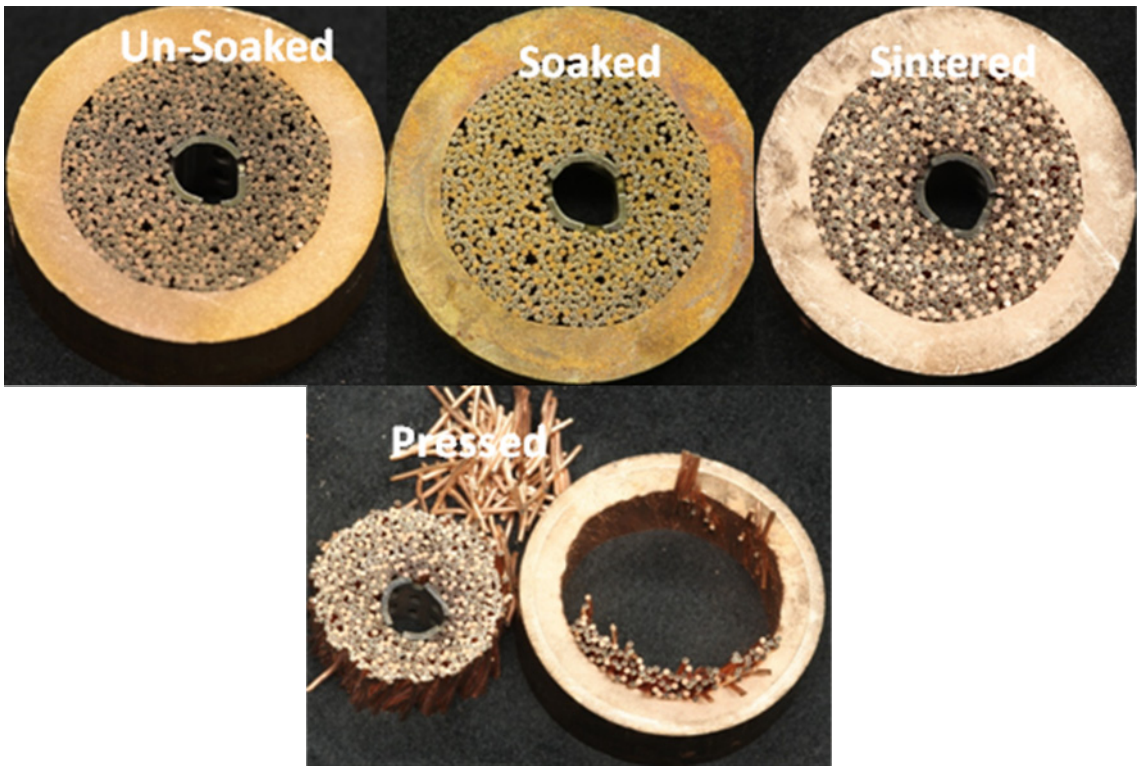


Figure A117: Sample 14X

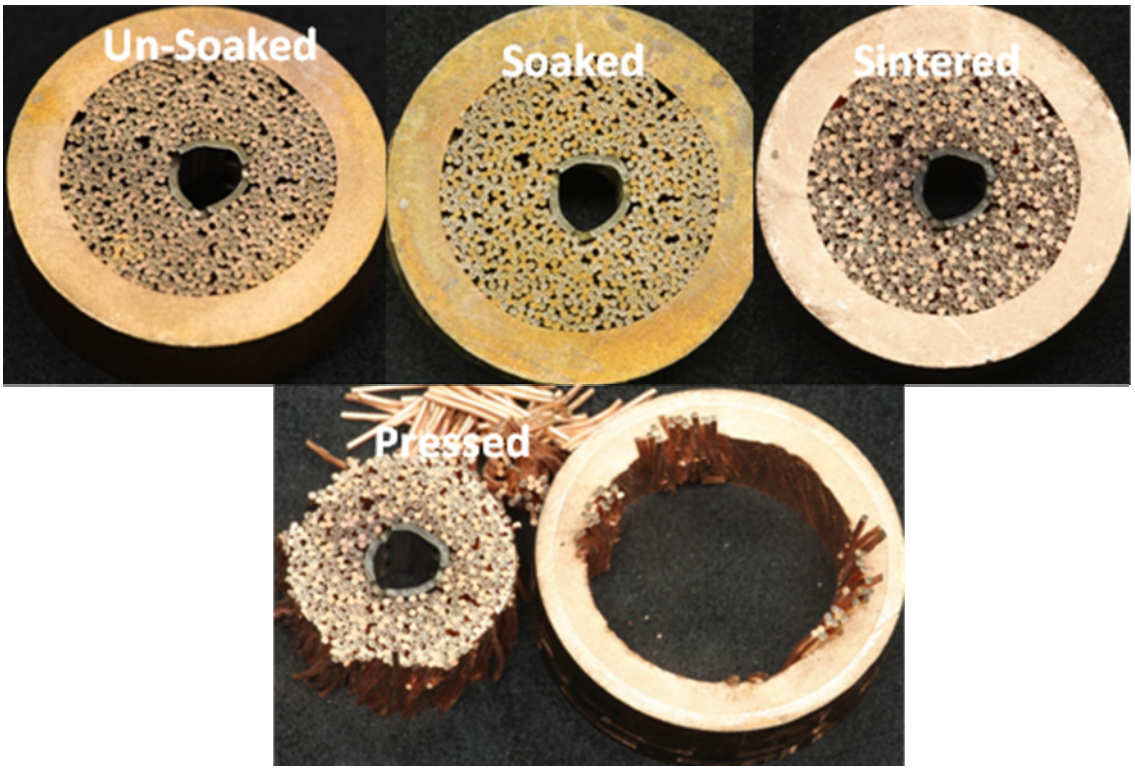


Figure A118: Sample 11X

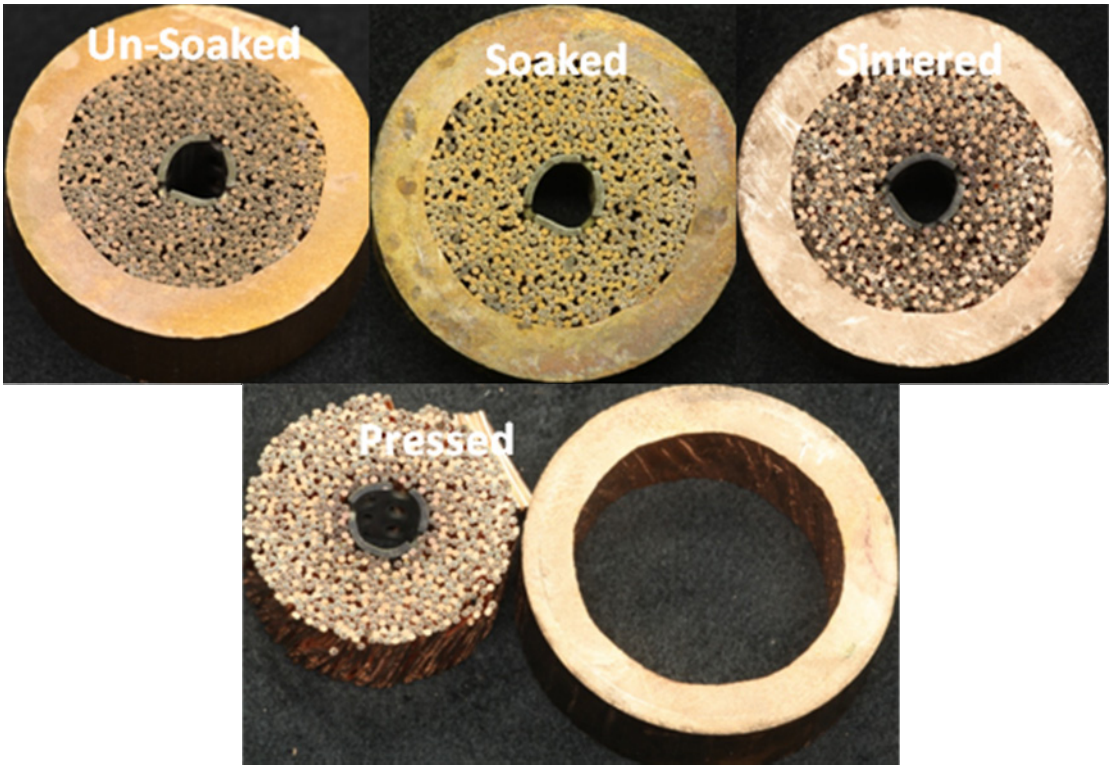


Figure A119: Sample 4X

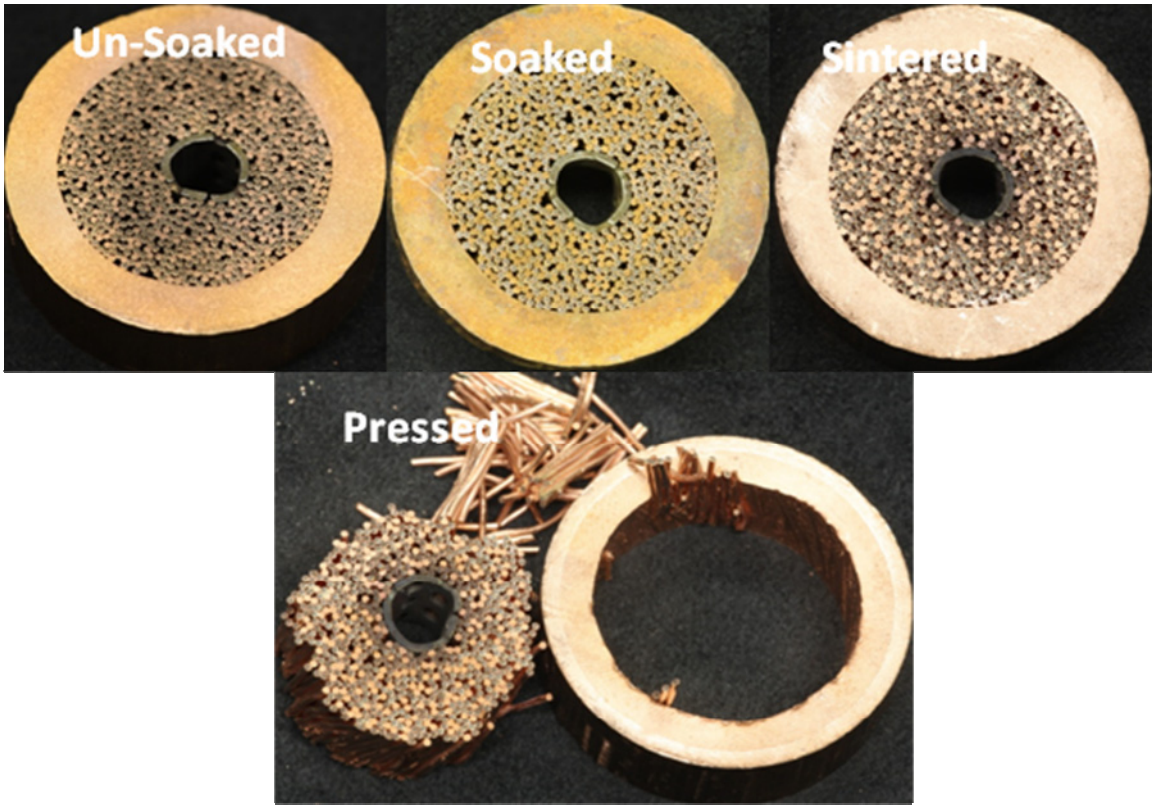


Figure A120: Sample 15X

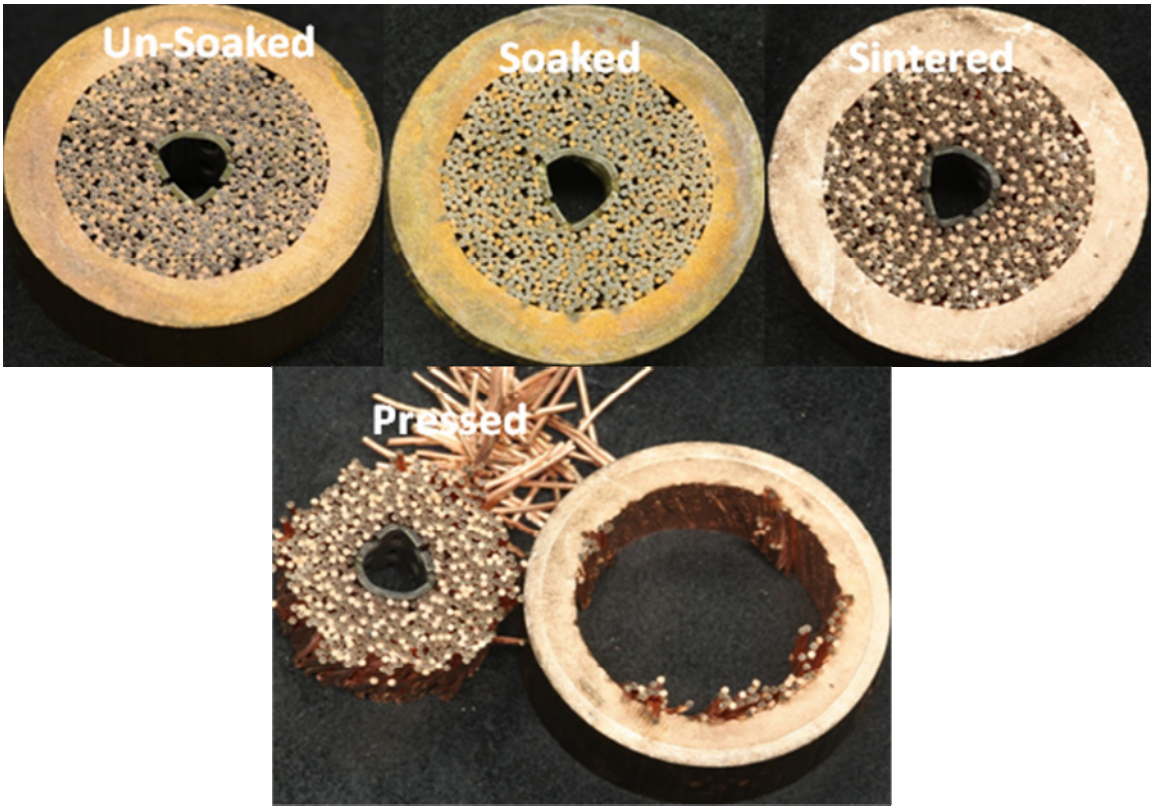


Figure A121: Sample 28X

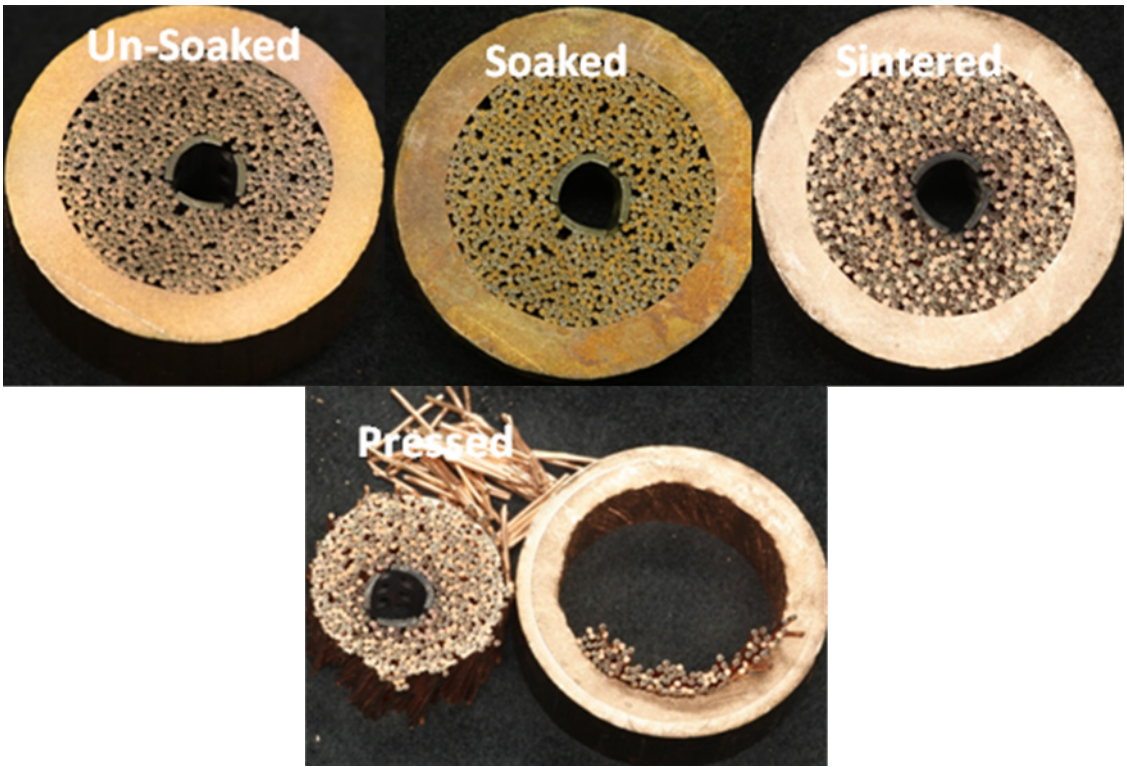


Figure A122: Sample 13X

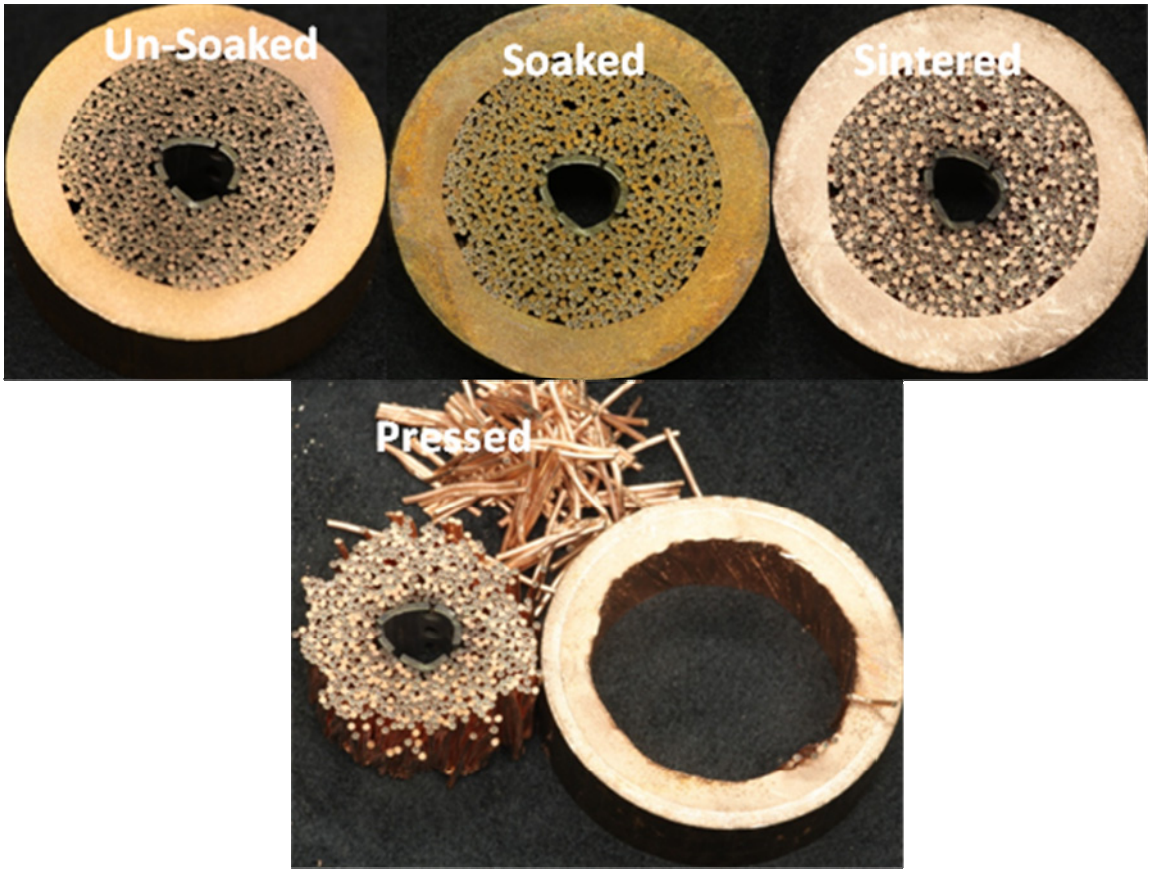


Figure A123: Sample 25X

Four Weeks 80˚C

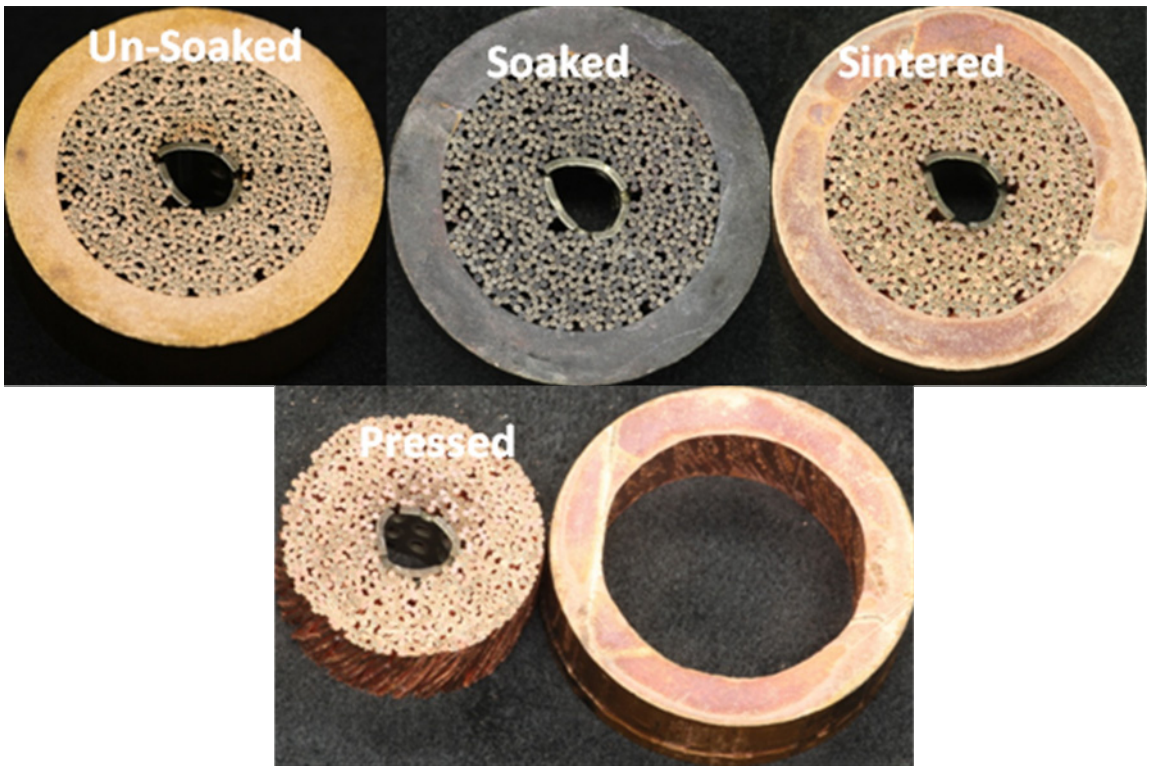


Figure A124: Sample 9X

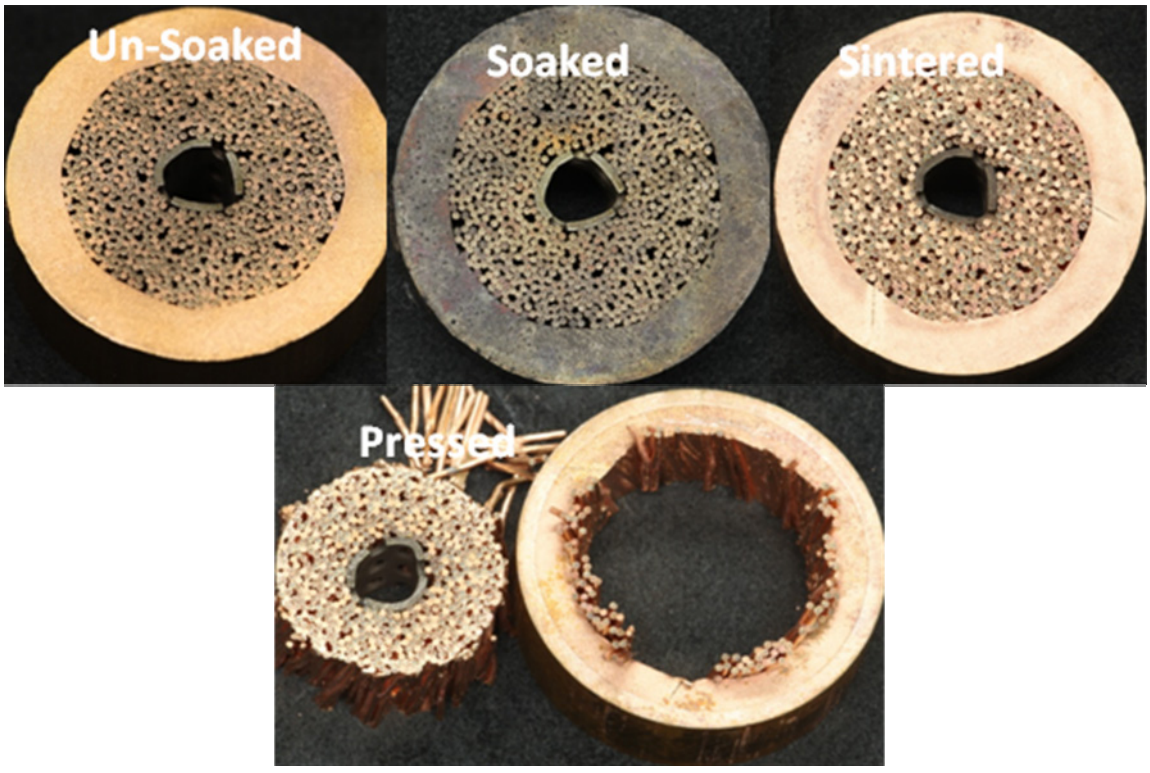


Figure A125: Sample 33X

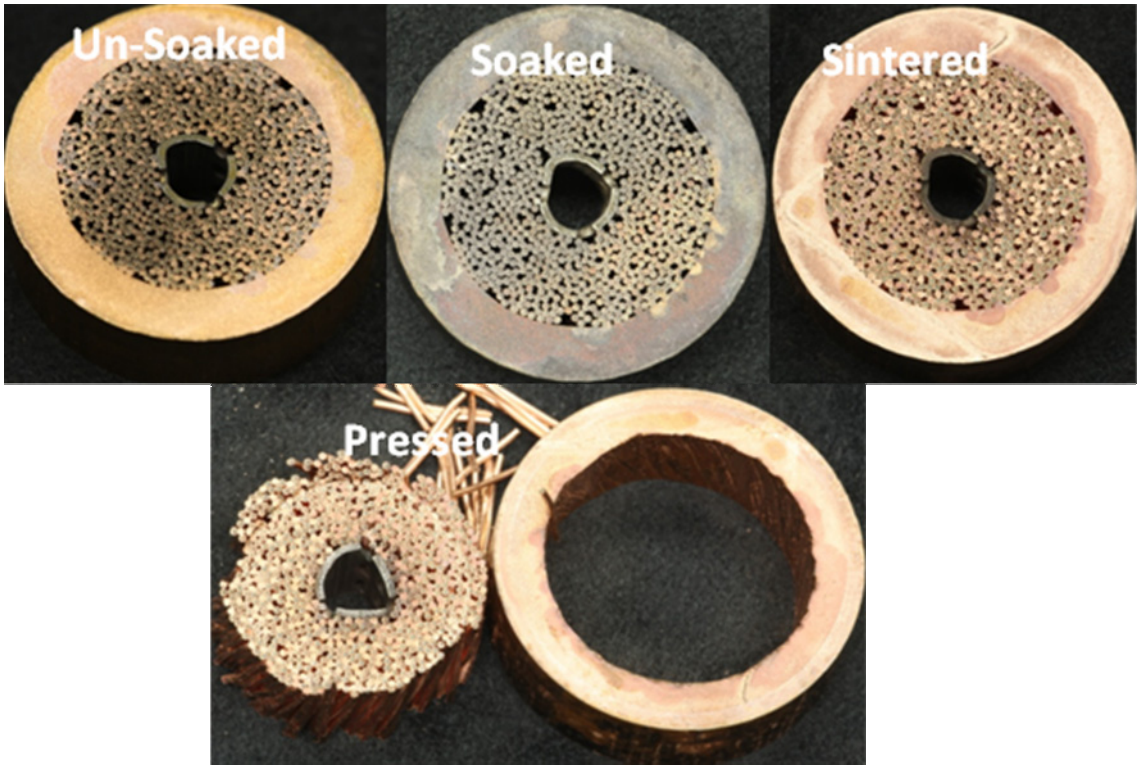


Figure A126: Sample 27X

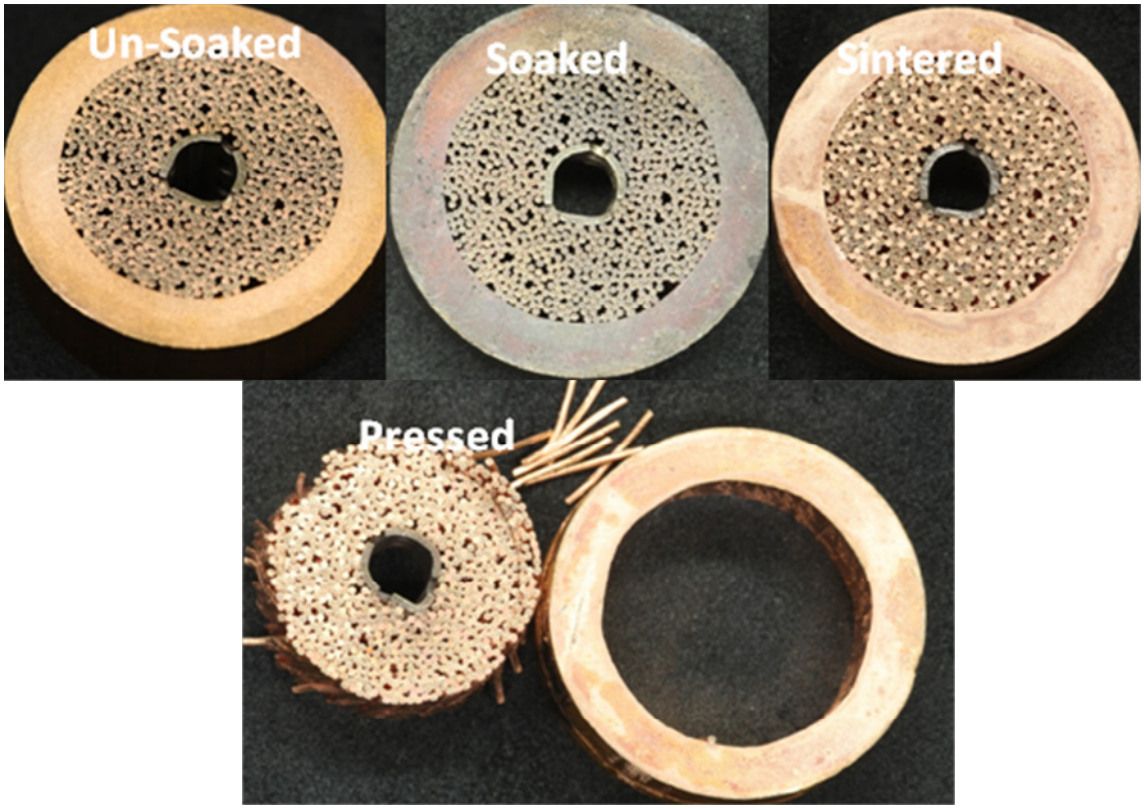


Figure A127: Sample 21X

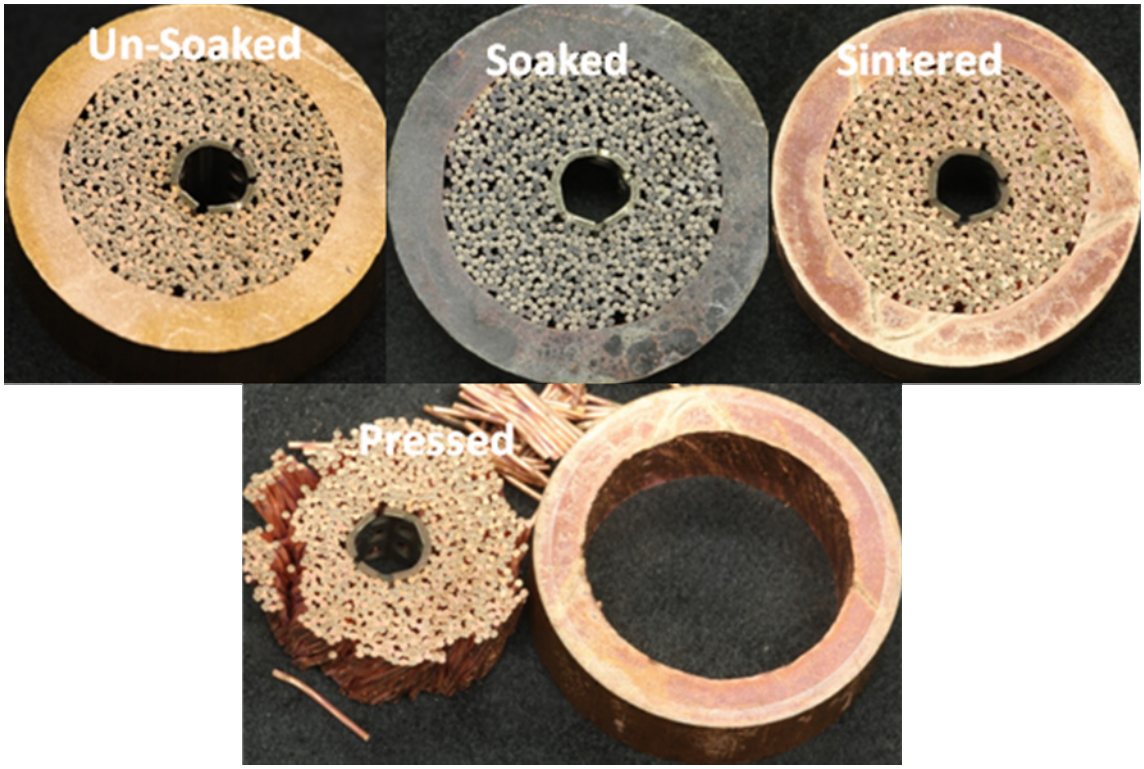


Figure A128: Sample 12X

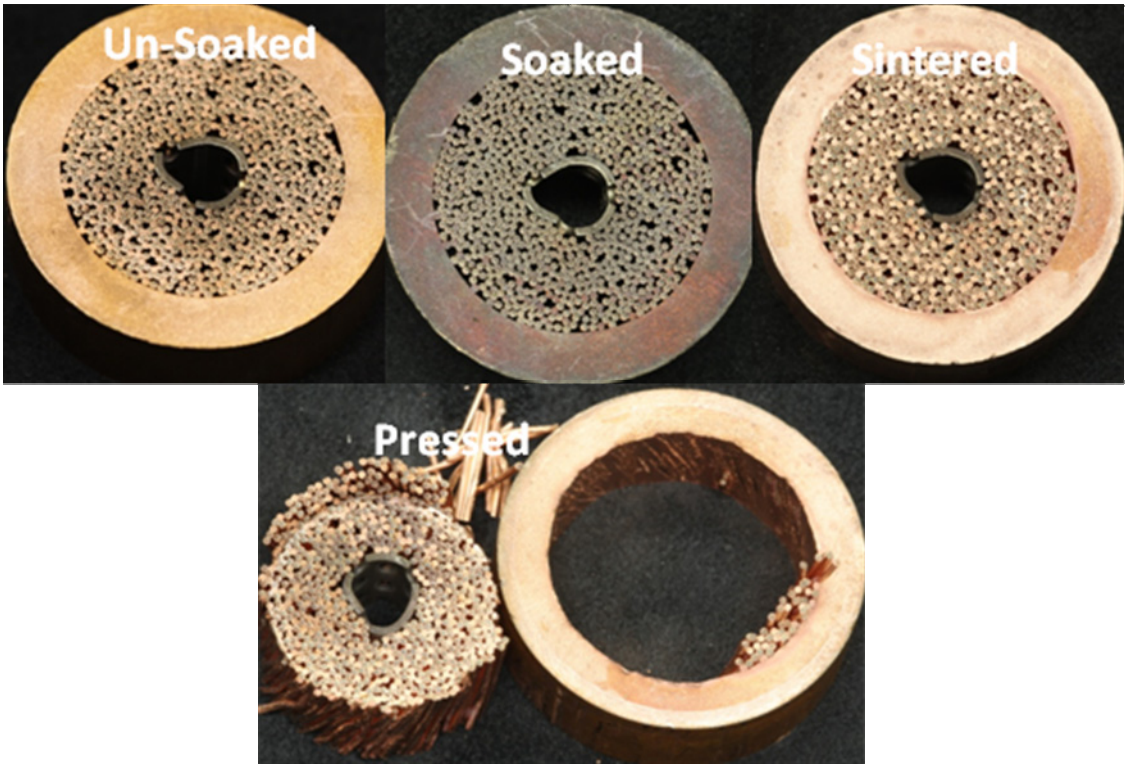


Figure A129: Sample 23X

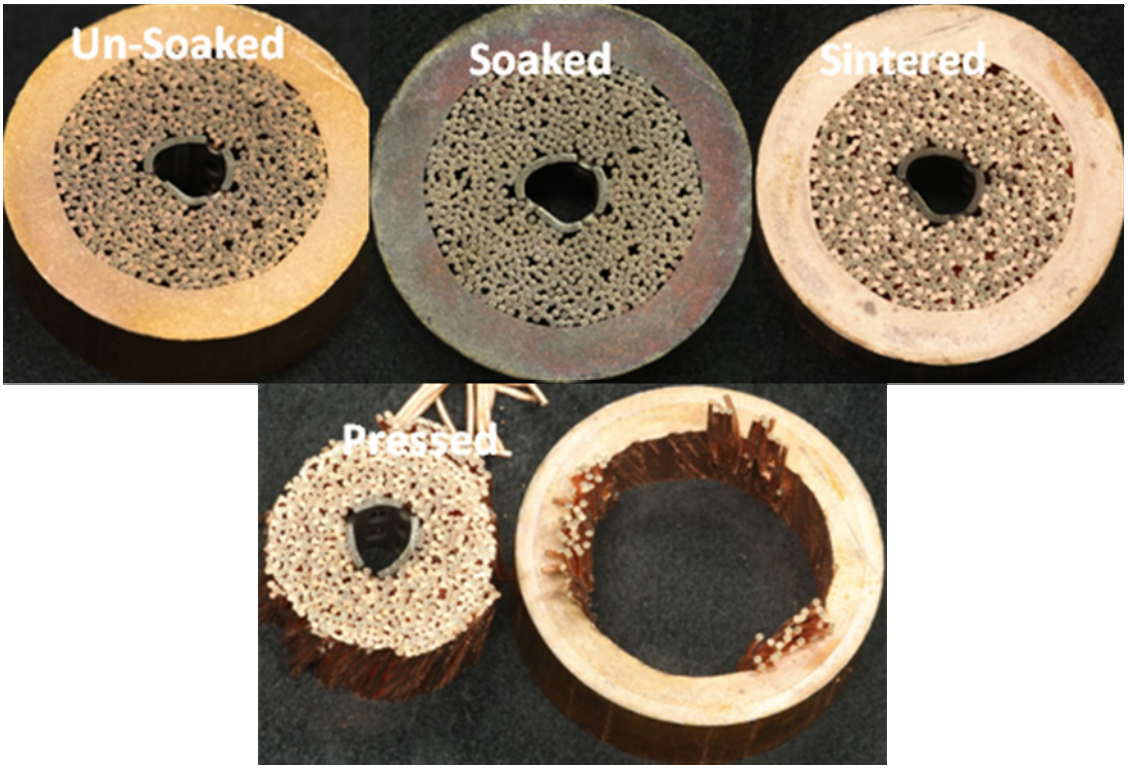


Figure A130: Sample 24X

Four Weeks 100˚C

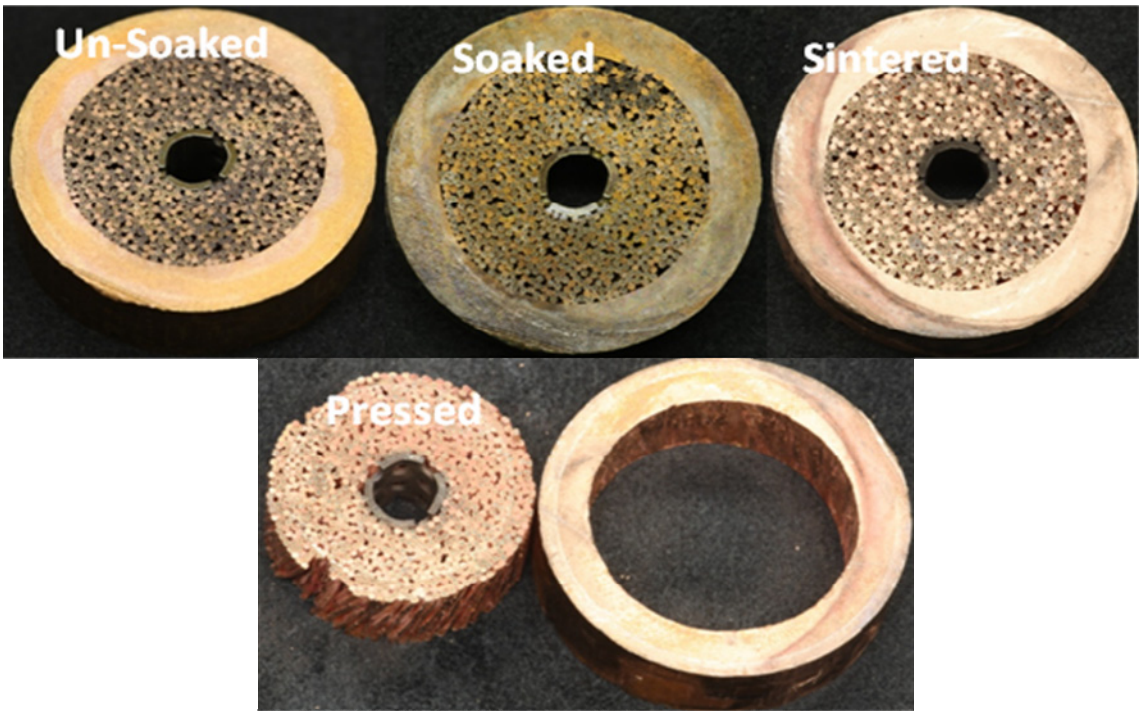


Figure A131: Sample 1X

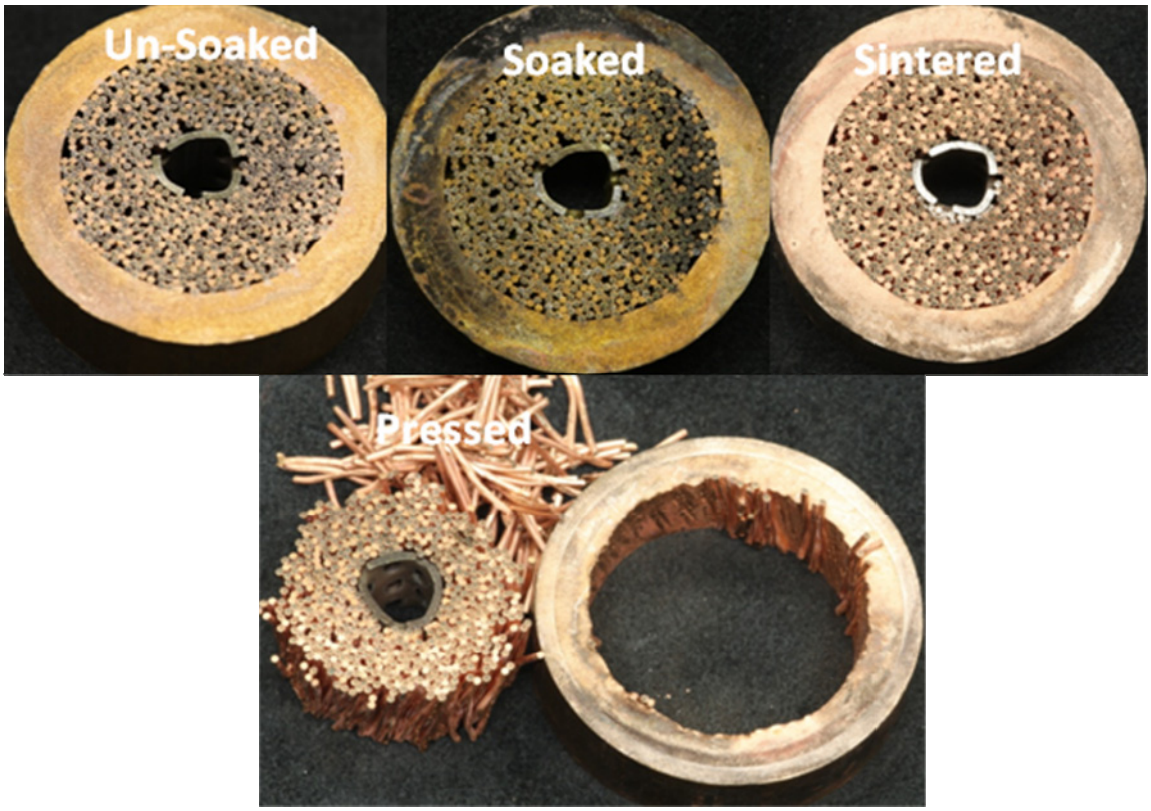


Figure A132: Sample 32X

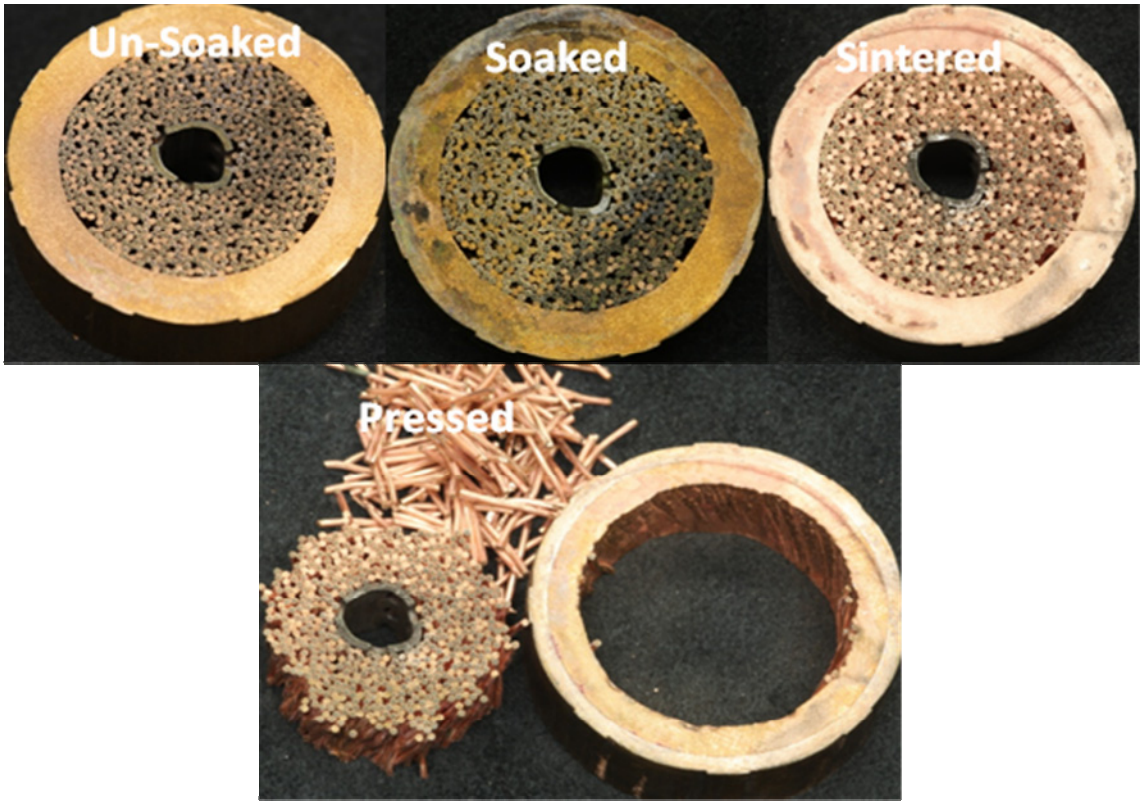


Figure A133: Sample 34X

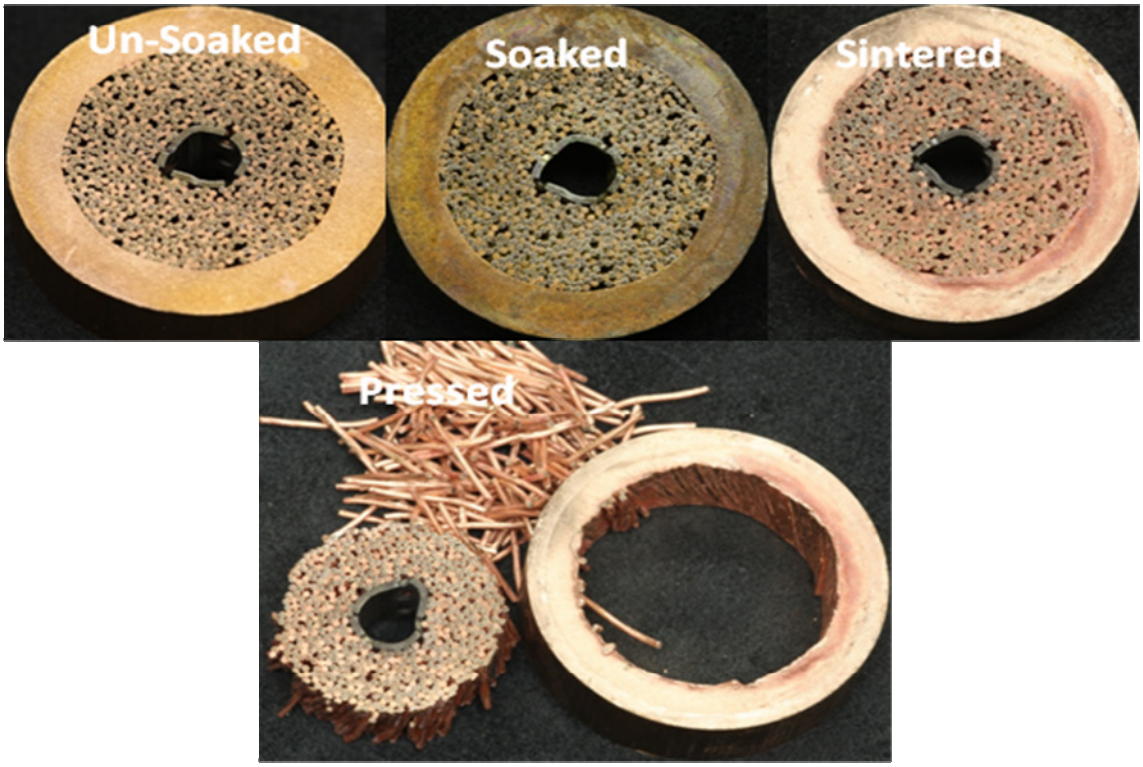


Figure A134: Sample 22X

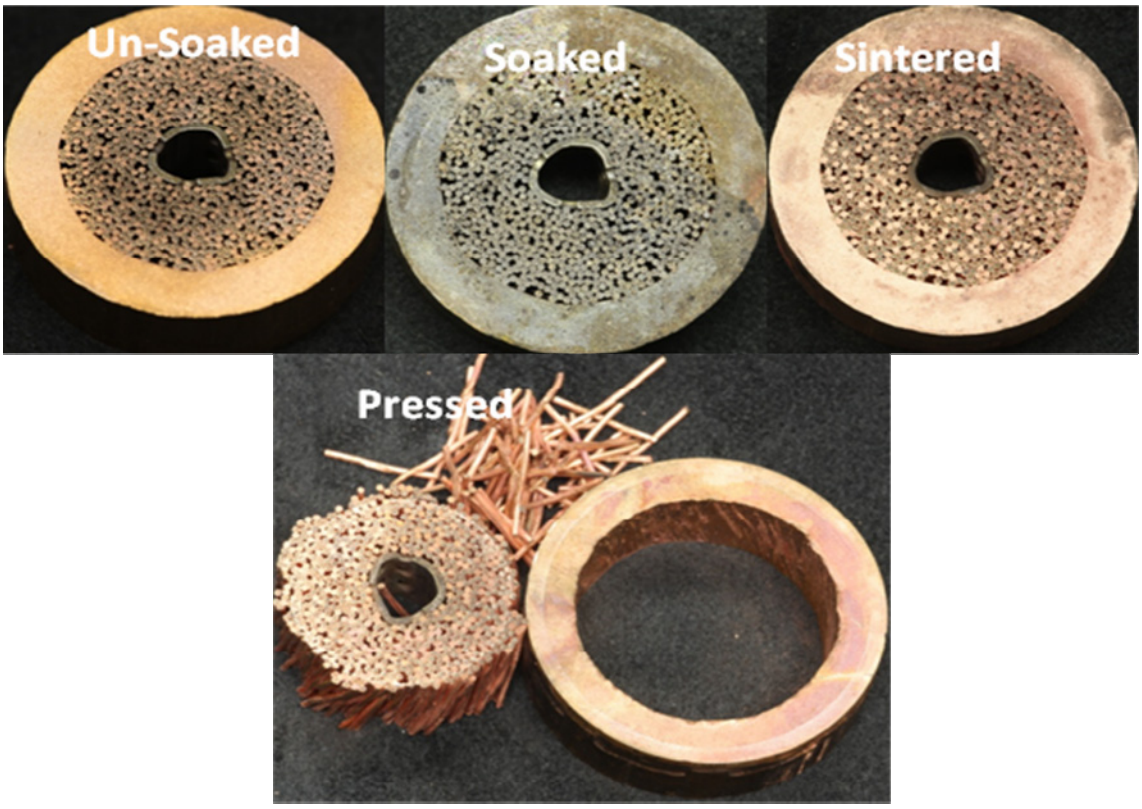


Figure A135: Sample 31X

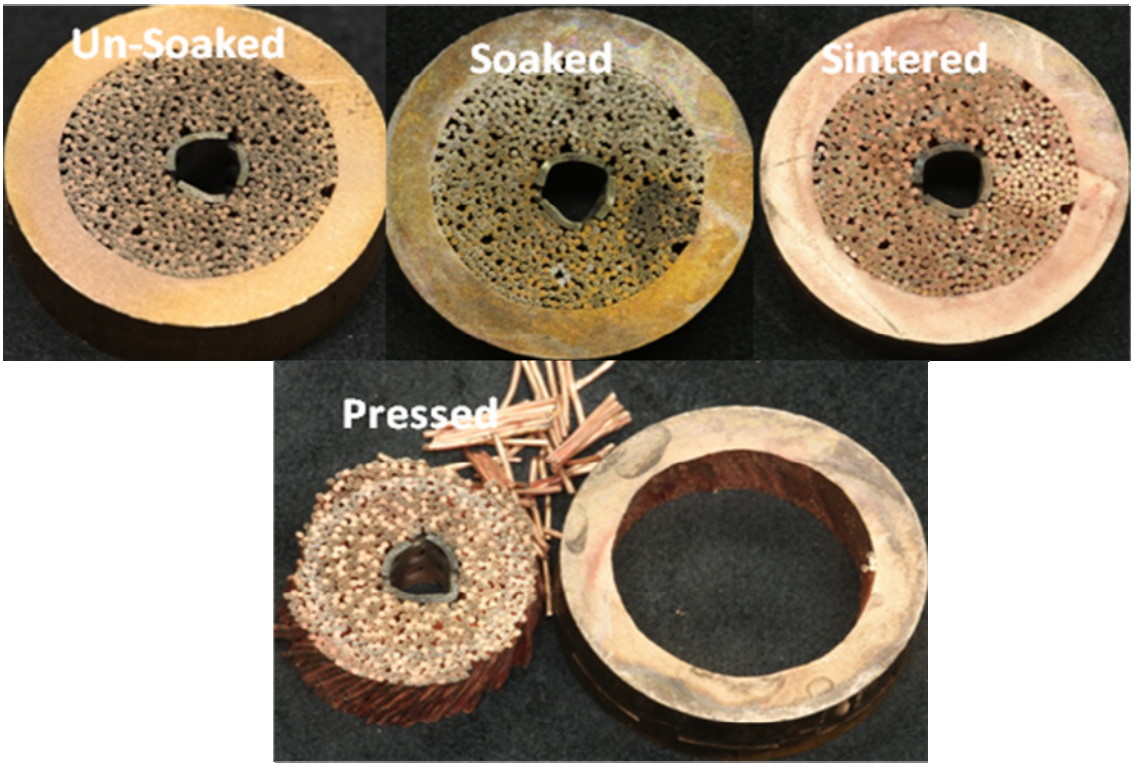


Figure A136: Sample 16X

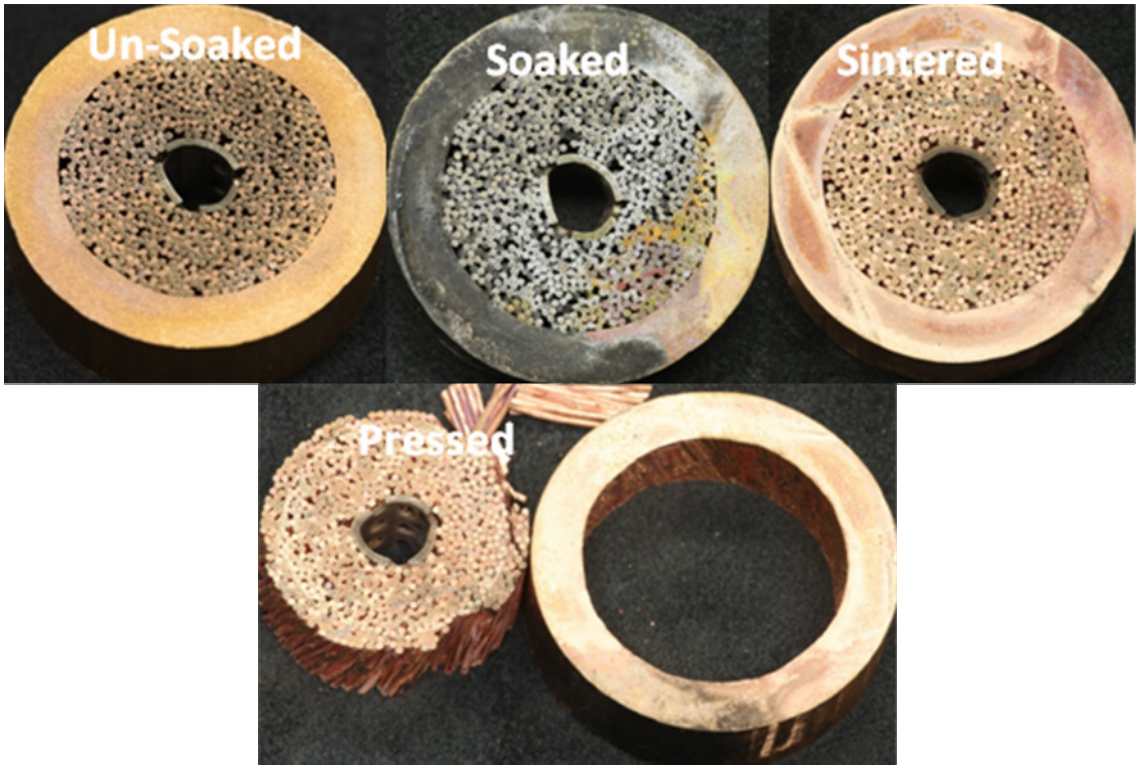


Figure A137: Sample 26X

VITA

Shaan Mohammed was born in 1985 in Houston, TX where he lived for less than one month before moving to Alliance, OH. Shaan lived in Alliance until he was seven years old when he moved to Knoxville, TN with his mother. He attended Maryville Christian School for high school and then attended Pellissippi State for two years before transferring to the University of Tennessee where he received his Bachelors of Science in Mechanical Engineering in May of 2009. During his college career Shaan had internships working for Michelin North America in Greenville, SC and Alcoa Inc in Alcoa, TN and Ferndale, WA. After graduation Shaan will be working for Alcoa Inc at the Tennessee Operations location in Alcoa, TN.